Université du Québec
INRS-ETE

Volcanology and metallogeny of a sector of the Blake River Group, Abitibi Subprovince, Québec and Ontario

Volcanology et métallogénie d'un secteur du Groupe de Blake River, Sous-province de l'Abitibi, Québec et Ontario

Par
Russell Rogers

Mémoire présenté
pour obtenir le grade de Maître ès sciences (M.Sc)
en Sciences de la Terre

Jury d'évaluation

Examinateur externe	Phil Thurston, Ph.D. Laurentian University
Examinateur interne	Michel Malo, Ph.D. INRS – ETE
Codirecteur de recherche	Patrick Mercier-Langevin, ing., Ph.D. Commission Géologique du Canada
Directeur de recherche	Pierre-Simon Ross, Ph.D. INRS – ETE

Abstract

A promising approach to enhance volcanogenic massive sulfide (VMS) exploration in regions outside of mining camps is to simultaneously (1) combine physical volcanology with chemo-stratigraphy to establish the location of effusive centers in the volcanic units; and (2) combine pyrite geochemistry in sulphide-bearing stratified horizons with whole-rock geochemistry in the underlying volcanic units to identify hydrothermal up-flow zones.

These concepts are illustrated by a study in the Archean Blake River Group within the Abitibi Subprovince of Quebec and Ontario. The Blake River Group contains numerous VMS deposits, yet large segments of it remain underexplored, including the area west of Lake Hébécourt. Five main tholeiitic units are identified in the Hébécourt Formation there: the Hébécourt basalt, the Hébécourt basaltic andesite, the main rhyolite (divided into low-Ti and high-Ti subunits), the upper rhyolite and the McDiarmid dacite. Even though the same units are present in both the east and the west, the stratigraphic order of these units is different. In addition, in the eastern region there are thin units of calc-alkaline geochemistry, which are similar to the younger Reneault-Dufresnoy Formation, intercalated within the units of the Hébécourt Formation.

The more detailed information available in the east allowed likely emplacement mechanisms and effusive centers to be identified, using physical volcanology, for three felsic units and a basaltic andesite unit. The low-Ti subunit was emplaced as an extrusive submarine lava dome from a single vent, while the high-Ti subunit was emplaced as submarine lava flows or domes from two separate vents. The upper rhyolite was emplaced as lava flows or domes in several episodes from separate vents and the basaltic andesite was emplaced as pillowed flows from a single vent. Vents in the west could not be located.

Known Zn-Cu mineralization includes sulphide stringers and disseminations located within the flank breccia of the low-Ti rhyolite dome, predominantly forming as replacement of the pore spaces of the fragmental units. Higher in the stratigraphy, this sector corresponds to the inferred volcanic vent area for the basaltic andesite unit.

Laser Ablation Induced Coupled Plasma Mass Spectrometry (LA-ICP-MS) analysis of pyrite grains sampled from several sulphide-bearing stratified horizons in the

eastern stratigraphy indicates two broad regions of higher Cu, Zn, Au and Ag contents. The same peaks were identified using two methods: (1) using all samples regardless of stratigraphic position and (2) using only samples from a single horizon, which could be correlated. The eastern region corresponds to known volcanic vents and mineralization. The western region also indicates up-flow of Cu-bearing hydrothermal fluids, and corresponds to a possible effusive centre for the high-Ti rhyolite. This western sector does not contain known mineralization at lower stratigraphic positions but it has not received significant exploration efforts yet.

R. J. Hannan
Student

Pierre Simard
Research Director

Acknowledgements

The author would like to express sincere gratitude to his research director, Pierre-Simon Ross, for consistently helpful and encouraging supervision during all stages of this project, including fieldwork, labwork and the drafting of publications, posters and figures.

Patrick Mercier-Langevin, the co-director, is also thanked for encouraging and helpful discussions on many aspects of the project and useful comments on the many products of this project.

Jean Goutier is also acknowledged for sharing his extensive knowledge of the Rouyn-Noranda area in general, and for many helpful comments on the publications and posters resulting from this project.

Benoit Lafrance, formerly at Cogitore Resources Inc., shared his knowledge of the Hébécourt property at the beginning of the project and supplied unpublished geological compilations and databases. Tony Brisson of Cogitore Resources Inc. is also thanked for discussions and supplying information. This study was funded in part by the Geological Survey of Canada's Targeted Geoscience Initiative program, phase 3, Abitibi project, led by Benoît Dubé, whom is thanked also for support. Financial and logistical support came from the Ministère des Ressources naturelles et de la Faune (Québec); with particular thanks to Sylvain Lacroix. Balz Kamber organized the use of the Laurentian University LA-ICP-MS lab, and Thomas Ulrich was the analyst. Jan Peter is thanked for invaluable discussion of the sulphide-bearing layered horizons. INRS-ETE provided an international fee-exemption scholarship. Philippe Robidoux served as a field assistant during summer 2008, and Erick Giroux during summer 2009.

Table of contents

List of Figures Page

List of Appendices Page

Sommaire en Francais

Introduction

Les gisements de sulfures massifs volcanogènes (SMV) constituent typiquement des amas polymétalliques formés sur le fond marin ou juste en dessous, en lien avec une activité volcanique (Franklin et al., 2005; Galley et al., 2007). À l'échelle mondiale, y compris au Canada, les SMV représentent des sources importantes de zinc, cuivre, plomb, argent et or.

Critères et méthodes d'exploration traditionnelles

Plusieurs critéres et guides et méthodes d'exploration pour les gisements de SMV sont reconnus. Citons, à l'échelle régionale : des séquences volcaniques ayant subi de l'extension; la présence d'intrusions sub-volcaniques composites ou mafiques riches en sodium; et des rhyolites de haute température (>900°C) qui définissent des environnements favorables (Galley et al., 2007). A une échelle plus locale, les méthodes d'exploration incluent la géophysique (méthodes électromagnétique et magnétique); la découverte de failles syn-volcaniques et de centres volcaniques (environnements proximaux); et la reconnaissance de systèmes hydrothermaux (Franklin et al., 2005; Galley et al., 2007). En général, sauf pour la géophysique, ces méthodes requièrent un échantillonnage abondant et de nombreuses analyses, ainsi que de bons affleurements ou beaucoup de forages au diamant.

Problématique : l'exploration hors des camps miniers est difficile

En général, l'exploration pour les SMV est plus difficile et risquée hors des camps miniers établis puisque la stratigraphie est prouvent mal connue; les horizons-repères sont rares ou non-documentés; et peu de forages sont disponibles. Aussi, dans certains cas, les affleurements sont également rares. La quantité limitée de travaux antérieurs ne permet pas d'utiliser une large base de données avec laquelle comparer toute nouvelle observation ou interprétation. Il peut alors devenir nécessaire de combiner plusieurs méthodes d'investigation imparfaites pour obtenir une meilleure compréhension géologique d'un secteur donné.

Objectifs et méthodes

L'objectif de cette étude était d'expérimenter une approche scientifique diversifiée pour comprendre l'histoire volcanique et hydrothermale d'un secteur considéré comme prospectif pour les SMV. Cette approche devait s'appliquer à l'intérieur ou à l'extérieur d'un camp minier dans des roches volcaniques archéennes ou plus jeunes. Elle combine des méthodes de terrain avec des techniques analytiques à haute résolution.

Spécifiquement, il fut décidé d'utiliser (1) la volcanologie physique et (2) la chimico-stratigraphie pour établir la position des centres effusifs pour les unités volcaniques de la séquence à l'étude. De plus, (3) la géochimie dans les roches volcaniques en lien avec (4) les mesures d'éléments en traces dans les pyrites provenant d'horizons stratifiés riches en sulfures rend possible l'identification de conduits hydrothermaux à l'échelle locale. Cette combinaison de techniques permet aussi de vérifier s'il existe une relation spatiale entre la localisation des centres effusifs volcaniques et des centres hydrothermaux. Quand c'est le cas, l'identification de nouveaux centres effusifs permet de suggérer de nouvelles cibles d'exploration.

La combinaison des techniques employées est nouvelle et puissante.

Contexte géologique et métallogénique

Géologie régionale

Le secteur d'étude est situé dans le Groupe de Blake River, à l'intérieur de la Sous-province de l'Abitibi, qui fait partie de la Province du Supérieur (Fig. 2.1). Cette dernière est constituée de roches archéennes et forme le cœur du Bouclier Canadien. La Province du Supérieur comprend une série de terranes dominés par des granites et des gneiss (terranes continentaux), des granitoïdes et des roches volcaniques (terranes océaniques), et des roches métasédimentaires. Ces terranes se sont assemblés entre 2,72 and 2,68 Ga (Percival, 2007).

La Sous-province de l'Abitibi (Fig. 2.2) est un de ces terranes océaniques qui couve une surface de 700 x 300 km au Québec et en Ontario (Goodwin, 1982). Il s'agit de la plus grande ceinture de roches vertes au monde et elle possède un âge de ~2,7 Ga (Laflèche et al., 1992).

Le Groupe de Blake River (GBR) est la plus jeune séquence volcanique sub-alcaline de la partie Sud de la Sous-Province de l'Abitibi (Thurston et al., 2008; Fig. 2.3). Le GBR est dominé par des laves sous-marines mafiques à intermédiaires avec des faibles quantités de roches volcaniques felsiques (Dimroth et al., 1982; Gélinas et al., 1984; Péloquin et al., 1990). Ces roches volcaniques sont recoupées par des plutons syn-volcaniques à tardifs (ex. Piercey et al., 2008) et des dykes et filons-couches dioritiques à gabbroïques (Pearson et Daigneault, 2009).

Au Québec, un arrêt possible dans le volcanisme du GBR a été identifié vers 2699,3 Ma à partir de la géochronologie U-Pb de haute précision (McNicoll et al., soumis). Les roches volcaniques plus anciennes sont attribuées au Blake River inférieur, alors que celles plus jeunes font partie du Blake River supérieur. Notons que ces divisions ne sont pas nécessairement équivalentes à celles qui prévalent dans le *Blake River Assemblage* en Ontario (Ayer et al., 2005).

Le GBR est connu pour ses gîtes minéraux, notamment ses dépôts de SMV. Plusieurs des gisements de Cu-Zn sont contenus dans le camp de Noranda, juste au nord de Rouyn-Noranda (Gibson et Watkinson, 1990). La plupart des SMV du camp de Noranda sont encaissés dans des roches qui appartiennent au Blake River supérieur (Goutier et al., 2009; McNicoll et al., *soumis*). Les SMV riches en or du camp minier de Doyon-Bousquet-LaRonde, plus à l'Est, sont aussi compris dans des roches volcaniques du Blake River supérieur (Lafrance et al., 2003; Mercier-Langevin et al., 2007a; 2007b; 2008)

Cependant, le Blake River inférieur est maintenant considéré comme intéressant pour l'exploration aussi, puisqu'il abrite les SMV riches en or de Horne et de Quemont (Goutier et al., 2009; McNicoll et al., *soumis*). Les roches du Blake River inférieur au

Québec et en Ontario représentent géographiquement une partie significative du GBR. Une meilleure compréhension de la géologie et de l'hydrothermalisme de ces régions est donc nécessaire pour pouvoir proposer des vecteurs d'exploration dans le Blake River inférieur.

SMV et exhalites

Il est important de bien cerner les caractéristiques et l'origine des gisements de SMV avant de débuter l'étude d'un territoire qui pourrait en contenir. Le modèle général des gisements de SMV proposé par Franklin et al (1995), d'après Lydon (1984, 1988), Galley (1993) et Franklin (1995), a six caractéristiques : (1) une source de chaleur (une intrusion) pour stimuler la circulation hydrothermale et potentiellement pour fournir des métaux; (2) une zone de réaction à haute température qui agit comme réservoir pour les métaux lessivés des roches encaissantes par interaction avec de l'eau de mer modifiée; (3) des failles syn-volcaniques permettant la décharge des fluides hydrothermaux vers le fond marin; (4) des zones d'altération hydrothermale, typiquement dans le mur du gisement, produites par le mélange des fluides ascendants avec de l'eau de mer; (5) le gisement polymétallique lui-même formé sur le fond marin ou juste en dessous; (6) des produits distaux de l'activité hydrothermale comme des exhalites (Fig. 2.4). On peut classifier les SMV en deux types selon le type de roches encaissantes, à savoir des coulées de lave ou des roches volcanoclastiques (Morton et al., 1987; Galley et al., 2007).

Les exhalites sont des sédiments chimiques d'origine surtout volcanique (Ridler, 1971). La présence d'exhalites dans une séquence volcanique sous-marine indique une activité hydrothermale pendant les hiatus du volcanisme. Les exhalites sont souvent minces mais étendues latéralement. Elles se composent de particules détritiques ou tuffacées et d'une composante exhalative comme le chert ou les sulfures (Franklin et al., 2005).

Variations de faciès typiques dans les coulées de lave et les dômes

Comme la grande majorité des roches volcaniques du secteur d'étude sont des coulées de lave ou des dômes de lave, il est utile de passer brièvement en revue les variations de

faciès typiques rencontrées dans ces roches, incluant les cas mafiques et felsiques en environnement sous-marin (Fig. 2.5)

Laves et dômes extrusifs felsiques

Le modèle de McPhie et al. (1993) (Fig. 2.5a et b) montre que les laves felsiques et les dômes extrusifs sous-marins comprennent un cœur massif (cohérent) qui comprend ou non des laminations d'écoulement laminaire. Ce cœur est constitué de nombreux lobes (Yamagashi et Dimroth, 1985) qui s'injectent l'un dans l'autre et dans le matériel fragmentaire environnant. Le cœur est surmonté et entouré de hyaloclastite *in situ* et resédimentée. Les dômes ont un point d'effusion central, alors que les laves sont plus asymétriques et peuvent être plus étendues.

Coulées coussinées mafiques

Dans une coulée de lave coussinée, on rencontre des parties coussinées et des parties fragmentaires (Gibson et al., 1999) (Fig. 2.5c). Les parties coussinées comprennent des coussins en empilement dense avec de la hyaloclastite interstitielle. La brèche de coussins est située au dessus des coussins et dans les parties distales de la coulée; elle comprend des coussins intacts ou brisés et des fragments anguleux dans une matrice de hyaloclastite. La hyaloclastite se compose de fragments vitreux anguleux, monomictiques, formés par refroidissement rapide de la lave dans l'eau. La proportion et la dimension des coussins intacts diminuent vers le haut et les parties distales de la brèche de coussins. On remarque aussi des parties massives dans certaines coulées; il peut s'agir de vraies parties massives, ou encore de méga-coussins.

Les variations de faciès idéalisées montrent les parties massives près de l'évent ou encore des parties coussinées. La taille des coussins diminue avec la distance de la source, alors que la proportion de matériel fragmentaire augmente (Dimroth et al., 1978; 1982; McPhie et al., 1993; Gibson et al., 1999).

Volcanologie et géochimie du secteur d'étude

Le secteur d'étude est situé dans la partie nord du GBR, à l'Ouest du lac Hébécourt, de part et d'autre de la frontière entre le Québec et l'Ontario (Fig. 3.1). Dans la partie québécoise du secteur d'étude, la polarité stratigraphique est vers le sud et le pendage des couches est très abrupt (Fig. 3.2). Le GBR s'y compose de deux formations : Hébécourt et Reneault-Dufresnoy.

La Formation d'Hébécourt y a été divisée en cinq unités tholéiitiques. La plus ancienne et la plus volumineuse est le basalte d'Hébécourt, lequel est interlité avec des niveaux d'andésite basaltique variolitique. À l'extérieur du secteur d'étude, on note aussi des niveaux de lave glomérophyrique dans la succession mafique (Legault et al., 2005). Les laves mafiques sont couvertes dans tout le secteur d'étude par une unité rhyolitique de ≤495 m d'épaisseur (rhyolite principale). Dans la partie Est du secteur, la rhyolite est elle-même surmontée par une andésite basaltique de 210 m d'épaisseur et une seconde unité de rhyolite de 45-75 m d'épaisseur (rhyolite supérieure). Les deux rhyolites ont donné des âges U-Pb sur zircons de 2703 Ma et 2702 Ma respectivement (McNicoll et al., *soumis*). Finalement, la Formation de Reneault-Dufresnoy repose en concordance sur la Formation d'Hébécourt dans le secteur d'étude et est représentée essentiellement par des laves mafiques à intermédiaires d'affinité magmatique variable.

Du côté ontarien, les formations québécoises ne sont pas reconnues officiellement mais elles sont utilisées ici pour simplifier la présentation (Fig. 3.3). Les unités chimico-stratigraphiques identifiées sont les mêmes, mais elles ne se présentement pas exactement dans le même ordre qu'au Québec comme on le verra ci-dessous.

Stratigraphie de la Formation d'Hébécourt à l'Est du forage HEB-04 au Québec

Basalte d'Hébécourt

Le basalte d'Hébécourt forme la grande majorité de la Formation d'Hébécourt à l'échelle régionale. En général, dans le secteur d'étude, il est surmonté de la rhyolite principale, mais des minces bandes de basalte sont aussi notées plus haut dans la séquence, notamment entre la rhyolite principale et la rhyolite supérieure. Aucune variation de

faciès systématique n'a été documentée dans le secteur d'étude pour le basalte d'Hébécourt : les laves sont massives à coussinées (Fig. 3.4). L'interprétation traditionnelle de cette unité est qu'elle forme une plaine de laves tholéiitiques (Dimroth et al., 1982). Les nouvelles analyses géochimiques confirment le caractère basaltique et tholéiitique de cette unité (Figs. 3.7 et 3.8). Les patrons d'éléments en traces rappellent les basaltes de dorsales médio-océaniques (MORB) (Fig. 3.9).

Andésite basaltique d'Hébécourt

Des andésites basaltiques aphyriques, massives à coussinées, intercalées dans le basalte d'Hébécourt, ont été observées en affleurement et dans le forage HEB-05. Ces intercalations font de 20 à 300 m d'épaisseur. De plus, l'andésite basaltique d'Hébécourt surmonte la rhyolite principale dans la partie Est du secteur d'étude. Son épaisseur vraie maximale est de 132 m, mais l'intrusion de minces mais nombreux dykes mafiques à intermédiaires a gonflé l'épaisseur « vraie □ de l'unité à 210 m. Les faciès volcaniques observés incluent les laves massives et coussinées, la brèche de coussins et la hyaloclastite sans coussins (Fig. 3.5). Toutes ces roches sont aphyriques.

Cette unité s'amincit nettement d'Est en Ouest, passant de 132 m d'épaisseur vraie (sans les dykes) à 56 m avant de disparaître au-delà du forage HEB-08 (Fig. 3.6). Le faciès massif se présente également en plus forte proportion dans la portion orientale (spécialement dans HEB-03). Le faciès coussiné domine en proportion dans chaque forage, mais on observe une diminution de la taille moyenne des coussins vers l'Ouest, de 90-100 cm dans les forages HEB-01 à HEB-03 à 40 cm dans le forage HEB-08. Enfin, la proportion de roches fragmentaires (brèche de coussins, hyaloclastite sans coussins) augmente vers l'Ouest de 0 % dans HEB-03 à 30 % dans HEB-08. Ces variations de faciès et d'épaisseur sont typiques des laves sous-marines mafiques à intermédiaires (Dimroth et al., 1978) et suggèrent que le centre effusif, de l'unité d'andésite basaltique d'Hébécourt, est situé dans les environs du forage HEB-03, à l'Ouest du lac Hébécourt.

En général, les analyses géochimiques de nos échantillons forment un groupe serré sur tous les diagrammes quand on tient compte des effets possibles de l'altération

hydrothermale. Sur le diagramme SiO_2 versus Zr/TiO_2 (Fig. 3.7a), les analyses sont situées dans la partie inférieure du champ andésite basaltique/andésite confirmant le nom attribué à cette unité. Sur le diagramme Zr/TiO_2 versus Nb/Y (Fig. 3.7b), les échantillons se projettent dans le champ des andésites. L'affinité magmatique tholéiitique est bien indiquée sur les diagrammes (Figs. 3.8 et 3.9).

Rhyolite principale

La rhyolite principale de la zone étudiée recouvre le basalte d'Hébécourt. Elle a été divisée en deux sous-unités selon la présence ou l'absence de phénocristaux (Fig. 3.12), ainsi que l'abondance en Ti (Fig. 3.10). L'unité la plus ancienne pauvre en Ti (porphyrique à quartz) est surmontée par la rhyolite riche en Ti (aphyrique).

Les faciès volcaniques observés au sein de ces deux sous-unités sont similaires, la seule différence étant le contenu en phénocristaux. Ces deux sous-unités sont composées de faciès cohérents avec localement des laminations d'écoulement laminaire et de faciès fragmentaires dominés par des tufs à lapilli non stratifiés avec des fragments monomictiques et anguleux interprétés comme de la hyaloclastite (Fig. 3.11).

La rhyolite pauvre en Ti est plus épaisse au centre et s'amincit de chaque côté. Elle est constituée de roches cohérentes au centre dans la région du trou de forage HEB-02. Ces roches sont surmontées et bordées par des roches fragmentaires. Ces variations de faciès peuvent être interprétés, selon le modèle de McPhie et al. (1993), comme un dôme de lave complètement extrusif à partir d'un unique évent dans la région du forage HEB-02.

La rhyolite riche en Ti est plus mince à l'endroit où la rhyolite pauvre en Ti est la plus épaisse, puis son épaisseur augmente vers l'Est et vers l'Ouest. Il y a deux zones de roches cohérentes dans la rhyolite pauvre en Ti, une dans la région du forage HEB-04 et l'autre entre les forages HEB-01 et HEB-03. On observe des roches fragmentaires autour de ces parties massives. Ceci peut être interprété comme des coulées de laves ou des dômes provenant de deux évents distincts à l'Est et à l'Ouest du Chemin de la Mine.

Du point de vue géochimique, la rhyolite principale tombe dans le champ rhyolitique sur les diagrammes de Winchester et Floyd (1977) (Fig. 3.13), mais s'étend aussi dans le champ des rhyodacites sur le graphe de SiO_2 vs. Zr/TiO_2, probablement à cause de la mobilité des éléments majeurs. Dans les graphiques montrant les affinités magmatiques, la rhyolite principale est clairement tholéïtique (Fig. 3.14). La méthode de discrimination des deux sous-unités est basée sur le contenu en Ti. On peut cette discrimination voir sur le graphe de TiO_2 vs. Zr (Fig. 3.14c). Les deux sous-unités forment également des groupes distincts sur le graphique Zr vs. Y (Fig. 3.14a). Le spectre des éléments en trace étendus est plat, avec une anomalie significative en titane correspondant à des profils de roches tholéïtiques (Fig. 3.15).

Rhyolite supérieure

La rhyolite supérieure forme le sommet de la Formation d'Hébécourt dans la partie Est du secteur d'étude, surmontant la dernière intercalation d'andésite basaltique. C'est l'unité la plus mince de la formation et elle se pince vers l'Ouest au delà du forage HEB-08 (Fig. 3.16). Les faciès observés incluent de la rhyolite sphérolitique massive ainsi que trois types de roches fragmentaires : (i) de la hyaloclastite typique; (ii) des tufs à lapilli avec fragments anguleux; et (iii) des tufs et tufs à lapilli, parfois stratifiés, et contenant des fragments arrondis. Enfin, on remarque aussi la présence de tufs felsiques fins laminés, interlités parfois avec des tufs mafiques et de l'argillite, indiquant que la rhyolite supérieure a été générée par plusieurs épisodes volcaniques.

L'épisode felsique le plus ancien a formé les dépôts les plus épais qui s'amincissent vers l'Ouest. Dans le forage HEB-01, la rhyolite supérieure est formée à 100% de roche massive alors que la proportion de roches fragmentaires augmente latéralement vers l'Ouest et vers l'Est, ce qui suggère que l'évent pour le premier épisode est situé dans le secteur de HEB-01. L'évent pour le second épisode est inconnu.

Les échantillons de la rhyolite supérieure se projettent largement dans le champ des rhyolites sur le diagramme SiO_2 vs Zr/TiO_2 (Fig. 3.13a), alors qu'ils chevauchent les champs rhyodacitiques et rhyolitiques sur le diagramme Zr/TiO_2 vs Nb/Y (Fig. 3.13b). La

principale distinction chimique par rapport à la rhyolite principale est le ratio Zr/TiO_2 plus faible pour la rhyolite supérieure en raison des contenu en titane plus élevé. Les diagrammes d'affinité magmatique montrent une tendance tholéiitique (Figs. 3.14 at 3.15).

Stratigraphie de la Formation d'Hébécourt en Ontario et à l'Ouest du forage HEB-04 au Québec

En général, dans la partie Ouest du secteur à l'étude, la quantité d'affleurements est très limitée et les forages peu nombreux. La géologie est ainsi mal connue. En Ontario, la plus ancienne unité felsique est la rhyolite riche en Ti qui contient au moins deux intercalations de rhyolite supérieure (Fig. 3.3). On note aussi la présence de la dacite de McDiarmid qui contient une mince intercalation de rhyolite pauvre en Ti. La dacite est surmontée par du basalte d'Hébécourt au sommet de la formation. Compte tenu des distances importantes entre la section ontarienne décrite ci-dessus et la séquence typique de la partie Est du secteur d'étude au Québec, puis des différences dans l'ordre stratigraphique des roches felsiques, les roches volcaniques du côté ontarien proviennent vraisemblablement d'évents différents, surtout pour les unités felsiques. Les roches mafiques de Formations d'Hébécourt en Ontario tombent dans les même champ que leur équivalent au Québec (Figs. 3.17, 3.18).

Les faciès observés en Ontario dans les deux sous-unités de la rhyolite principale sont les mêmes que ceux vus au Québec. La rhyolite riche en Ti contient 4-5% de phénocristaux de quartz et autant de feldspath en Ontario contrairement à son caractère aphyrique au Québec. Une corrélation directe est impossible malgré la correspondance géochimique comme le montre aussi la position stratigraphique différente.

La rhyolite supérieure du côté ontarien est bien plus épaisse que son équivalent au Québec et prend la forme de plusieurs occurrences dans la stratigraphie ontarienne. Les faciès observés sont massifs et fragmentaires.

La dacite de McDiarmid est une unité felsique tholéiitique définie par cette étude. Elle s'étend de l'Ontario (forage MD-01) jusqu'aux forages HEB-04 et HEB-09 au Québec. Elle comprend des faciès massifs et lobés, ainsi que des roches volcanoclastiques (tufs et tufs à lapilli). Sur les diagrammes de Winchester et Floyd (1977) (Fig. 3.19), la dacite de McDiarmid tombe surtout dans les champs rhyodacite/dacite, mais avec une grande dispersion. Le diagramme TiO_2 vs. Zr (Fig. 3.20b) montre que cette unité est bien distincte de toutes les autres dans le secteur d'étude, mais suggère également un patron de différentiation à l'intérieur de l'unité. Possiblement la dacite de McDiarmid deviendrait divisible en sous-unités si plus d'information devenait disponible.

Formation de Reneault-Dufresnoy au Québec et en Ontario

L'unité stratigraphique la plus jeune dans le secteur d'étude est la Formation de Reneault-Dufresnoy. Seuls les premiers 250 à 300 m de cette unité ont été étudiés, sur six affleurements et dans sept forages. Les roches volcaniques mafiques à intermédiaires observées sont massives à coussinées avec une faible proportion de roches fragmentaires. Plus au sud, la proportion de matériel volcanoclastique augmente (Ross et al., 2008a).

Sur les diagrammes de Winchester et Floyd (1977) (Fig. 3.7), les nouveaux échantillons ont une composition variant de basalte à andésite. Deux groupes ont été définis à partir des diagrammes d'affinités magmatiques et des diagrammes multi-éléments (Figs. 3.8 at 3.9). Ces groupes ne sont pas nécessairement présents ensemble dans chaque forage, mais quand ils le sont, les échantillons du Groupe 2 se trouvent plus haut dans la stratigraphie que ceux du Groupe 1. Les échantillons du Groupe 1 sont d'affinité tholéiitique à transitionnelle, alors que ceux du Groupe 2 sont transitionnels à calco-alcalins, suggérant une évolution vers des affinités plus calco-alcalines avec le temps dans la Formation de Reneault-Dufresnoy. Considérés ensemble, les deux groupes couvrent la gamme des compositions représentées par le champ des analyses antérieures par un secteur plus étendu. Sur les diagrammes multi-éléments (Fig. 3.9), les échantillons du Groupe 1 ont des pentes douces à modérées, de faibles anomalies négatives en Nb-Ta, de petits plateaux Zr-Hf et de faibles anomalies négatives (parfois positives) en Ti. En revanche, ceux du Groupe 2 ont des pentes plus fortes, des anomalies en Nb-Ta et de titane plus

prononcées, et des plateaux Zr-Hf plus marqués. Cette dernière signature est typique des magmas d'arcs volcaniques.

La figure 3.21 montre un résumé schématique de l'histoire volcanique de la zone d'étude.

Altération et minéralisation

Le diagramme "*Alteration Box Plot*" (Large et al., 2001; Gifkins et al., 2005; Fig. 4.1) consiste en deux indices d'altération allant de 0 à 100 : l'indice d'Ishikawa (AI: Ishikawa et al., 1976) et l'indice chlorite-carbonate-pyrite (CCPI). L'AI est un bon marqueur pour l'altération à chlorite et séricite, ainsi que pour la destruction du plagioclases, alors que le CCPI permet de différencier les altérations à chlorite et séricite ainsi que les carbonates et la pyrite. La combinaison des deux indices peut aussi être utilisée pour identifier des tendances diagénétiques comme épidote + calcite ± albite et albite + chlorite, tout comme les roches fraîches, qui tombent dans certaines boîtes dépendant de leur composition chimique.

Le graphique *alteration box plot* montre que les roches volcaniques mafiques sont largement fraîches (Fig. 4.1a), suggérant que les quantités mineures à modérées de chlorite et de séricite observées macro- et microscopiquement sont des minéraux métamorphiques. Les roches felsiques (Fig. 4.1b), au contraire, montrent plusieurs altérations incluant des altérations hydrothermales, composées de chlorite ± pyrite ± séricite et de séricite + chlorite + pyrite, avec un peu d'altération carbonatée. Il y a également une tendance diagénétique à albite+chlorite, ainsi qu'une à épidote+calcite±albite. Ces tendances d'altération suggérées par la géochimie peuvent être confirmées par les observations en forages et en lames minces (Fig. 4.3) sur les roches felsiques avec cependant quelques limites comme expliqué ci-dessous.

La carte thématique (Fig. 4.2) des indices d'altération (AI) a été créée pour localiser les zones les plus altérées. Les valeurs inférieures à 20 montrent les tendances diagénétiques, les roches fraîches ont des valeurs entre 20 et 60-65 et les roches avec des valeurs plus élevées sont altérées (Gifkins et al., 2005). Les valeurs AI ont été calculées pour des

données compilées d'échantillons de surface anciens et récents ainsi que de forages. La rhyolite pauvre en Ti est plus altérée que la rhyolite riche en Ti qui la surmonte près du Chemin de la Mine. Les différents degrés d'altération de la rhyolite principale ont été vus dans les forages plus à l'Est (Fraser, 1991; Martin, 1994; Bambic, 1998). Les échantillons ayant subi de la diagénèse sont localisés à l'Ouest du Chemin de la Mine dans la rhyolite riche en Ti dans la région proposée pour l'évent de cette unité.

La carte de contours des valeurs en cuivre et zinc a été créée à partir des données d'analyses économiques disponibles (Fig. 4.4). Les minéralisations et les valeurs anomales en métaux se retrouvent dans deux zones appelées informellement A et B. La zone A est localisée dans la région centrale de la rhyolite principale (surtout au sein de la sous-unité riche en Ti) et est dominée par des valeurs en Zn anomales avec presque pas de Cu. Les valeurs les plus élevées en Zn (6,17% sur 0,1 m) sont rencontrées dans le trou de forage SC-13 et représentent des sulfures semi-massifs ou des filonnets de pyrite et de sphalérite (Cloutier, 1975; Martin, 1994; Bambic 1998). Il y a des valeurs plus faibles au Sud de cette zone ainsi qu'à l'Ouest et à l'Est. Légèrement plus à l'Ouest dans le trou de forage 77738, le Zn se situe dans des disséminations riches en pyrite et une zone mince contrôlée par les fractures. Dans le trou de forage SC-14 à l'Est, les minéralisations sont principalement des filonnets de pyrite et de sphalérite associés à du quartz.

La zone B, qui est caractérisée par de meilleures teneurs que la zone A, est localisée dans le coin Nord-est de la zone d'étude. Il s'agit d'une zone minéralisée allant jusqu'à 40 m de longueur d'intersection en forage, au sein d'une zone d'altération chloritique et séricitique (Cloutier, 1975; Bambic, 1998). Les valeurs en cuivre et zinc proviennent de sulfures disséminés et de zones de filonnets (Cloutier, 1975) avec le zinc plus largement répandu que le cuivre. Les disséminations de pyrite, sphalérite et chalcopyrite sont présentes principalement dans la région la plus à l'Ouest de la zone B, alors que les filonnets dominés par la pyrite sont trouvés plus à l'Est (Cloutier, 1975). Les plus fortes teneurs en Cu (0,19% Cu sur 1,9 m), ainsi que les roches les plus altérées (AI = 80 à 95, dû à des altérations chloritiques et séricitiques) se trouvent dans le trou de forage 753-07, où la minéralisation se trouve dans la matrice des brèches de la rhyolite pauvre en Ti qui

contient des fragments anguleux d'en moyenne 3-4 cm (Cloutier, 1975). Cette brèche fait partie du flanc Est du dôme de rhyolite pauvre en Ti. Des valeurs plus faibles en Cu-Zn apparaissent plus haut au sein de la rhyolite riche en Ti. La meilleure intersection de zinc se trouvant dans la zone B montre des valeurs de 11,6% Zn sur 1,1 m au sein du forage 753-01 (Cloutier, 1975).

Il est intéressant de noter que les roches les plus altérées et minéralisées se situent dans les brèches de la rhyolite et que les minéralisations se sont probablement formées par remplacement sous le fond marin comme le montrent les textures (sulfures disséminés et en filonnets).

Horizons stratifiés riches en sulfures et leur utilité dans l'identification de zones de remontée de fluides hydrothermaux

Deux horizons stratifiés riches en sulfures, historiquement présentés comme étant d'origine exhalative, ont été auparavant identifiés au contact entre la rhyolite principale et les andésites basaltiques les plus jeunes de la Formation d'Hébécourt, ainsi qu'au contact entre la rhyolite supérieure et la Formation de Reneault-Dufresnoy (Fraser, 1991; Carignan et Lafrance, 2008; Figs. 5.1 et 5.2). Cogitore Resources Inc. a obtenu des valeurs en Zn allant jusqu'à 1,2% sur quelques décimètres au niveau de ces horizons (Carignan et Lafrance, 2008). Pendant l'observation et l'échantillonnage de ces horizons dans les trous de forages HEB-01 à HEB-09, il a été noté qu'ils n'étaient pas toujours localisés aux contacts mentionnés plus haut et que le nombre de ces horizons dans un trou de forage particulier va de un à trois. Quelques horizons sont trouvés dans la Formation de Reneault-Dufresnoy. De plus, il est proposé que les sulfures au sein de ces horizons se sont mis en place principalement par remplacement, plutôt que par précipitation et sédimentation à partir d'un panache hydrothermal dans la colonne d'eau de mer (Fig. 5.3). Les fluides hydrothermaux ont remonté dans les fractures au travers d'une épaisseur de lave cohérente, ou au sein de la porosité primaire de dépôts volcanoclastiques. Les fluides ont ensuite rencontré des horizons lités de tuf ou de sédiment, et ont changé de chemin pour migrer latéralement le long de ces horizons, où ils ont précipité des sulfures.

Les horizons stratifiés riches en sulfures comprennent (i) des intervalles finement laminés à finement lités sur une épaisseur de 20 cm en moyenne (localement pouvant aller à 50-60 cm d'épaisseur) consistant en une alternance de cendres, chlorite, argillite et de pyrite à grains fins, et (ii) des intervalles généralement plus épais de tuf, de 60-70 cm d'épaisseur en moyenne, qui n'ont typiquement pas de stratification interne (Fig. 5.4).

La position stratigraphique et l'extension latérale de ces horizons stratifiés riches en sulfures sont variables d'un trou de forage à l'autre (Fig. 5.1). La majorité de ces horizons sont inclus dans la Formation d'Hébécourt et seulement deux se situent dans la Formation de Reneault-Dufresnoy (Figs. 5.1 et 5.2). Un horizon stratiforme riche en sulfure au sommet de la rhyolite supérieure (horizon A) a été corrélé entre quatre trous de forages : HEB-03, HEB-01, HEB-02 et HEB-08. Un deuxième horizon (A') a été corrélé au sommet de la dacite de McDiarmid à l'Ouest dans les trous de forages HEB-09 et HEB-04. Les deux horizons sont à la base de la Formation de Reneault-Dufresnoy.

Des lames épaisses (~100 μm d'épaisseur) ont été préparées pour 19 des échantillons les plus représentatifs des intervalles finement laminés à finement lités des horizons stratifiés riches en sulfures. Chaque horizon trouvé pendant l'étude est représenté par une ou deux lames. Celles-ci ont été faites dans les zones où la carotte était caractérisée par une abondance de pyrite, peu importe le style de minéralisation (ex. pyrite dans des veines vs. laminations riches en pyrite, grains fins ou grossiers). Entre 10 et 20 points ont été analysés par LA-ICP-MS par section épaisse à l'Université Laurentienne (Fig. 5.5). Le site de résidence des éléments traces dans les pyrites peut être dans la structure cristalline ou sous forme d'inclusions (Fig. 5.6).

Un diagramme des teneurs en métaux (Cu, Zn, Au, Ag) par rapport à la position latérale du trou de forage est présenté (Fig. 5.7). Deux pics peuvent être observés : un premier à l'Ouest, centré autour du trou HEB-04, et un second à l'Est, dans la région des trous HEB-02 et HEB-03, avec une vallée entre les deux. Ces patrons existent aussi pour les éléments suivants: As, Bi, Cd, Hg, Mn, Pb, Sb et Tl, ce qui suggère l'existence de deux

zones distinctes de remontée de fluides hydrothermaux dans les roches volcaniques de la partie supérieure de la Formation d'Hébécourt : une à l'Ouest dans le secteur des trous HEB-09 à HEB-04, et l'autre à l'Est dans le secteur des trous HEB-02 à HEB-03. Les fluides hydrothermaux ont aussi circulé dans des niveaux inférieurs de la Formation de Reneault-Dufresnoy comme le montrent les hautes valeurs en Cu et Zn dans cette formation dans le trou HEB-09.

De plus, le même type de graphique pour les horizons A et A' présente aussi deux pics (Fig. 5.8), à l'Est et à l'Ouest, avec des valeurs plus basses au centre autour de HEB-08. Cette bonne correspondance entre les patrons des éléments en trace pour des pyrites d'un horizon relativement continu avec des patrons équivalent pour toutes les données qui incluent des horizons multiples, principalement discontinus, suggère que l'activité hydrothermale s'est poursuivie sur une longue période de temps, permettant l'infiltration de fluides dans plusieurs horizons à des niveaux stratigraphiques différents. La corrélation entre les patrons des multiples horizons et au sein d'un même horizon suggère fortement que les patrons ne sont pas des anomalies statistiques, mais reflètent clairement la présence de remontées de fluides hydrothermaux.

Discussion

La discussion reprend les principales interprétations des sections précédentes et les combine pour arriver à une reconstitution de l'histoire géologique du secteur d'étude (Fig. 6.1).

Le basalte d'Hébécourt répresente une plaine de laves massives à coussinées ressemblant géochimiquement à des MORB, ce qui suggère une mise en place dans un environnement sous-marin en extension. Bien que la majeure partie de cette unité soit située stratigraphiquement sous la rhyolite principale, de minces niveaux de basalte tholéiitique ont été découverts au-dessus de celle-ci. Ceci suggère que la mise en place de la rhyolite principale ne représente pas la fin des éruptions de tholéiites mafiques dans la Formation d'Hébécourt. Soit que les rhyolites proviennent d'une chambre magmatique distincte de

celle des basaltes, ou bien que la chambre magmatique unique a été rechargée par des magmas basaltiques après l'éruption de la rhyolite.

L'andésite basaltique d'Hébécourt située au-dessus de la rhyolite principale ressemble aux horizons d'andésite basaltique variolitique intercalés avec les basaltes plus bas dans la séquence, tant d'un point de vue chimique qu'en termes de textures volcaniques. La plus jeune interdigitation constitue donc une autre manifestation de volcanisme tholéiitique relativement mafique intercalé entre deux rhyolites. Dans l'andésite basaltique d'Hébécourt, les variations d'épaisseur et de faciès suggèrent que le centre effusif était situé dans la partie Est de l'unité.

Les variations de faciès volcaniques pour la sous-unité pauvre en Ti de la rhyolite principale peuvent être interprétées comme un dôme de lave provenant d'un seul évent dans la région de HEB-02, alors que la sous-unité riche en Ti est interprétée comme des laves sous-marines ou des dômes provenant de deux évents distincts, un à l'Est et l'autre à l'Ouest du Chemin de la Mine.

Même si moins épaisse que les sous-unités de la rhyolite principale, la rhyolite supérieure d'Hébécourt semble avoir été formée par de multiples évents avec au moins deux épisodes de mise en place et un hiatus dans l'activité effusive entre ces deux épisodes. L'épisode le plus vieux et le plus épais a la plus grande proportion (100%) de rhyolite massive dans le trou HEB-01, suggérant que ce trou de forage se situe à proximité de l'évent.

Les premiers 250 à 300 m de la Formation de Reneault-Dufresnoy contiennent des roches volcaniques mafiques à intermédiaires qui se classent en deux groupes géochimiques. Le Groupe 1 d'affinité tholéiitique à transitionnelle se trouve à la base de l'unité, alors que le Groupe 2 d'affinité transitionnelle à calco-alcaline se situe plus haut dans la stratigraphie, suggérant qu'avec le temps, les magmas de la Formation de Reneault-Dufresnoy sont devenus plus calco-alcalins et apparentés géochimiquement à des magmas d'arcs volcaniques modernes. Les travaux de Ross et al. (*soumis*) démontrent également des

variations géochimiques importantes dans la même formation plus au Sud dans le secteur du lac Monsabrais.

Dans la zone d'étude, il existe un lien entre les centres effusifs, les altérations hydrothermales, les minéralisations de métaux de base et les concentrations en métaux dans les pyrites d'horizons stratifiés riches en sulfures. En particulier, l'évent proposé pour la dernière manifestation des andésites basaltiques d'Hébécourt est situé immédiatement au Sud de la principale minéralisation connue (zone B) et de l'altération la plus intense en séricite-chlorite dans les brèches de la rhyolite principale plus bas dans la stratigraphie. Ceci suggère que les magmas des andésites basaltiques ont utilisé les mêmes structures synvolcaniques, ou tout au moins des structures proches, pour arriver à la surface que le fluide hydrothermal qui a altéré la rhyolite principale et produit la minéralisation. Les pyrites dans les horizons stratifiés riches en sulfures contiennent également des valeurs appréciables en Ag, Au, Cu et Zn, entre autres, dans le secteur. Les fortes valeurs en métaux dans de telles pyrites définissent en fait une zone plus étendue à l'Est du Chemin de la Mine et correspondent alors à une zone contenant le centre éruptif du dôme de rhyolite pauvre en Ti, le centre effusif principal pour la rhyolite supérieure, et un des évents pour la rhyolite riche en Ti, ainsi que la faible minéralisation en Zn (zone A).

Les fortes valeurs en métaux dans les pyrites des horizons stratifiés riches en sulfures à l'Ouest du Chemin de la Mine, qui sont aussi hautes que les valeurs à l'Est, ne semblent pas associées avec les minéralisations de métaux de base et de l'altération hydrothermale plus bas dans la stratigraphie. Ceci pourrait être le résultat d'exploration très limitée dans cette zone comparée au secteur Est, particulièrement dans la rhyolite principale, plutôt qu'une absence de minéralisation et d'altération. Le pic Ouest de teneur en métaux dans les pyrites pourrait potentiellement être associé avec le centre effusif proposé pour la rhyolite riche en Ti dans le trou HEB-04, ou avec un autre centre volcanique non défini et associé à de potentielles zones de remontées hydrothermales. Ceci démontre le potentiel d'utiliser la cartographie de faciès volcaniques en affleurement et en forage et la chimico-

stratigraphie détaillée, en parallèle avec des analyses d'éléments en trace dans les pyrites, pour définir des vecteurs d'exploration vers les gisements de SMV.

Il est intéressant de comparer les rhyolites de la Formation d'Hébécourt avec celles du bloc de Horne, puisqu'elles ont approximativement le même âge. En termes volcanologiques, elles présentent certaines similitudes (forte proportion de roches volcanoclastiques) mais aussi des différences (pas de roches pyroclastiques dans le secteur d'étude). La géochimie montre aussi des différences (Fig. 6.2).

Conclusions

L'exploration pour les SMV devient plus difficile hors des camps miniers dans le GBR et ailleurs, notamment parce que la stratigraphie volcanique est mal connue; parce qu'il existe comparativement peu de forages et parfois peu d'affleurements; et parce que des horizons marqueurs sont absents ou non documentés. Il devient alors nécessaire de combiner plusieurs méthodes d'investigation pour obtenir une meilleure compréhension d'un secteur donné.

Dans la région d'étude, la stratigraphie est différente entre les secteurs Ouest et Est, surtout pour les unités felsiques. Dans l'Est, la chimico-stratigraphie est maintenant bien établie et plusieurs centres effusifs ont été identifiés grâce à la volcanologie physique : un centre effusif unique pour la sous-unité pauvre en Ti de la rhyolite principale; deux centres effusifs distincts pour la sous-unité riche en Ti de cette même rhyolite; un évent unique pour la plus jeune intercalation d'andésite basaltique; et un des évents de la rhyolite supérieure. Dans l'Ouest, la position des centres effusifs n'est pas connue en général. Dans l'Est, il existe clairement un lien entre la localisation des centres effusifs (environnements volcaniques proximaux) et les zones de remontées hydrothermales. Ces dernières se manifestent par des roches volcaniques altérées, de la minéralisation en Zn-Cu, et des valeurs élevées en éléments traces dans les pyrites des horizons stratifiés riches en sulfures. Les valeurs en éléments traces sont aussi élevées dans l'Ouest, ce qui suggère un potentiel d'exploration. Il est intéressant de noter que les horizons stratifiés riches en sulfures sont porteurs d'information même s'il ne s'agit pas d'exhalites classiques, mais

plutôt de niveaux volcano-sédimentaires ayant subi un remplacement partiel suite à la circulation/percolation de fluides hydrothermaux.

Légendes de figures en français

Fig. 2.1. Carte montrant la Province du Supérieur et les sous-provinces de celle-ci. La Sous-province de l'Abitibi est mise en évidence. D'après Thurston et al. (2008).

Fig. 2.2. Carte de la Sous-province de l'Abitibi, d'après Thurston et al. (2008).

Fig. 2.3. Carte géologique simplifiée du Groupe de Blake River avec la localisation de la zone d'étude.

Fig. 2.4. Modèle général de formation de dépôts de SMV montrant les caractéristiques du système hydrothermal. D'après Franklin et al. (2005).

Fig. 2.5. Schéma montrant les variations de faciès typiques des laves sous-marines et des dômes. (A) Volcan mafique ou intermédiaire coussiné, d'après Gibson et al. (1999). (B) Dôme felsique sous-marin extrusif, d'après McPhie et al. (1993). (C) Coulée de lave sous-marine felsique, d'après McPhie et al. (1993).

Fig. 3.1. Carte de la partie supérieure de la Formation d'Hébécourt ainsi que de la partie inférieure de la Formation de Renault-Dufesnoy à l'Ouest du lac Hébécourt. La géologie est basée sur des cartes au 1 : 20 000 du Ministère des Ressources naturelles et de la Faune (Québec), d'une compilation non-publiée de Ressources Cogitore Inc., ainsi que de nouvelles données cartographiques.

Fig. 3.2. Section entre les points A et A' de la fig. 3.1. Cette section a été créée en utilisant les informations du trou de forage HEB-02 ainsi que des observations de terrain. Elle montre l'ordre stratigraphique typique des unités dans la région à l'Est du trou HEB-04. Les basaltes d'Hébécourt sont à la base, intercalés avec des andésites basaltiques et surmontés par la rhyolite principale. La rhyolite principale est divisée en une sous-unité plus ancienne, pauvre en Ti, et une sous-unité plus jeune, riche en Ti. La rhyolite principale est surmontée d'une mince unité de basalte d'Hébécourt et d'une séquence

d'andésite basaltique, puis finalement par la rhyolite supérieure et la Formation de Reneault-Dufresnoy.

Fig. 3.3. Section entre les points B et B' de la fig. 3.1. Cette section a été créée en utilisant les informations des trous de forage MD-01 et MD-02 et montre la seule stratigraphie connue dans le secteur d'étude en Ontario. Il est supposé que la sous-unité de rhyolite riche en Ti (rhyolite principale) se met en place au dessus des basaltes d'Hébécourt, mais le contact n'a pas été observé. La rhyolite supérieure est intercalée avec la rhyolite riche en Ti, et la rhyolite supérieure est plus épaisse qu'au Québec. Ces deux unités sont recouvertes par la dacite de McDiarmid qui contient une fine interdigitation de rhyolite pauvre en Ti. Le tout est finalement recouvert par les basaltes d'Hébécourt, puis la Formation de Reneault-Dufresnoy.

Fig. 3.4. Photomicrographies d'unités mafiques de la Formation d'Hébécourt. LN : Lumière naturelle, LP : lumière polarisée. (A)-(B) Les textures de refroidissement des basaltes d'Hébécourt en LN et en LP, respectivement. (C)-(D) Le caractère in situ des fragments d'une hyaloclastite typique dans les andésites basaltiques d'Hébécourt en LN et en LP. (E)-(F) La zonation des minéraux au sein des fragments des andésites basaltiques d'Hébécourt en LN et en LP.

Fig. 3.5. Photographies des andésites basaltiques d'Hébécourt. A) Faciès massif montrant une forte concentration en varioles. L'échelle est graduée en centimètres. B) Point triple entre des coussins avec de la hyaloclastite (Hy) intersticielle. Les varioles (VAR) sont abondantes dans les bordures des coussins. (C) Un coussin de lave complet avec une augmentation de la concentration en varioles et en vésicules près des bordures. (D) Faciès de brèche de coussins en forage comprenant de la hyaloclastite in situ et des clastes plus gros qui représentent des fragments de coussins. La règle est graduée en centimètres et en millimètres. (E)-(F) Faciès hyaloclastique en forage montrant de la fragmentation in situ et des petits fragments chloritisés. L'échelle est une règle de 15 cm, dans les deux photos.

Fig. 3.6. Variations de faciès volcaniques dans les andésites basaltiques d'Hébécourt. En haut: Diagraphies des quatre trous de forage où cette unité est observée. Tous les diagraphies ont la même échelle, qui représente l'épaisseur vraie après l'inflation due aux intrusions. Les épaisseurs avec les intrusions retirées sont : HEB-03 : 127 m; HEB-01 : 132 m; HEB-02 : 85 m et HEB-08 : 56 m. Les graphiques en pointe de tarte montrent les proportions des faciès volcaniques dans chaque forage. En bas : carte montrant les variations de faciès intégrant les observations de surface et les observations en forage projetées le long d'un plan penté à 72°S. La carte n'est pas dans la même orientation que sur la figure 3.1.

Fig. 3.7. Géochimie des roches volcaniques mafiques à intermédiaires dans la zone d'étude. (A)-(B) Diagramme de classification de Winchester et Floyd (1977). Les analyses illustrées par des symboles sur toutes les figures géochimiques ont été obtenues chez Activation Laboratories Ltd. à Ancaster, Ontario, en utilisant la méthode ICP-AES (suite à une fusion) pour les éléments majeurs et la méthode ICP-MS (suite à une fusion) pour les éléments en traces. Les champs des figures 3.8, 3.13 et 3.14 représentent les données compilées de Ressources Cogitore Inc., ainsi que des données non publiées de la Commission Géologique du Canada (courtoisie de E. Grunsky).

Fig. 3.8. Géochimie des roches volcaniques mafiques à intermédiaires dans la zone d'étude. (A)-(C) Diagrammes d'affinités magmatiques d'après Ross et Bédard (2009). Le graphique (A) inclue également les limites de Barrett et MacLean (1999).

Fig. 3.9. Diagramme d'éléments en traces étendu pour les roches volcaniques mafiques à intermédiaires de la zone étudiée : (A) basalte d'Hébécourt; (B) andésite basaltique d'Hébécourt; (C) Formation de Reneault-Dufresnoy, Groupe 1; (D) Formation de Reneault-Dufresnoy, Groupe 2, et un basalte calco-alcalin de la Formation d'Hébécourt. Les valeurs des normalisations au manteau primitif et des compositions de MORB proviennent de Sun et McDonough (1989). Deux analyses non publiées de basalte d'Hébécourt (le Ta n'est pas déterminé) ont été fournies par E. Grunsky.

Fig. 3.10. (A) Carte de la rhyolite principale dans la Formation d'Hébécourt montrant les sous-unités délimitées par les échantillons riches et pauvres en Ti, et les observations de rhyolite porphyrique ou aphyrique. Les observations et les échantillons de forages ont été projetés à la surface en utilisant le pendage régional de 72°S et une direction perpendiculaire à S_0. (B) Carte montrant la distribution des faciès dans la rhyolite pauvre en Ti, basée sur les observations de forages et de terrain, et sur les travaux statutaires. La forme des roches volcanoclastiques au dessus de la partie centrale massive est définie d'après les forages et trois affleurements; il se peut qu'il ne s'agisse pas d'une représentation précise des faciès en surface. Seuls les forages compilés sont montrées sur cette figure. (C) Carte montrant la distribution des faciès dans la rhyolite riche en Ti.

Fig. 3.11. Photographies de roches felsiques de la Formation d'Hébécourt. (A) Faciès massif dans la sous-unité pauvre en Ti de la rhyolite principale avec des veines de séricite et des phénocristaux de quartz de 1-2 mm. (B) Faciès bréchique de la rhyolite pauvre en Ti, clairement riches en matrice avec de larges clastes. (C) Faciès de brèche de la rhyolite riche en Ti. (D) Faciès massif de la rhyolite supérieure avec des sphérules coalescentes irrégulières. (E) Tuf à lapilli dans la rhyolite supérieure avec des fragments anguleux. Les plus petits clastes sont épidotisés et les plus gros clastes montrent une texture sphérulitique. (F) Tuf laminé et argillite provenant de la limite entre le premier et le second épisode volcanique de la rhyolite supérieure.

Fig. 3.12. Photomicrographies des unités de la Formation d'Hébécourt. LN : Lumière naturelle, LP : lumière polarisée. (A)-(B) Phénocristaux de quartz dans la rhyolite pauvre en Ti en LN et en LP, respectivement. (C)-(D) Fibres radiales dans des sphérules de la rhyolite supérieure en LN et en LP. (E)-(F) Vésicules remplies de quartz dans le basalte calco-alcalin en LN et en LP.

Fig. 3.13. Géochimie des roches volcaniques felsiques de la Formation d'Hébécourt dans la région d'étude. (A)-(B) Diagrammes de classification de Winchester et Floyd (1977) pour toutes les unités à l'Est du trou de forage HEB-04.

Fig. 3.14. Géochimie des roches volcaniques felsiques de la Formation d'Hébécourt dans la région d'étude (à l'Est du trou de forage HEB-04). (A)-(B)-(D) Diagrammes d'affinités magmatiques d'après Ross et Bédard (2009) : (A) pour les deux sous-unités de la rhyolite principale; (B) pour la rhyolite supérieure et la rhyodacite calco-alcaline; (D) pour toutes les unités. (C) Graphique de TiO_2 vs. Zr pour toutes les unités. Les graphiques (A) et (B) incluent également les limites d'affinité magmatique de Barrett et MacLean (1999).

Fig. 3.15. Diagrammes d'éléments en traces étendus, normalisés au manteau primitif, pour les roches volcaniques felsiques de la Formation d'Hébécourt : (A) rhyolite pauvre en Ti; (B) rhyolite riche en Ti; (C) rhyolite supérieure; (D) rhyodacite calco-alcaline. Les valeurs de normalisation proviennent de Sun et McDonough (1989).

Fig. 3.16. Variations de faciès volcaniques dans la rhyolite supérieure d'Hébécourt, montres par les diagraphies des trous HEB-03, -01, -02 et -08, tracés à la même échelle verticale. L'axe horizontal montre l'échelle de granulométrie. La ligne rouge représente la limite entre les deux épisodes volcaniques de la rhyolite supérieure, marquée par des cendres finement laminées et de l'argillite, et dans le trou HEB-08 par une unité plus épaisse de tuf mafique.

Fig. 3.17. Géochimie des roches mafiques à intermédiaires dans la zone d'étude. (A)-(B) Diagramme de classification de Winchester et Floyd (1977) pour les échantillons pris à l'Ouest du trou de forage HEB-04 avec un champ montrant les échantillons pris à l'Est.

Fig. 3.18. Géochimie des roches volcaniques mafiques à intermédiaires dans la zone d'étude. (A)-(C) Diagrammes d'affinités magmatiques d'après Ross et Bédard (2009). Le graphique (A) inclut également les limites de Barrett et MacLean (1999). Tous les graphes montrent des échantillons provenant de l'Ouest du trou de forage HEB-04 ainsi que des champs montrant les échantillons pris à l'Est de ce même trou de forage. Le champ pour la Formation de Reneault-Dufresnoy inclut également des échantillons provenant du Sud de la zone d'étude.

Fig. 3.19. Géochimie des roches volcaniques felsiques de la Formation d'Hébécourt à l'Ouest du trou HEB-04. (A)-(B) Diagrammes de classification de Winchester et Floyd (1977). Les graphiques montrent une bonne corrélation entre les échantillons à l'Ouest de HEB-04 et le champ formé à l'Est de ce trou pour la rhyolite supérieure et la rhyolite principale. De plus, la composition de la dacite de McDiarmid au travers de la zone d'étude est montrée.

Fig. 3.20. Géochimie de roches volcaniques felsiques de la Formation d'Hébécourt à l'Ouest du trou HEB-04. (A) Diagramme de Zr vs. Y pour les échantillons pris à l'Ouest de HEB-04 tracés dans un champ formé par les échantillons à l'Est de HEB-04. (B) Graphe TiO_2 vs. Zr pour toutes les unités à l'Ouest de HEB-04 tracés dans des champs formés par les échantillons à l'Est de HEB-04. (C) Affinité magmatique d'après Ross et Bédard (2009).

Fig. 3.21. Histoire géologique de la zone d'étude avec un accent sur la partie supérieure de la Formation d'Hébécourt, illustrée par des sections schématiques (pas à l'échelle). (A) Déposition du basalte d'Hébécourt et de la sous-unité pauvre en Ti de la rhyolite principale. Les triangles représentent les faciès fragmentaires et les tirets orientés de manière aléatoire représentent les faciès massifs. (B) Éruption de la sous-unité riche en Ti de la rhyolite principale par deux conduits séparés. (C) Éruption de l'intercalation la plus jeune d'andésite basaltique d'Hébécourt. Les triangles pleins représentent les hyaloclastites et la taille des coussins diminue vers l'Ouest. (D) Éruption de la rhyolite supérieure provenant de l'évent le plus à l'Est, étant donné que le centre effusif à l'Ouest est inconnu.

Fig. 4.1. Altération hydrothermale dans la zone étudiée. (A)-(B) *Alteration box plot* montrant l'indice d'Ishikawa (AI) vs. l'indice chlorite-carbonate-pyrite (CCPI) (Large et al., 2001; Gifkins et al., 2005) pour les échantillons mafiques et felsiques, respectivement. Les analyses géochimiques utilisées proviennent de cette étude ainsi que de données compilées fournies par Ressources Cogitore Inc. La boîte de basaltes non altérés provenant de rides océaniques jeunes a été compilée d'après la base de données

GEOROC (http://georoc.mpch-mainz.gwdg.de/georoc/), les quatre autres boîtes de jeunes roches non altérées sont tirées de Gifkins et al. (2005).

Fig. 4.2. Altération hydrothermale dans la zone étudiée. (A)-(B) Cartes de l'indice d'altération d'Ishikawa (AI; Ishikawa et al., 1976) pour les échantillons de surface et prélevé dans les carottes, respectivement. Les frontières géologiques sont fournies comme référence. Notez que par souci de simplicité, les échantillons prélevés dans les carottes sont projetés verticalement vers la surface et peuvent ne pas tomber exactement dans l'unité géologique auxquels ils appartiennent (le pendage de la stratigraphie est à 72°S). Les grilles aux 10 m de l'AI furent créées par interpolation entre les échantillons avec un rayon de recherche de 100 m et un minimum de deux échantillons pour chaque point de la grille.

Fig 4.3. Photographies et photomicrographies de roches felsiques altérées. LN = lumière naturelle, LP = lumière polarisée. (A)-(B) Altération séricitique de la matrice provenant d'un échantillon de surface de la rhyolite pauvre en Ti, en LN et en LP, respectivement. (C)-(D) Veinules de séricite avec les épontes altérées en la séricite, en LN et en LP. (E) Altération quasiment complète (surtout une silicification) rendant les textures primaires difficiles à observer dans la rhyolite riche en Ti (HEB-04). (F) Fausse texture fragmentaire formée par l'altération de la rhyolite supérieure dans le trou HEB-01.

Fig. 4.4. Minéralisation de métaux de base et géochimie des pyrites pour la zone d'étude. (A)-(B) Contours de cuivre et de zinc représentant les zones minéralisées A et B, respectivement (voir le texte pour descriptions), avec les grilles de l'indice d'altération d'Ishikawa pour des échantillons de forage, préparé comme pour la figure 4.2. Les contours de cuivre et de zinc sont basés sur une grille aux 5 m autour des trous de forage en utilisant les interpolations entre les échantillons avec un rayon de 50 m et un minimum de deux échantillons par point. Les échantillons sont projetés verticalement vers la surface.

Fig 5.1. Diagramme de corrélation géologique basée sur la chimico-stratigraphie pour six des trous de forage étudiés lors de cette étude. L'échelle est donnée en mètres et représente l'épaisseur vraie de chaque unité. Le zéro représente la base de la Formation de Reneault-Dufresnoy. La position stratigraphique des horizons stratifiés riches en sulfures est montrée, avec les possibles corrélations des horizons A et A'.

Fig. 5.2. Carte thématique pour les valeurs en Cu (A), Zn (B), Au (C) et Ag (D) des pyrites provenant des horizons stratifiés prélevés en forage, basées sur les analyses au LA-ICP-MS. Les échantillons sont projetés à la surface en utilisant le pendange régional de 72°S, donc leur projection est à la bonne position stratigraphique.

Fig 5.3. (A) Illustration des mécanismes de mise en place pour une exhalite typique : remontée de fluides hydrothermaux formant un panache dans l'eau de mer, et précipitation et déposition de sulfures à partir du panache. (B) Mise en place des sulfures par remplacement : les fluides hydrothermaux remontant dans une zone large se propagent le long des horizons laminés avec les sulfures précipitant au sein de la stratigraphie existante.

Fig. 5.4. Photographies d'horizons stratifiés riches en sulfures. (A) Intervalles finement laminés à très finement laminés contenant du tuf et de l'argillite. Les pyrites sont présentes dans les veines et les amas entre et dans les lits. (B) Intervalles de tuf à lamines fines et épaisses montrant des déformations synvolcaniques. Les pyrites concordantes à grain fin sont associées à des laminations. (C) Un exemple d'intervalle tuffacé qui forme les segments plus épais entre les lits et lamines plus riches en sulfures. (D) Un exemple de fragments laminés dans des sédiments chaotiques et perturbés. (E) Une image composite d'horizon minéralisé dans le trou HEB-04 montrant une progression vers le haut de tuf grossier à plus fin et finalement des intervalles laminés qui ont une forte concentration en pyrite.

Fig 5.5. (A) Pyrite concordante à grain fin. (B) Pyrite grossière associée à une veine. (C) Un grain de pyrite riche en inclusions de sulfures et de silicates. (D) Cristal de pyrite

idiomorphe avec peu d'inclusions. Sa forme et l'absence d'inclusions laissent penser que c'est le résultat d'une recristallisation métamorphique. Les dépressions dans la surface de la lame sont le résultat de l'ablation laser et sont entourés en rouge.

Fig 5.6. Les trois groupes d'éléments en traces dans les pyrites sont définis selon leur position au sein du grain de pyrite qui est vu par comparaison du spectre de l'élément avec celui du fer, en coups par seconde (CPS). (A) Éléments sélectionnés du Groupe 1, qui se trouvent toujours dans une inclusion au sein de la pyrite. (B) Le Ni est toujours au sein de la structure cristalline. (C) Éléments sélectionnés du Goupe 2 qui peuvent se situer soit dans les inclusions, soit dans la structure cristalline.

Fig. 5.7. Variations géochimiques dans les pyrites provenant d'analyses LA-ICP-MS dans les horizons stratifiés riches en sulfures, en fonction des différents forages; A) le cuivre, (B) le zinc, (C) l`or et (D) l`argent.

Fig. 5.8. Variations géochimiques dans les pyrites, provenant des horizons laminés riches en sulfures A et A' identifiés sur la fig. 5.1, basées sur les analyses LA-ICP-MS, en fonction des différents forages; (A) le cuivre, (B) le zinc, (C) l`argent et (D) l`or. Aucune pyrite de l'horizon A dans le forage HEB-08 ne contenait d'or détectable.

Fig. 6.1. Histoire géologique de la zone d'étude, avec une emphase sur la partie supérieure de la Formation d'Hébécourt, illustrée par des sections schématiques (pas à l'échelle). La remontée hydrothermale au sein des unités volcaniques a probablement été plus ou moins continue pendant la période montrée. (A) Déposition de la sous-unité pauvre en Ti de la rhyolite principale. Les triangles représentent les faciès fragmentaires et les tirets orientés de manière aléatoire représentent les faciès massifs. (B) Éruption de la sous-unité riche en Ti de la rhyolite principale, par deux évents séparés. Les altérations et minéralisations de la Zone A et de la Zone B sont aussi illustrées. Les épaisses lignes oranges représentent les horizons stratifiés contenant des sulfures (certains horizons peuvent être plus continus que montré ici). (C) Éruption de l'intercalation la plus jeune d'andésite basaltique d'Hébécourt. Les triangles pleins représentent les hyaloclastites et la

taille des coussins diminue à l'Ouest. (D) Éruption de la rhyolite supérieure provenant de l'évent le plus à l'Est, étant donné que le centre effusif à l'Ouest est inconnu.

1. Introduction

Volcanogenic massive sulphide (VMS) deposits typically form as polymetallic sulphide lenses at or near the seafloor in submarine volcanic successions (Franklin et al., 2005; Galley et al., 2007). Worldwide, VMS deposits are major sources of Zn, Cu, Pb, Ag, and Au, and significant sources for Co, Sn, Se, Mn, Cd, In, Bi, Te, Ga, and Ge. Some also contain significant amounts of As, Sb, and Hg (Galley et al., 2007). Historically, VMS deposits have accounted for 27% of the copper and 49% of the zinc production in Canada (Galley et al., 2007) and they remain important producers of these metals as well as some precious metals today. For example, the LaRonde Penna VMS deposit, 50 km east of Rouyn-Noranda in the Abitibi region, is the largest gold deposit currently mined in Canada (Mercier-Langevin et al., 2007a).

1.1 Traditional exploration criteria and methods for VMS deposits

Traditional exploration for VMS deposits has involved certain key criteria, such as the presence of volcanic rocks, evidence for extension indicated by tholeiitic to transitional bimodal volcanic successions and times of major ocean closing or terrane accretion (e.g. Late Archean (2.8-2.69 Ga), Paleoproterozoic (1.92-1.87 Ga), Cambro-Ordovician (500-450 Ma), Devono-Mississippian (370-340 Ma), and Early Jurassic (200-180 Ma)) (Galley et al., 2007). VMS deposits are also associated with large mafic to composite, Na-rich syn-volcanic intrusions, and where these are present, a deposit may be in the 3000 m up section of the intrusions. In addition, rhyolites with high Zr (>300 ppm), negative chondrite-normalized Eu anomalies, $(La/Yb)_N$ values of less than 7, $(Gd/Yb)_N$ values of less than 2, and Y/Zr ratios of less than 7 define high-temperature (>900°C) felsic volcanic environments favourable for VMS formation (Galley et al., 2007). VMS mineralization has also been seen in rhyolites with F1 through to F4 geochemsitry (Hart et al., 2004).

Geophysical surveys are also a common tool in VMS exploration. Magnetic surveys can be used to look for magnetic halos around synvolcanic intrusions which act as a heat source, to look for laterally extensive iron formations which mark hydrothermally active horizons, or to directly detect sulphide bodies containing enough magnetite if they are not

too deeply seated (Galley et al., 2007). Airborne and ground electromagnetic surveys can allow direct detection of VMS deposits when conductive sulphides, such as pyrrhotite and chalcopyrite, are abundant, within a few hundred metres from the surface and physically connected (Moon et al., 2006).

For deeper or zinc-rich mineralization though, indirect techniques are needed, and these typically involve non-geophysical vectors, such as zonation from sericite to Fe rich-chlorite or quartz-rich alteration assemblages, which mark an increase in proximity to a hydrothermal system in most systems (Large et al., 2001). Sodium depletion zones in the footwall can extend over wider zones than the chlorite-sericite alteration, and may be associated with iron and magnesium enrichment zones (Large et al., 2001). Other useful criteria indicative of potential mineralization are syn-volcanic faults and volcanic centres, located through the use of physical volcanology and facies interpretation. Both volcanic centres and syn-volcanic faults are commonly associated with each other and with hydrothermal systems (Franklin et al., 2005; Galley et al., 2007). These methods require extensive sampling and analysis and for physical volcanology and to locate syn-volcanic faults, good outcrop and extensive exposure are generally preferred.

"Exhalite" is a common term applied to horizons such as the iron formations mentioned above and other more sulphide-rich hydrothermal sediments. These horizons can grade laterally into VMS deposits and have been used successfully for exploration within mining camps, such as the Noranda camp (Knuckey et al., 1982; Kalogeropoulos and Scott, 1989) and the Bathurst mining camp (Peter et al., 2003a; 2003b). However, outside of established mining camps, exhalites may be more discontinuous, or the continuity may not be known because correlation is impossible if the stratigraphy is not established.

1.2 The problem: VMS exploration outside of mining camps

In general, exploration is hindered outside of mining camps because the stratigraphy is not well known, there is a lack of marker horizons or they are undocumented, and there are fewer historical drill holes to provide information. In some cases, there is also a lack of outcrop. In many districts, no one technique is possible due to the lack of exposure

inhibiting observations and sampling, and the limited amount of previous work does not provide a large database of legacy data to be compared with and expand new findings. It is often necessary to use a combination of imperfect techniques to gain a full understanding of the region.

1.3 Aims and methods

The aim of this project was to develop an improved approach to mapping prospective areas in Archean or younger volcanic sequences, within or outside of existing mining camps, by combining field-based and high-precision analytical techniques.

To do this, it was decided to combine (1) physical volcanology with (2) chemostratigraphy to establish the location of effusive centers in the volcanic units, and combine (3) pyrite geochemistry in sulphide-bearing stratified horizons with (4) whole-rock geochemistry in the surrounding volcanic units to identify hydrothermal up-flow zones. The combination of all four of these techniques is a new process for VMS exploration.

The combination of chemostratigraphy and physical volcanology is essential when working with drill core, limited outcrop and highly deformed sequences. Physical volcanology alone is not able to determine a stratigraphy with such limited information, it is necessary to rely on the geochemical character of units to determine the stratigraphy. In addition, any interpretation of facies variations observed is meaningless unless they are interpreted within a single stratigraphic unit.

Laser ablation induced coupled plasma mass spectrometry (LA-ICP-MS) is useful for determining the trace metal contents of single pyrite grains as the technique has a very high resolution. The trace metal contents of pyrites from several horizons can establish lateral peaks in trace element contents, which is interpreted as an indication of where hydrothermal up-flow was active. When combined with assay data, any correlation between them will help indicate where the hydrothermal system was most active and where a VMS deposit is most likely to have been formed.

This combination of four techniques can establish whether or not there exists a spatial link between volcanic and hydrothermal centers. When this is the case, it can provide new exploration targets where there is a known volcanic center and hydrothermal activity but as yet undiscovered potential mineralization.

The studied area is part of the Blake River Group of the Abitibi Subprovince. The Noranda mining camp, north of Rouyn-Noranda within the Blake River Group, had over 20 VMS deposits discovered over an 85 year period (Gibson and Galley, 2007). The Noranda area has been used to develop the genetic model of the Noranda-type VMS deposits (Morton and Franklin, 1987), and also used to establish classic facies variations of submarine volcanic rocks (e.g., Dimroth et al., 1978). Yet outside the Noranda camp, some areas of the Blake River Group have seen less intense exploration but still hold good VMS potential.

The study area in the northern part of the Blake River Group, some 45 km NW of Rouyn-Noranda, was selected because although the Hébécourt Formation forms a lava plain regionally and it does not host known VMS deposits, in the study area it contains an unusually large accumulation of felsic rocks that are associated with some Zn-Cu mineralization and hydrothermal alteration zones, as well as sulphide-bearing stratified horizons of variable lateral extent, indicating a potential for economic mineralization.

1.4 Structure of the memoir

Chapter 2 will present the geological information that was necessary to complete this project, including a summary of the regional geology of the Superior Province, the Abitibi Subprovince and the Blake River Group. In addition to regional geology, more specific geological information is presented, related to VMS deposits and to the submarine emplacement of felsic and mafic lavas, and the facies variations generated by such emplacement.

Chapter 3 will present a chemo-stratigraphic framework for the volcanic rocks of the study area in Québec, and this framework will be applied to the rocks in the study area in

Ontario which, as will be shown, have a different eruptive history to those in Québec. The volcanic facies present within each unit will be documented and the lateral and vertical variations between the facies will be interpreted using the models presented in Chapter 2, with the objective of locating the volcanic vent area for each unit.

Chapter 4 will discuss the alteration and mineralization in the study area. Specifically, the alteration will be described using three techniques: alteration box plots to quantify the intensity of the alteration, thematic maps of alteration indices to locate the most altered zones spatially, and hand sample and thin section observations to confirm the mineralogy of the alteration. Mineralization will be described based on statutory files since the available diamond drill holes did not intersect the main known mineralized area.

Chapter 5 will describe the sulphide-bearing stratified horizons found in the study area and show their position within the stratigraphy. In addition, this chapter will document LA-ICP-MS measurements on pyrites from sulphide-bearing stratified horizons to identify potential high-temperature hydrothermal up-flow zones.

Chapter 6 will discuss the interpretation of the data presented in the preceding chapters, and Chapter 7 will outline the conclusions of the study.

Appendix A and B contain the descriptions of the drill core and the geochemical analysis, respectively. Outcrop descriptions have been incorporated into the SIGEOM system of the Ministére de Ressouces naturelles et de la Faune. Appendix C contains a larger scale map of the study area and appendix D contains the photographs of the sulphide bearing horizons described in chapter 5.

1.5 Previous publications

Before writing this memoir, the author produced three documents in collaboration with several co-authors, i.e. two government reports (published) and one paper for the journal Economic Geology (submitted in April 2010):

1. Rogers, R., Ross, P.-S., Goutier, J., Lafrance, B., and Mercier-Langevin, P., 2010, Étude volcanologique et métallogénique d'un segment de la Formation d'Hébécourt, Sous-province de l'Abitibi : résultats préliminaires: Ministère des Ressources naturelles et de la Faune (Québec), report RP-2010-06, p. 1-18.

2. Rogers, R., Ross, P.-S., Goutier, J. and Mercier-Langevin, P., 2010, Étude volcanologique et géochimique des roches volcaniques mafiques à intermédiaires du Groupe de Blake River entre les lacs McDiarmid et Hébécourt, Sous-province de l'Abitibi: Ministère des Ressources naturelles et de la Faune (Québec), report RP-2010-08, p. 1-11.

3. Rogers, R., Ross, P.-S., Goutier, J., and Mercier-Langevin, P., *submitted*, Using physical volcanology, chemo-stratigraphy and pyrite geochemistry as tools for VMS exploration outside of mining camps in the Blake River Group, Abitibi Subprovince: Economic Geology.

The information presented in these three documents has been entirely integrated into the current traditional-style memoir, which in addition contains numerous extra explanations, details and figures which could not be integrated into the previous publications due to space limitations or because they were developed later.

In the previous publications, the senior author has been responsible for collecting the data presented, including field mapping and whole-rock geochemistry sampling; re-logging diamond drill holes for physical volcanology and alteration; and sampling the cores for whole-rock geochemistry and LA-ICP-MS analysis of sulphides. The first author was also responsible for the interpretation of the data, the integration of the data collected with existing data, and the drafting of the initial figures and text for each of the publications. The second author translated the two government reports into French, from English versions finalized by the first author, and also did the proof-reading of these two reports.

All co-authors provided comments and suggestions on various drafts of each publication as is customary.

2. Geological and metallogenic context

This chapter will outline the geological knowledge necessary for this project to have been developed. The study area is located in the southern part of the Abitibi Subprovince, which is part of the Superior Province. The Abitibi Subprovince contains numerous volcanogenic massive sulphide (VMS) deposits, and the study area in the Blake River Group is considered prospective for this type of mineralization. Knowledge of these subjects was necessary to reach the objectives laid down in the beginning of the project. As the rocks of the study area were emplaced in a volcanic-dominated geological environment, a good understanding of submarine volcanology is essential. This chapter will also explain the nomenclature used in the following chapters.

2.1 Regional geology

2.1.1 Superior Province

The Superior Province (Fig. 2.1) consists of metamorphic rocks of Archean age and forms the core of a large Precambrian craton, the Canadian Shield. It consists of a series of terranes dominated by either granitoids and greenstones (oceanic terranes), granites and gneissic rocks (continental terranes), or metasedimentary rocks, which were assembled between 2.72 and 2.68 Ga (Percival, 2007). The region is believed to have been tectonically stable since 2.66 Ga, with the exception of some rifting at the margins and some large-scale rotation at 1.9 Ga (Percival, 2007). The Superior Province is considered to have formed allochthonously from a series of continental and oceanic terranes, with metasedimentary terranes separating some of the oceanic and continental terranes, which were deposited, deformed and metamorphosed during the process of accretion (Percival, 2007). However a competing view is that many of the greenstone assemblages originated through autochthonous or parautochthonous means, based on the presence of mapped unconformities, geochemical evidence of contamination by continental crust and the presence of assemblages representing the juxtaposition of multiple volcanic environments (Thurston, 2002).

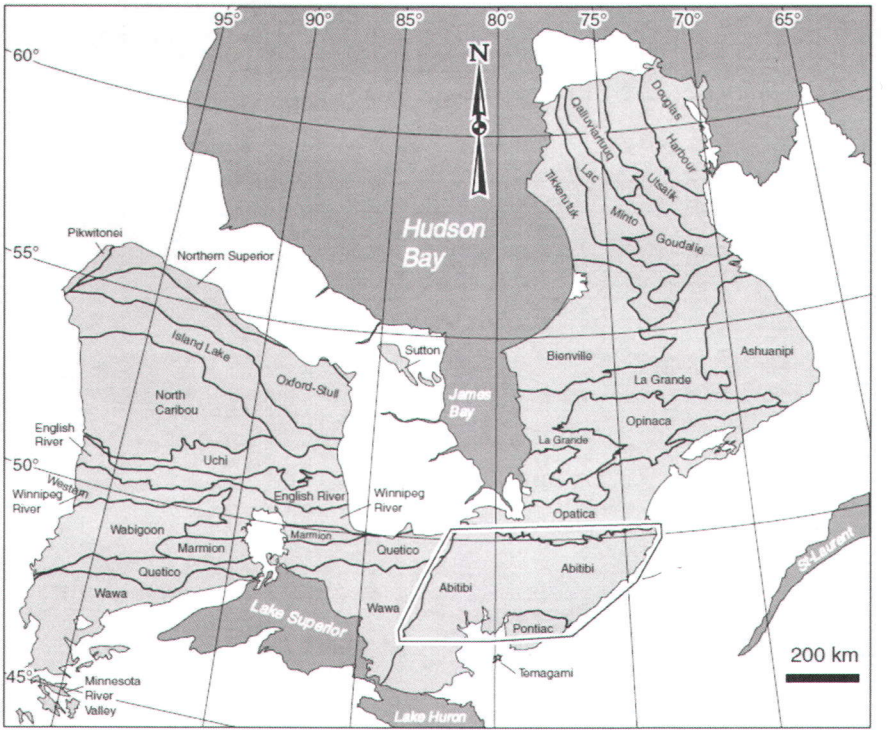

Fig. 2.1: Map showing the Superior Province and the subprovinces within it, with the Abitibi Subprovince highlighted after Thurston et al. (2008).

The terranes form linear subprovinces of distinct lithological and structural character, often with late sub-parallel boundary faults. The trend of these subprovinces is east-west in the southern Superior Province, west-northwest in the northwestern Superior Province and northwest in the northeastern Superior Province (Percival, 2007).

While the oldest of the continental fragments is the Hudson Bay terrane (O`Neil et al., 2008; Maurice et al., 2009) which occurs in the northern Superior, the fragment believed to form the core or nucleus of the continental accretion is the North Caribou Superterrane. This terrane has 3.0 Ga basement of metaplutonic rocks and minor metavolcanic assemblages, with overlying rift and arc metavolcanics and then further re-worked by continental arc magmatism at 2.75 to 2.70 Ga (Corfu et al., 1998; Percival, 2007).

The oceanic terranes, which separate most of the continental terranes, are formed of granitoids and greenstones. These belts generally have long strike lengths and include ocean floor, plateaus and island arc/back arc metavolcanics (Percival, 2007). The greenstone belts in the Superior Province can be divided into two type assemblages. The older type represents the products of arc- and plume-related processes, whereas the younger type has been compared to pull-apart basins (Thurston, 2002).

For brevity, in the rest of the memoir, the prefix "meta" is omitted since for the regions of interest, the metamorphism is low-grade and the protoliths are easily recognizable.

2.1.2 Abitibi Subprovince

The Archean Abitibi Subprovince is a granite-greenstone terrane that covers an area of 700 km by 300 km in Ontario and Québec (Goodwin, 1982; Fig. 2.2), has an age of ~2.7 Ga and is the world's largest (Laflèche et al., 1992). It is bounded to the north by the Quetico (Opatica in Québec) gneissic belt, grades into the sedimentary Bellecombe (Pontiac in Québec) gneiss sequence in the south and is bounded to east and west by younger tectonic structures, called the Grenville Front and the Kapuskasing Structural Zone, respectively (Fig. 2.2) (Dimroth et al., 1982).

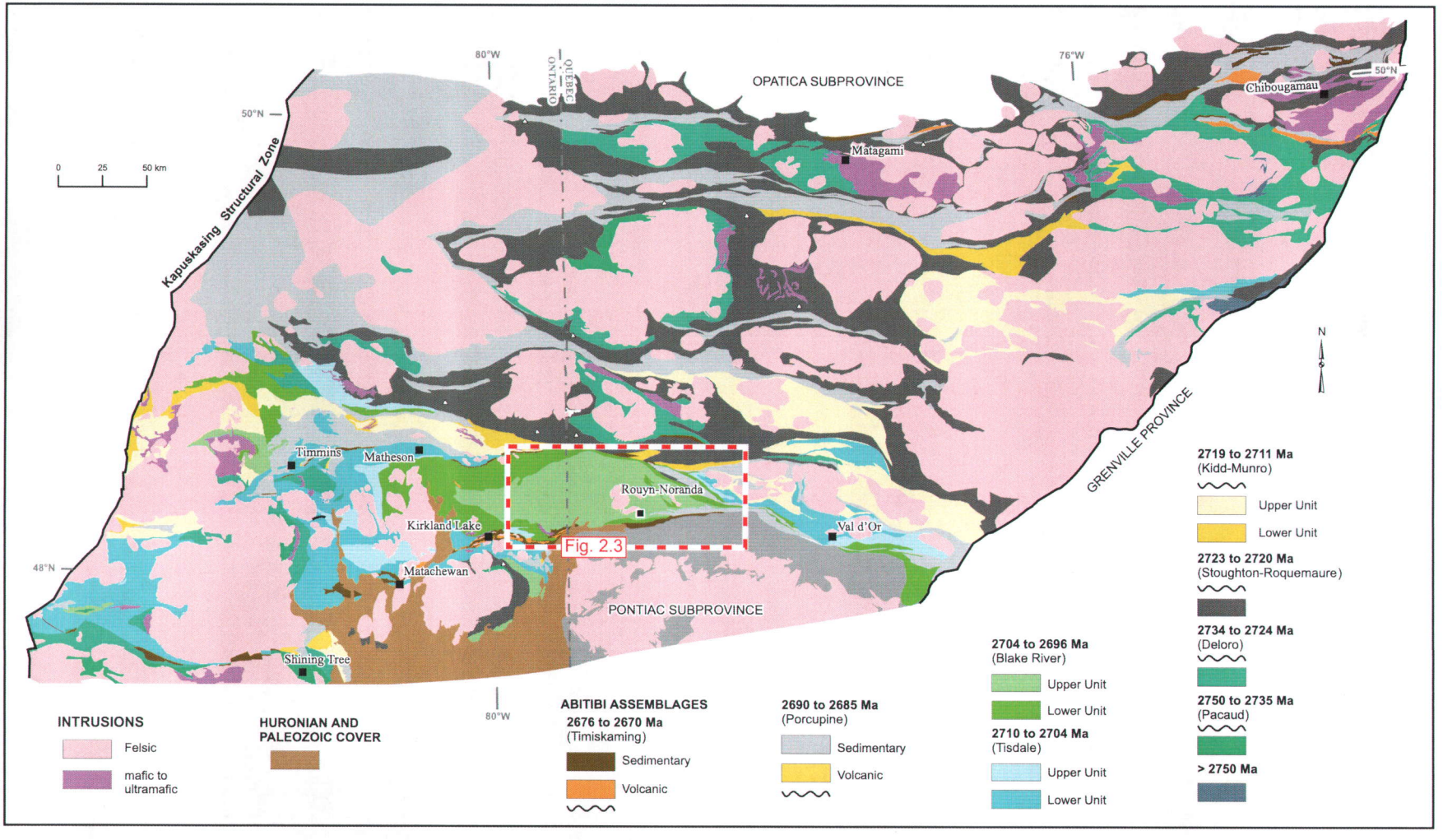

Fig. 2.2 A map of the Abitibi Subprovince showing the Ontario assemblages applied to both provinces, after Thurston et al. (2008).

The metamorphic history of the Abitibi Subprovince is complex, consisting of several metamorphic events affecting the Superior Province basement prior to the eruption of the lavas, creating high grade facies within the basement, which were overprinted by regional prehnite-pumpellyite facies and greenschist and amphibolite facies after the eruption of the voluminous basalts (Jolly, 1978; Powell et al., 1995).

The northern region of the Abitibi Subprovince is characterized by subaqueous basalt, central volcanic complexes and linear sedimentary basins (Chown et al., 1992). Different volcano-sedimentary cycles are distinguished within the northern area, characterized by the development of an extensive subaqueous basalt plain, followed by the evolution of felsic volcanic centers and sedimentary sequences formed by subsequent uplift and erosion of these volcanic centers (Chown et al., 1992).

Ayer et al. (2002) divided the southern Abitibi Subprovince of Ontario into nine distinct lithological assemblages; Pacaud, Deloro, Stoughton-Roquemaure, Kidd Munro, Tisdale, Kinojevis, Blake River, Porcupine and Timiskaming, from oldest to youngest. The two youngest assemblages are mostly sedimentary (with some alkaline volcanic rocks in the latter) and are deposited unconformably on the older volcanic-dominated assemblages. The volcanic assemblages show intercalations of tholeiitic, komatiitic and calc-alkaline volcanic rocks, suggesting a range of different mantle sources and geodynamic environments (Ayer et al., 2002). The Kinojevis Assemblage was subsequently renamed "Lower Blake River Assemblage" by Ayer et al. (2005) to avoid confusion with the older Kinojévis Group in Québec, with the former Blake River Assemblage becoming the "Upper Blake River Assemblage". The Blake River Group of Québec corresponds to the two Blake River assemblages of Ayer et al. (2005).

The northern and southern volcanic areas of the Québec side were previously believed to have evolved separately (and then to have been assembled by a tectonic collision (Daigneault et al. 2002; Mueller et al., 1996), with the northern zone mostly older than the southern zone, but recent geochronology and mapping shows a more complicated

story, and suggests autochthonous construction of the whole Abitibi Subprovince (Ayer et al., 2002; Thurston et al., 2008).

2.1.3 Blake River Group

The Blake River Group (BRG) (Fig. 2.3) is the youngest subalkaline volcanic succession in the southern Abitibi Subprovince (Thurston et al., 2008). The BRG is dominated by submarine mafic to intermediate lavas with subsidiary felsic volcanic rocks and mafic to intermediate volcaniclastic rocks (Dimroth et al., 1982; Gélinas et al., 1984; Péloquin et al., 1990; Laflèche et al., 1992; Goutier et al., 2007; Ross et al., 2007, 2008a, 2008b, submitted-a, submitted-b; Mercier-Langevin et al., 2008). The volcanic rocks of the BRG are intruded by felsic to intermediate syn-volcanic and syntectonic plutons (Piercey et al., 2008, and references therein), as well as a series of gabbroic to dioritic dikes and sills (Pearson and Daigneault, 2009).

The base of the Lower Blake River Assemblage in Ontario is marked by an abrupt change to transitional volcanic rocks from the underlying tholeiitic volcanic rocks (Ayer et al., 2002). On most sides, the BRG is bounded by important regional faults such as the Porcupine-Destor Fault and the Cadillac-Larder Lake Fault, so undisturbed contacts with older or younger units are rare. Younger sedimentary packages such as the Kewagama Group or the Cadillac Group are tectonically juxtaposed against the BRG. The ambient metamorphism in the BRG is prehnite-pumpellyite grade to greenschist grade, but with metamorphic aureoles around late intrusions (Gélinas et al., 1984).

The BRG has been interpreted as a caldera cluster by Pearson and Daigneault (2009), and Mueller at al. (2009) whereas Ross et al. (2007, submitted a and b) and other workers ho see the BRG as a series of overlapping volcanoes built on a mafic lava plain (e.g. Dimroth et al., 1982), with no evidence for subsidence except in the Noranda cauldron (Gibson and Watkinson, 1990).

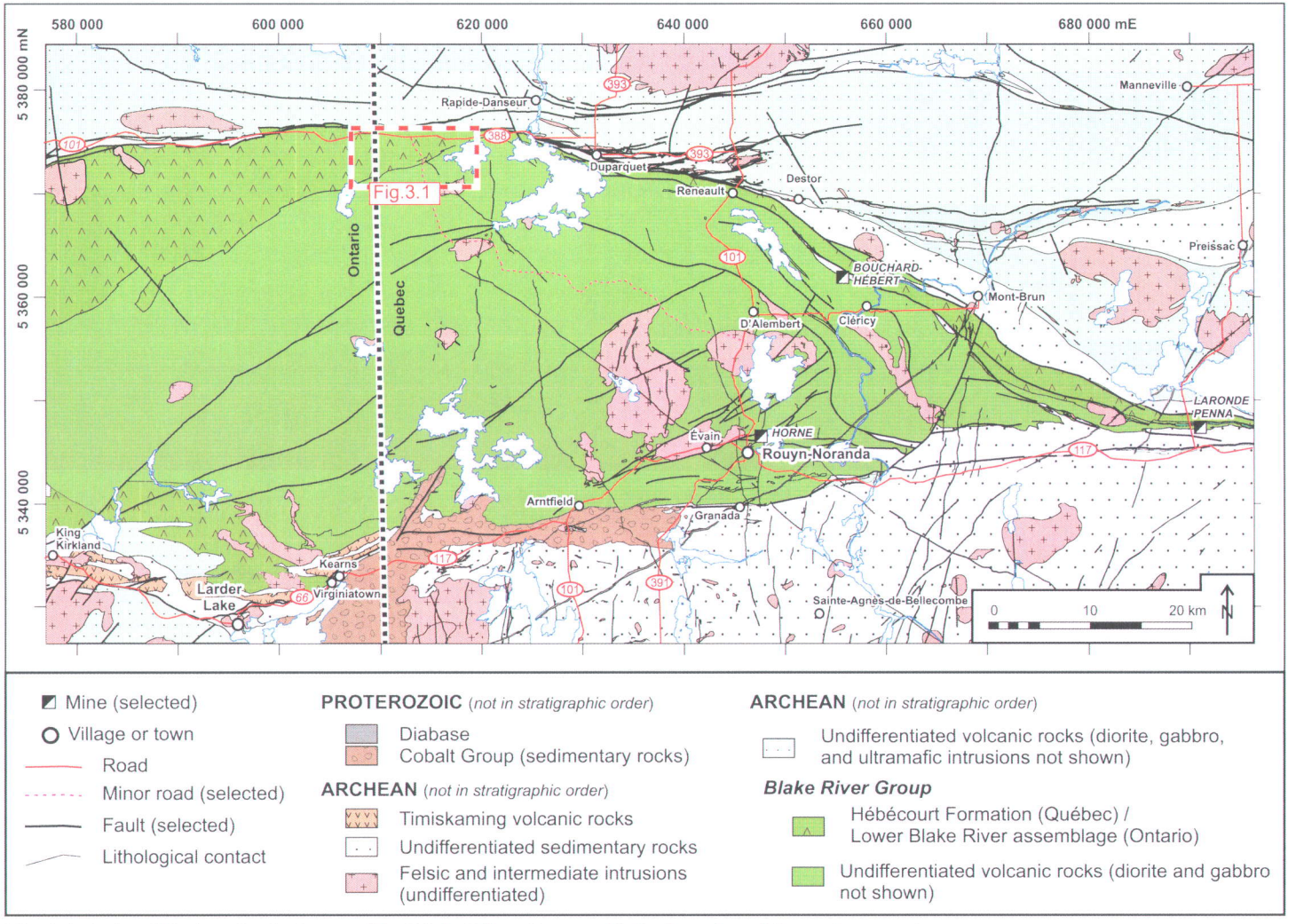

Fig. 2.3: A simplified geological map of the Blake River Group with the location of the study area given.

A number of workers have proposed stratigraphic divisions in the BRG, including Goodwin (1982), Gélinas et al. (1984), Péloquin et al. (1990), Couture and Goutier (1996), Goutier (1997), and Goutier et al. (2007, 2009). Most of these divisions are based on a combination of mapping and geochemistry of the volcanic rocks. McNicoll et al. (submitted) presents the secular evolution of the BRG volcanism along with the metallogenic periods favourable for VMS mineralization. In Québec, a gap in volcanic deposition has been identified at about 2699.3 Ma based on precise U-Pb geochronology: volcanic rocks older than this belong to the lower BRG, whereas younger rocks are part of the upper BRG. Note that whether or not these "lower" and "upper" divisions of the BRG in Québec are equivalent or not to the "lower" and "upper" Blake River assemblages in Ontario has not been established.

The BRG is well known for mineral deposits, particularly of the VMS type. A number of the Cu-Zn VMS deposits of the BRG are located within the Noranda mining camp, which contains 22 known deposits north of Rouyn-Noranda (Gibson and Watkinson, 1990), including the world-class Horne deposit which was mined from 1927 to 1976 and produced 53.7 Mt of ore at grades of 6.1 g/t Au, 2.2% Cu and 13.0 g/t Ag (Kerr and Gibson, 1993; Gibson et al., 2001).

Many of the deposits in the Noranda camp are associated with the "mine sequence" (Gibson and Watkinson, 1990), or Noranda Formation, which belongs to the upper BRG (Goutier et al., 2009; McNicoll et al., submitted). The gold-rich VMS deposits of the Doyon-Bousquet-LaRonde mining camp, further east, are also hosted by upper BRG volcanic rocks, belonging to the Bousquet Formation (Lafrance et al., 2003; Mercier-Langevin et al., 2007a; 2007b; 2008). The Doyon-Bousquet-LaRonde mining camp includes the LaRonde Penna deposit, formed of stacked massive to semi-massive sulphide lenses, which contains reserves and geologic resources of 46.5 million tons (Mt) of ore or more than 250 t of Au, at an average grade of 4.3 g/t Au, 0.3% Cu and 2.2% Zn (Mercier-Langevin et al., 2010a).

However, the lower BRG stratigraphy is now considered highly prospective as well, as both the Horne and Quemont gold-rich VMS deposits have recently been shown to sit in rocks of this age range, using precise U-Pb geochronology (Goutier et al., 2009; McNicoll et al., submitted). Rocks of the lower BRG in Québec and Ontario cover a vast area and spatially represent a significant part of the group. Improved understanding of the geology and hydrothermalism is therefore needed to vector exploration towards prospective sectors in the lower BRG (Fig. 2.3).

The study area (Fig. 3.1) is located in the lower BRG in Québec and Ontario. Two formations are present in the study area: the Hébécourt Formation, overwhelmingly of tholeiitic magmatic affinity, and the younger Reneault-Dufresnoy Formation, of variable magmatic affinity (Goutier, 1997; Ross et al., submitted a). Regionally, the Hébécourt Formation is dominated by basaltic lavas (e.g., Lafrance et al., 2003; Legault et al., 2005), whereas the Reneault-Dufresnoy ranges in composition from basalt to rhyolite (e.g., Laflèche et al., 1992; Lafrance and Dion, 2004).

2.2 VMS deposits and exhalites

The Abitibi Subprovince and the Blake River Group in particular are well endowed in VMS deposits, and the area under study has characteristics that indicate VMS potential, so knowledge of this deposit type is essential for completion of this project.

VMS deposits are also known as volcanic-associated, volcanic-hosted and volcano-sedimentary-hosted massive sulphide deposits (Galley et al., 2007). The mineralization typically occurs as a conformable component and a discordant component. The conformable part of the deposits consists of lenses or mounds of polymetallic sulphides that are generated at or near the seafloor in spatial, temporal and genetic association with contemporaneous volcanism (Barrie and Hannington, 1999; Franklin et al., 2005; Galley et al., 2007). Stringer-type mineralization is located in the footwall strata, and is commonly called the stringer or stockwork zone in the model presented by Franklin et al. (2005) after Lydon (1984, 1988), Galley (1993) and Franklin (1995).

This general model (Fig. 2.4) has six characteristics: 1) a heat source to drive hydrothermal systems and potentially contribute metals; 2) a high temperature reaction zone that acts as a reservoir from which metals are leached from volcanic and/or sedimentary rocks by interaction with evolved seawater (this zone includes an impermeable barrier, cap rock, or aquacludes that restricts and insulates the hydrothermal system); 3) syn-volcanic faults or fissures that permit focused discharge of hydrothermal fluids from the reservoir; 4) footwall and less commonly hanging wall alteration zones produced by high temperature fluid-rock interaction involving mixtures of ascending hydrothermal fluid and locally heated ambient seawater; 5) the massive sulphide deposit itself formed at or near the seafloor; and 6) distal products which represent a hydrothermal contribution to background sedimentation, such as exhalites (see below). VMS deposits have been classified into two types based on the dominant host rock, volcaniclastic rocks or lava flows (Morton and Franklin, 1987; Galley et al., 2007).

2.2.1 Alteration pipes

In lava flow-hosted type deposits there are vertically extensive alteration pipes that narrow with depth (Morton and Franklin, 1987; Gibson et al., 1999). They are localised around the structure controlling hydrothermal discharge, usually a synvolcanic fault (Gibson et al., 1999). The pipes are well defined by chlorite ± quartz inner zones surrounded by a less well defined zone of sericite-quartz, and the top of the pipes are often the width of the VMS deposit (Morton and Franklin, 1987; Gibson et al., 1999). In volcaniclastic-hosted type deposits, the alteration pipes are commonly poorly defined and wider than the massive sulphide deposit (Gibson et al., 1999; Gifkins et al, 2005). This is believed to be due to the more permeable nature of the host rocks (Gibson et al., 1999).

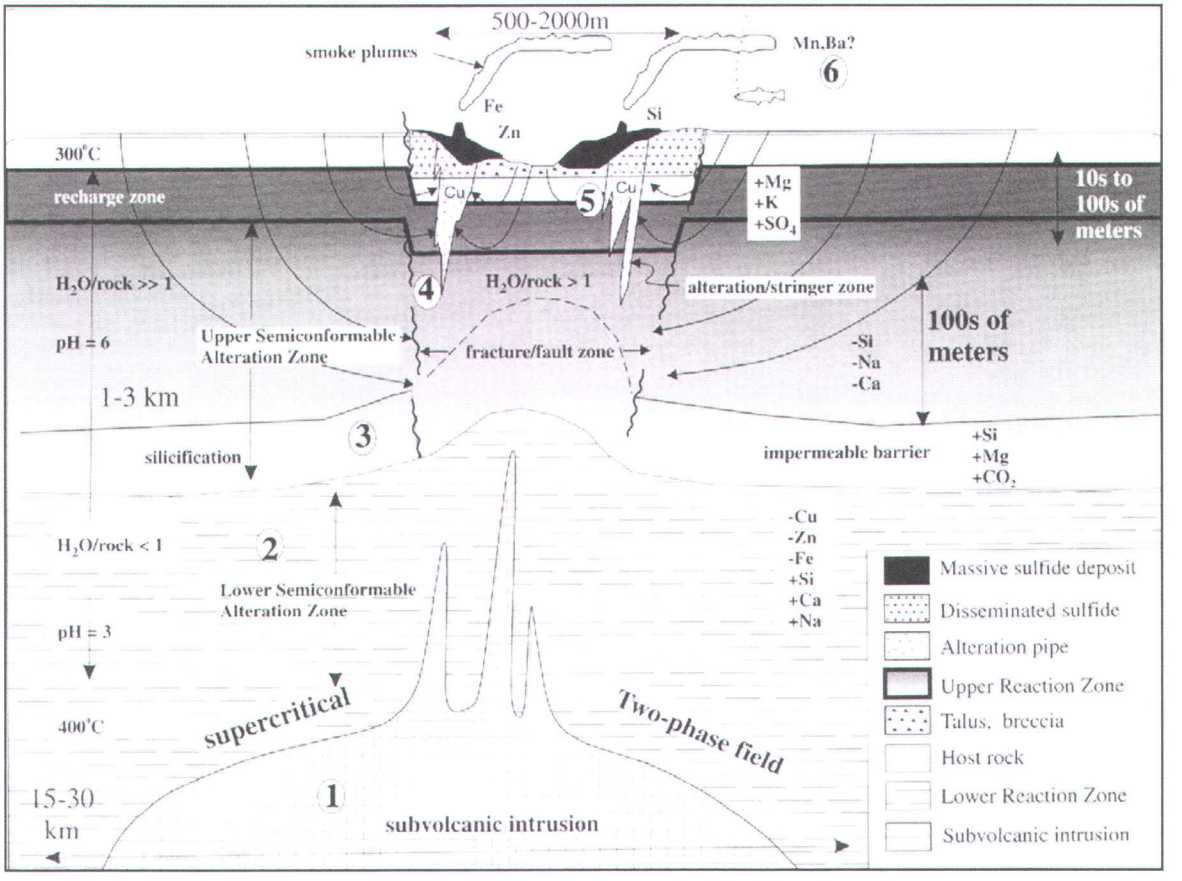

Fig. 2.4. A model of the formation of VMS deposits, showing the general characteristics of the hydrothermal system. After Franklin et al. (2005).

2.2.2 Semi-conformable alteration zones

Semi-conformable alteration zones have strike lengths of up to several kilometres and thicknesses up to 1 km (Galley, 1993). The alteration is generally irregularly distributed, preferentially along zones of high permeability such as flow-top breccias and hyaloclastite. These zones are of similar size in both types of VMS deposit, but stratigraphic height varies; they are higher in predominantly volcaniclastic-hosted deposits (Morton and Franklin, 1987).

2.2.3 Exhalites

Exhalites are defined as a class of chemical sediment of predominantly volcanic origin (Ridler, 1971). The presence of exhalites in a submarine volcanic succession is a first-order indicator that a hydrothermal system was active during a hiatus in volcanism. Exhalites are often thin but laterally extensive; they are formed of terrigenous or tuffaceous particles and an exhalative component (Franklin et al., 2005), for example pyrite or chert. Hydrothermal discharge on the seafloor can be extensive, diffuse, low-temperature and unfocused, or high temperature discharge from a small area; it may be synchronous, preceding or post-VMS formation (Franklin et al., 2005). The chemical component may be from the fallout of ferromanganese particles, silts and clays from the hydrothermal plumes (Franklin et al., 2005). Particles of pyrite up to 25 μm in diameter can be deposited up to 5 km from a hydrothermal vent and, in modern oceanic environments, distance from vent decreases with increased particle diameter (Feely et al., 1987).

In the Noranda camp (Knuckey et al., 1982; Kalogeropoulos and Scott, 1989) and elsewhere in the Abitibi Subprovince and around the world (e.g., Liaghat and MacLean, 1992; Spry et al., 2000), exhalites have been used for mineral exploration, since many VMS deposits occur at the intersection of a synvolcanic fault and an exhalite (Franklin et al., 2005), or at least along the stratigraphic level marked by an exhalite (Peter and Goodfellow, 1996; Spry et al., 2000). However, the term "exhalite" is sometimes overused or misused in VMS exploration, with laminated sulphide-bearing horizons automatically assumed to represent laterally extensive marker horizons formed by

sulphide precipitation and sedimentation in seawater, following venting of a hydrothermal fluid coming from a source such as a field of black smokers as in the work of Peter et al. (2003a; 2003b) and Chapman et al. (2008). This automatic assumption is not always valid, as will be discussed below.

2.3 Volcanic emplacement mechanisms

In this section, the typical variations in submarine volcanic facies for mafic and felsic lavas and domes are presented. Such lavas and domes make up the bulk of the studied volcanic succession.

2.3.1 Felsic lava flows and extrusive domes

The model of McPhie et al. (1993) for subaqueous lava flows and subaqueous extrusive domes (Figs. 2.5a and 2.5b) suggests that the internal facies variation for these two types of effusive products are relatively similar, with extrusive domes having a more limited lateral extent and more evidence of remnant feeder dikes. A typical subaqueous felsic flow or dome consists of a coherent (massive) core, which may or may not display flow banding. The core is formed by a number of coherent lobes (Yamagashi and Dimroth, 1985) which are injected into one another and into the surrounding fragmental material. This core is overlain and surrounded by in situ hyaloclastite, and subsequent mass-flow of the hyaloclastite due to oversteepening of the dome may lead to stratified re-sedimented hyaloclastite (McPhie et al., 1993; Fig. 2.5a). In situ hyaloclastite in felsic flows and domes is characterized by angular, monomictic clasts that have a jig-saw fit aspect but can vary in size from less than 1 mm to 10s of centimetres. Re-sedimented hyaloclastite consists of a deposit that shows some evidence of transport; stratification, rounding of clasts or a mixture of clasts with different textures. When felsic lavas are compared to domes, the effusive point should be more centered on the eruptive products for domes than for flows. Polygenetic dome complexes may consist of alternating intervals of coherent lava and hyaloclastite representing many resurgences of activity (McPhie et al., 1993).

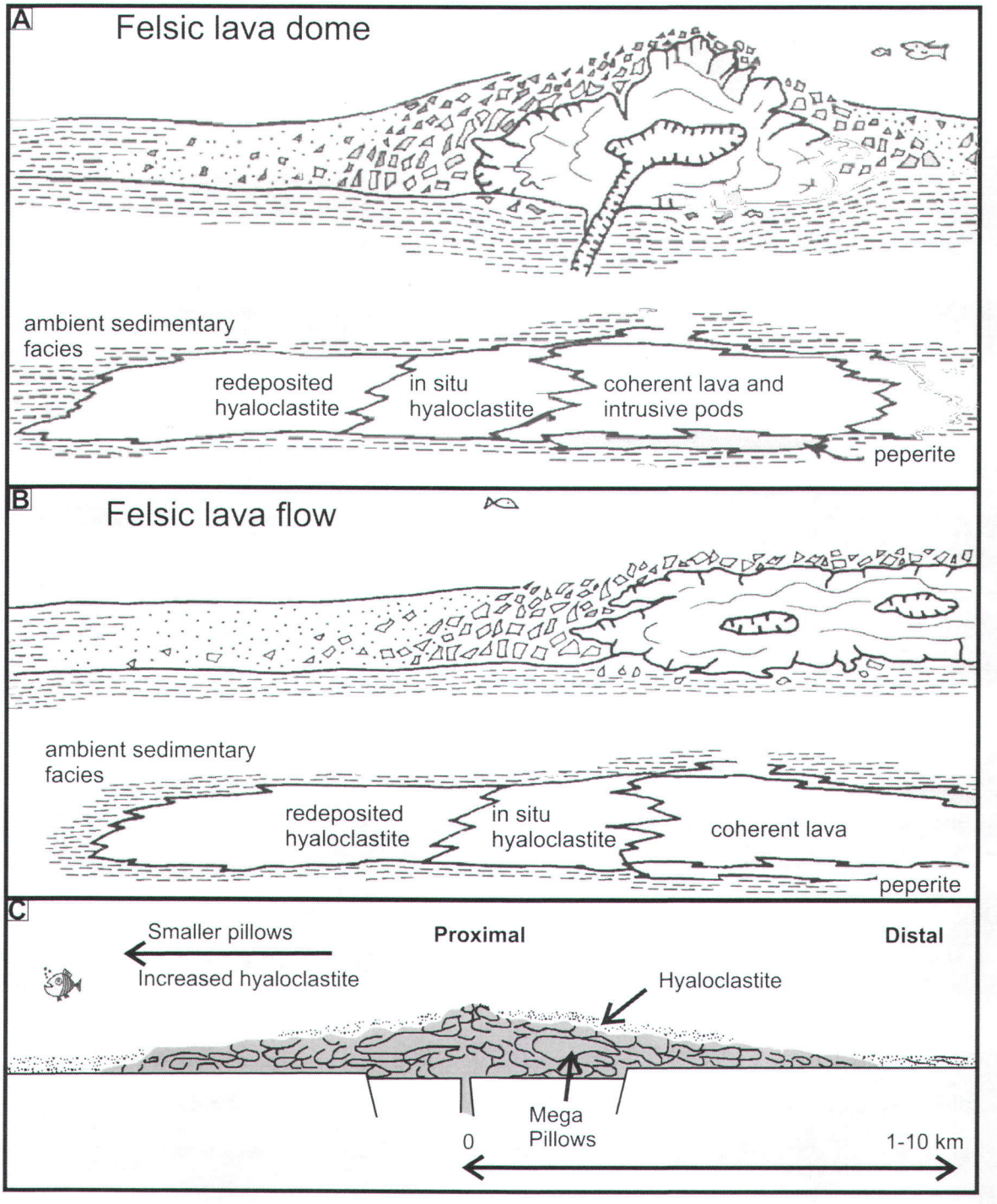

Fig. 2.5. Diagrams showing typical facies variation in submarine lavas and domes. A) Fully extrusive submarine felsic lava dome, after McPhie et al. (1993). B) Felsic lava flow, after McPhie et al. (1993). C) Pillow volcano, after Gibson et al. (1999).

2.3.2 Mafic to intermediate lava flows

Pillowed flows are the most easily recognized, especially in weakly deformed areas, and commonly observed form of sub-aqueous basaltic and andesitic volcanism, believed to be the result of sustained eruptions with low effusion rates (Gibson et al., 1999). Pillowed flows are compound flows with each individual pillow representing a small scale flow unit that cools independently (McPhie et al., 1993; Gibson et al., 1999).

Gibson et al. (1999) divide pillowed flows into two facies; the pillow facies and the pillow breccia facies. The pillow facies consists of densely packed pillows separated by thin regions of in situ hyaloclastite (inter-pillow material). The pillow breccia facies occurs at the top of the stack or at the terminus of the flow and consists of intact pillows, incipiently brecciated pillows, in situ brecciated pillows or blocky angular fragments of pillows in a matrix of in situ hyaloclastite. The hyaloclastite consists of angular, monomictic glassy fragments formed by quench brecciation in seawater. The proportion and size of intact pillows decreases upwards and distally within the breccia (McPhie et al., 1993; Gibson et al., 1999).

Although massive units can occur within the pillow stacks new pillows are often seen budding form them, suggesting that the massive regions are mega-pillows rather than truly massive (Gibson et al., 1999). However there are also true submarine massive lavas (Gregg and Fink, 1995; Chadwick et al., 1999), which may grade laterally into a pillow facies, or directly into hyaloclastite (Dimroth et al., 1978). The massive lavas are typically formed from moderate to high flow rates, moderate to high slopes and moderate to low cooling rates and from lineated sheets or jumbled sheets as the other (Gregg and Fink, 1995).

The idealized variation in facies for massive to pillowed lavas would have massive flows and large pillows as the proximal facies, with pillow size decreasing and proportion of pillow breccia and hyaloclastite increasing distally (Fig. 2.5c; Dimroth et al., 1978; 1982; McPhie et al., 1993; Gibson et al., 1999).

2.4 Nomenclature

In the following chapters, nomenclature of all volcaniclastic rocks follows the system proposed by White and Houghton (2006) and references therein. In this nomenclature system, modified from Fisher (1961) for grain sizes, the term "volcanic breccia" is restricted to volcaniclastic rocks containing more than 75% blocks, which are angular particles larger than 64 mm across. Therefore, many of the volcaniclastic rocks which are part of felsic lava domes or flows are in fact lapilli-tuffs and tuff-breccias, rather than true "breccias". In a similar way, the "flow-top breccias" at the top of some subaqueously emplaced mafic lavas are not true "breccias" in terms of grain size. Hyaloclastite is defined as a primary volcaniclastic rock forming during effusive volcanism when extruding magma or flowing lava is chilled and fragmented from contact with water and fragments are deposited under the influence of the continued lava emplacement (White and Houghton, 2006). This includes pillow breccia and is not restricted to small, angular, jigsaw-fit glass fragments. In this document, the latter is referred to as "typical hyaloclastite". The term "coherent" as applied to volcanic rocks in this memoir should be taken to mean unfragmented. In terms of grain size for coherent rocks, very fine grained or aphanitic means grains invisible to the naked eye, fine grained is <1 mm, medium grained is 1-5 mm and coarse grained is >5 mm. The term microphenocryst is used informally to refer to phenocrysts that are less than 500 μm. Stratification thickness in volcaniclastic and sedimentary rocks (e.g., "thinly laminated") is after Ingram (1954).

For Archean volcanic rocks having experienced metamorphism and hydrothermal alteration, magmatic affinities cannot be consistently determined using major elements. Therefore, ratios of immobile trace elements such as Zr/Y, La/Yb or Th/Yb are used to assign magmatic affinities (Barrett and MacLean, 1999; Ross and Bédard, 2009). 'Transitional' is employed to describe rocks which plot between tholeiitic and calc-alkaline fields.

3. Volcanology and geochemistry of the study area

3.1 Introduction

In the study area, stratigraphic younging is to the south and the beds dip steeply to the south in a homoclinal sequence (Figs. 3.1, 3.2 and 3.3). The Hébécourt Formation in the area from diamond drill hole (DDH) HEB-04 eastward – where the most information is available from outcrops and drill holes – consists of four well defined tholeiitic chemo-stratigraphic (informal) units, two felsic and two mafic (Fig. 3.1). The oldest unit is the Hébécourt basalt, which is intercalated with the Hébécourt basaltic andesite, and is also seen within the younger felsic rocks. The oldest felsic unit is the main rhyolite, which is further divided into two sub-units, the low-Ti rhyolite and the high-Ti rhyolite. A thick intercalation of the basaltic andesite overlies the main rhyolite, and is in turn overlain by the upper rhyolite (Fig. 3.2). There are also several intercalations of calc-alkaline rhyodacite and basalt in the easternmost DDH in Québec.

From DDH HEB-04 to the Ontario border, the chemo-stratigraphy is not well defined due to lack of outcrops and drill holes, but a new felsic unit, the tholeiitic McDiarmid dacite, becomes important at the top of the Hébécourt Formation (Fig. 3.1).

In the Ontario portion of the study area, the stratigraphy comprises the same chemo-stratigraphic units as in Québec, but not in the same order; nevertheless, the same chemo-stratigraphic names are used informally for clarity (although the Hébécourt and Reneault-Dufresnoy Formations are not recognized stratigraphic units in Ontario). Several intercalations of the upper and high-Ti rhyolites occur, and only one thin instance of the low-Ti rhyolite. The McDiarmid dacite is present, but not at the top of the Hébécourt Formation, since the highest stratigraphic position in this formation is occupied by the Hébécourt basalt (Fig. 3.3). The geology of McDiarmid Township was previously described by Jensen (1978), but he did not have access to the new DDHs in the rhyolite, and used a small number of whole-rock geochemical analyses focused on major elements.

The transitional to calc-alkaline Reneault-Dufresnoy Formation overlies the Hébécourt Formation in both provinces and the base of the Reneault-Dufresnoy Formation represents the best-controlled stratigraphic position since it is marked by a rather abrupt change in magmatic affinity in the volcanic succession.

This chapter will outline the details of these units including facies descriptions, the lateral variations in the facies and the chemical methods of defining these units. Facies descriptions and variations have been documented using a combination of drill core and outcrop observations. Additional information was compiled from historical company drill core logs obtained from the statutory files of the ministère des Ressources naturelles et de la Faune du Québec, especially for the main rhyolite. Petrography was done on 55 thin sections to supplement the field and core observations. Facies variations will be used to interpret emplacement mechanisms for each volcanic unit and also to estimate the location of the vent areas.

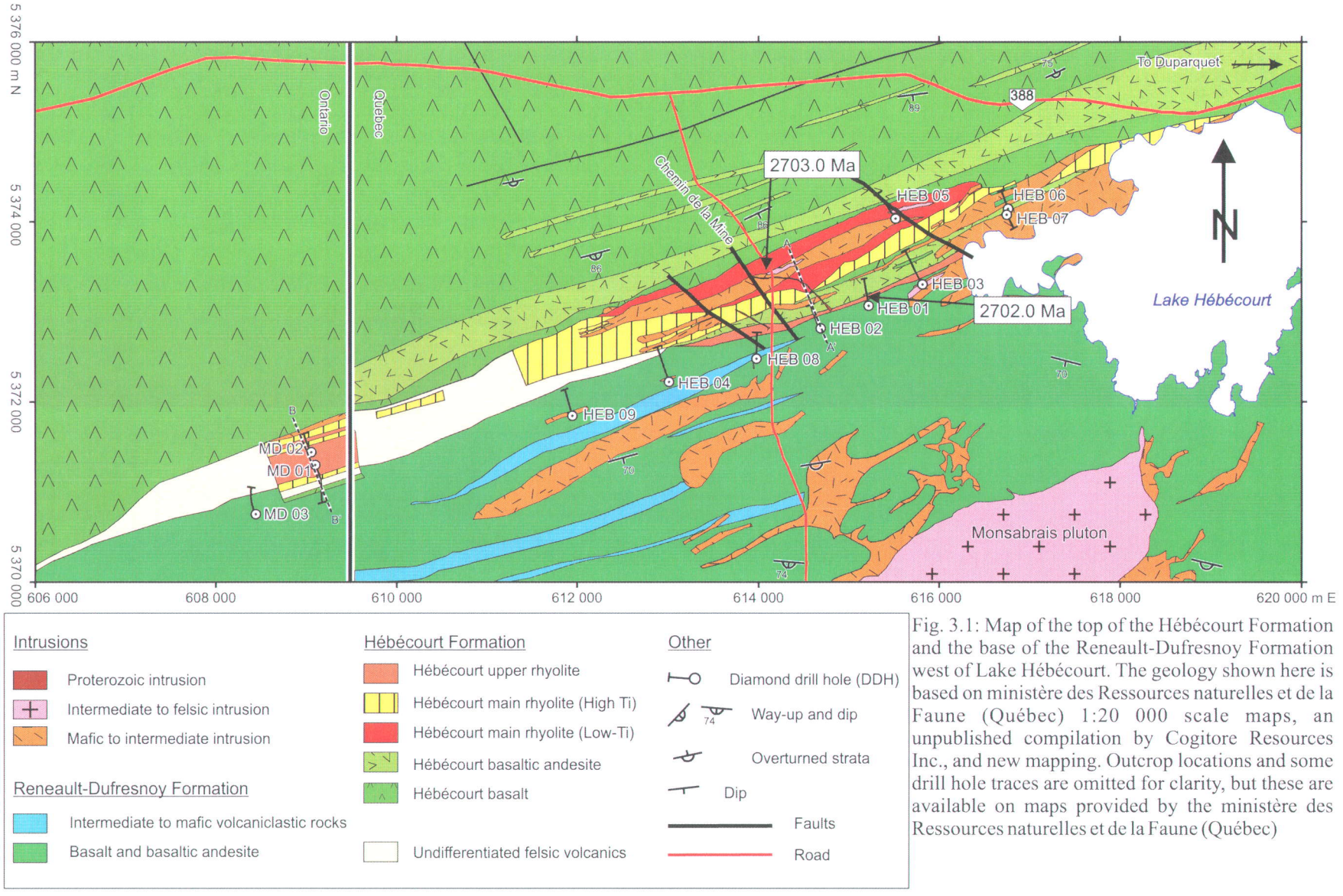

Fig. 3.1: Map of the top of the Hébécourt Formation and the base of the Reneault-Dufresnoy Formation west of Lake Hébécourt. The geology shown here is based on ministère des Ressources naturelles et de la Faune (Québec) 1:20 000 scale maps, an unpublished compilation by Cogitore Resources Inc., and new mapping. Outcrop locations and some drill hole traces are omitted for clarity, but these are available on maps provided by the ministère des Ressources naturelles et de la Faune (Québec)

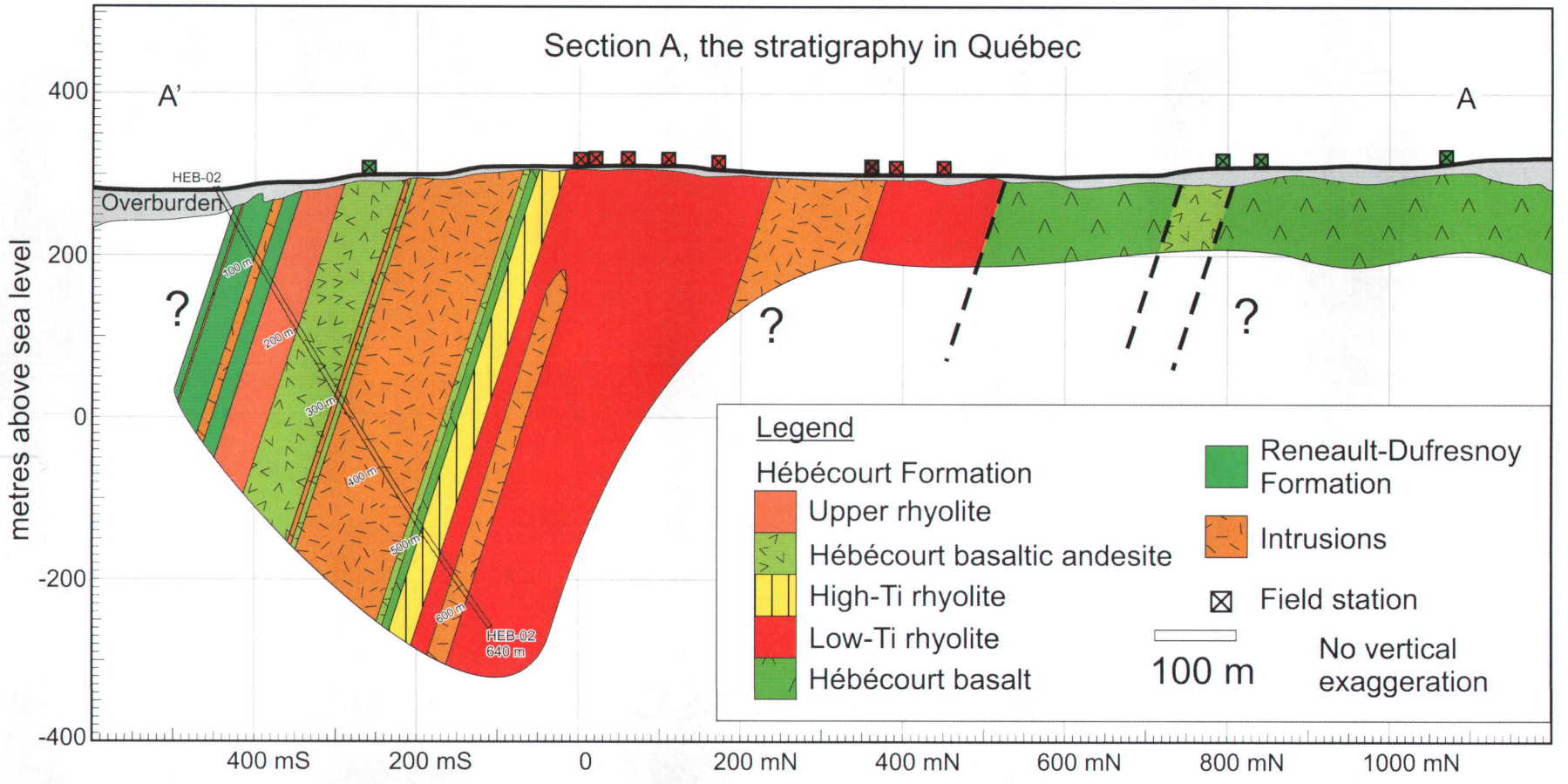

Figure 3.2. A cross-section along the line A-A' on fig. 3.1, looking approximately westward. The section was created using information from DDH HEB-02 and field observations. The section demonstrates the typical stratigraphic order of the units in the region east of DDH HEB-04; Hébécourt basalt at the base, intercalated with basaltic andesite, and overlain by the main rhyolite. The main rhyolite is divided into an older, low-Ti subunit and a younger, high-Ti subunit. The main rhyolite is overlain by a thin unit of the Hébécourt basalt and an intercalation of the basaltic andesite, in turn overlaid by the upper rhyolite. The Reneault-Dufresnoy Formation overlies the Hébécourt Formation. The horizontal axis of the section is the local exploration grid. Note that the section was drawn at the point where the low-Ti sub-unit is thickest; sections drawn elsewhere would show a greater proportion of the high-Ti rhyolite.

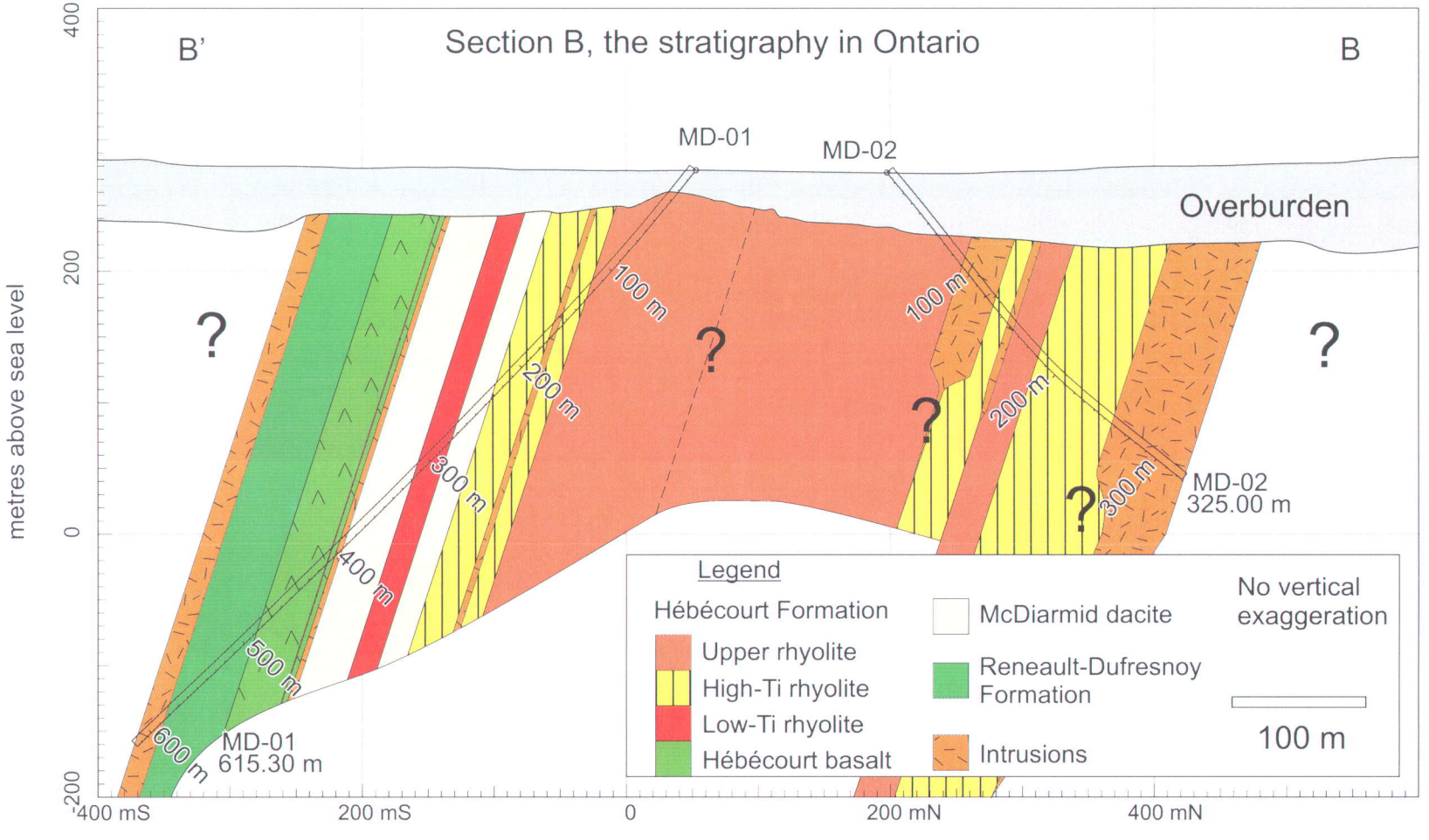

Figure 3.3. A cross-section along the line B-B' on fig. 3.1, looking approximately westward. The section was created using information from DDHs MD-01 and MD-02. The section demonstrates the only known stratigraphic section in Ontario; it is assumed that the high-Ti subunit of the main rhyolite overlies the Hébécourt basalt, but the contact is not seen. The upper rhyolite is intercalated with the high-Ti rhyolite, with the upper rhyolite being thicker. Both are overlain by the McDiarmid dacite which has a thin intercalation of the low-Ti rhyolite. This is then overlain by another intercalation of the Hébécourt basalt, and finally by the Reneault-Dufresnoy Formation. The horizontal axis of the section is the local exploration grid.

3.2 Mafic tholeiitic rocks of the Hébécourt Formation in Québec from DDH HEB-04 eastward

In the field area (Fig. 3.1), mafic to intermediate tholeiitic volcanic rocks of the Hébécourt Formation can be divided in two intercalated aphyric units: (1) the volumetrically dominant Hébécourt basalt, which is typically variole-free, and (2) the variably variolitic Hébécourt basaltic andesite. In addition, glomeroporphyritic mafic lavas are known in the Hébécourt Formation outside of the field area, for example east of Duparquet (Legault et al., 2005; MRNF maps).

3.2.1 Hébécourt basalt

The Hébécourt basalt forms the bulk of the Hébécourt Formation regionally. In general, the Hébécourt basalt is overlain by the Hébécourt main rhyolite in the study area (Fig. 3.1), but thinner occurrences of tholeiitic basalt are also observed in stratigraphically higher positions. For example, in DDH HEB-01 (Fig. 3.1), 36 m of Hébécourt basalt occurs above the main rhyolite, and there it is composed of pillow breccia.

In the field area, the basalts are pillowed to massive with no clear patterns to the facies distribution observed.

3.2.1.1 Pillowed facies. The pillows in the Hébécourt basalt are 60-80 cm across on average, with a very fine-grained texture. Fresh surfaces are medium to dark gray. Quartz amygdales up to 2 mm across make up 0-3% of the rock. Pale-colored varioles, up to 1 cm in size, are very rare and were only seen at one outcrop. The pillows are densely packed with only a small amount of inter-pillow material, typically consisting of angular hyaloclastite shards (former volcanic glass) up to 1 cm across.

In thin sections from the pillow facies, a radial quench texture can be observed (Figs. 3.4a and 3.4b), when not obscured by alteration. In some slides, microphenocrysts are visible (100-200 μm), predominantly of feldspar, but in rare cases olivine phenocrysts are observed. The rock is very fine-grained with the groundmass mostly being irresolvable, although where details can be seen, feldspar is visible.

3.2.1.2 Massive facies. Massive lavas consist of fine-grained to aphanitic basalt that is a medium gray in color on fresh surfaces. These rocks are non-vesicular and display irregularly shaped chlorite spots 2-3 mm across on several outcrops; these could represent former mafic phenocrysts. There are also epidote alteration spots locally. In places, there is up to 3% pyrite blebs, which can be up to 3 mm across.

In thin section, the same quench texture is also visible, but no phenocrysts were observed. The groundmass is predominantly irresolvable, although in some slides 20-30% feldspar, possibly microphenocrysts, are visible.

3.2.1.3 Mode of emplacement. The traditional interpretation of the Hébécourt basalt is that it represents a tholeiitic lava plain, perhaps a submarine flood basalt sequence (Dimroth et al., 1982). An alternative interpretation, apparently not proposed before, is that the Hébécourt basalt consists of overlapping low shields ("scutulums"), i.e. the submarine equivalent of the subaerial scutulums such as those found in the Quaternary Snake River Plain in Idaho, USA (Greeley, 1982). The slopes of such broad volcanic edifices can be as low as 0.5° (Greeley, 1982), so distinguishing between these and a flood basalt sequence is difficult for the Hébécourt basalt.

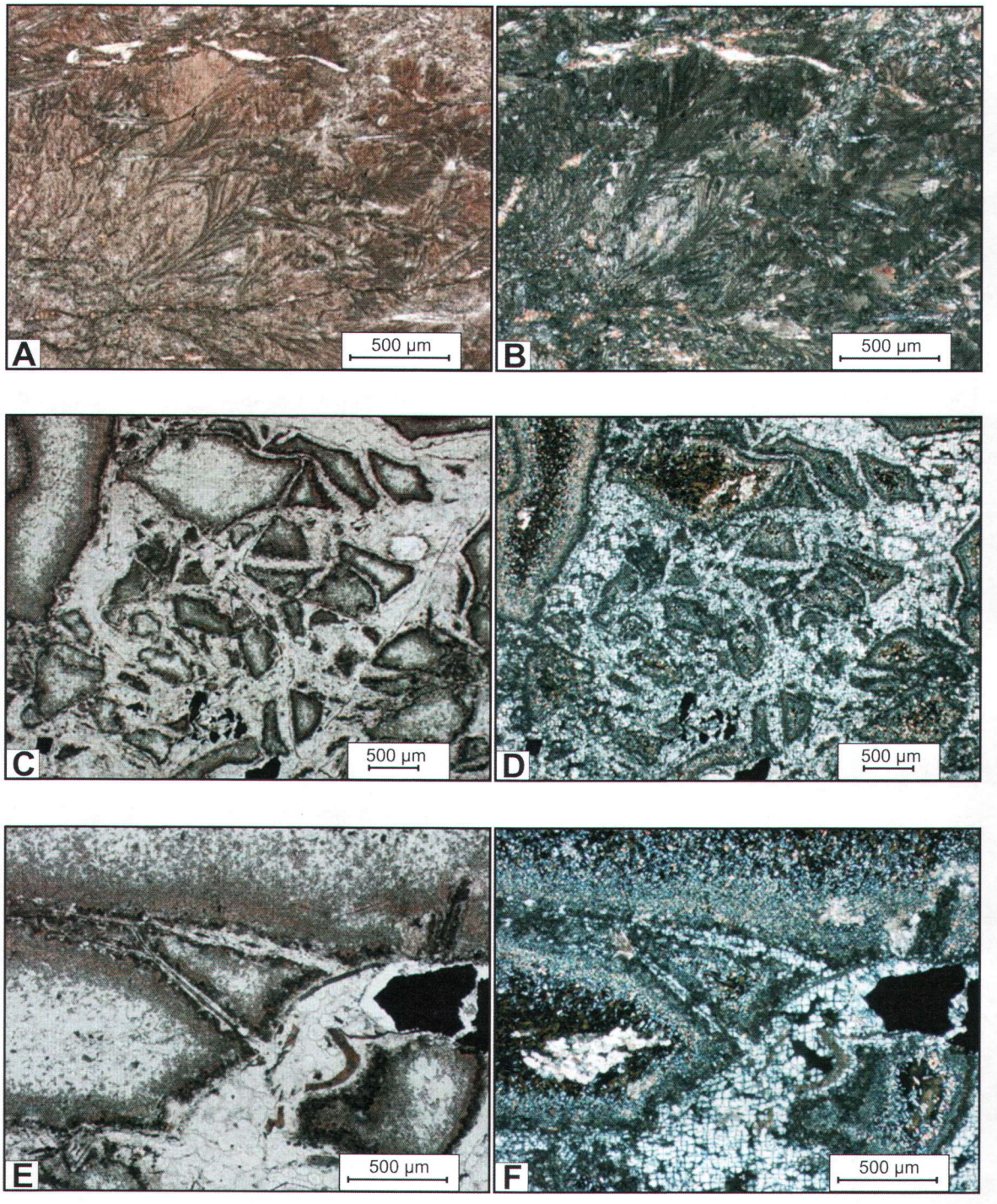

Fig. 3.4. Photomicrographs from sections of the mafic units of the Hébécourt Formation. PPL=Plane Polarised Light, CPL=Cross Polarised Light. A) The quench texture from the Hébécourt basalt in PPL. B) The same as A but in CPL. C) The in situ characteristics of the fragments in the typical hyaloclastite of the Hébécourt basaltic andesite in PPL. D) The same as C but in CPL. E) The zonation of minerals in fragments from the Hébécourt basaltic andesite in PPL. F) the same as E but in CPL.

3.2.2 Hébécourt basaltic andesite

Variably variolitic basaltic andesite intercalations occur at several levels in the Hébécourt Formation (Figs. 3.1 and 3.2). The best-known occurrence is a 132 m-thick basaltic andesite intercalation found between the main rhyolite and the upper rhyolite (Fig. 3.1), so the following descriptions focus on this particular occurrence. Thin mafic to intermediate dikes and sills, not shown on the map, have inflated the basaltic andesite unit to a total thickness of 210 m.

Volcanic facies observed in the Hébécourt basaltic andesite include massive lava, pillow lava, pillow breccia and hyaloclastite.

3.2.2.1 Massive facies. The massive rocks are fine-grained, aphyric, medium gray to green in fresh surface, with variable abundances (1-2% but up to 20% locally) of quartz, chlorite or calcite amygdales. The latter are typically circular in shape and average 2-3 mm in dimension, although they can be up to 5 mm across. There are also varioles visible in many cases; these are typically circular, 5 mm to 1 cm across, and between 10 and 90% in abundance (Fig. 3.5a). The varioles are often highlighted by the presence of chlorite in the surrounding material (giving it a darker color relative to the varioles) and locally may preserve radial fibers, although this is not typical. These massive regions greatly resemble the pillows in texture (see below) and may only appear to be massive due to the angle of drilling not showing regularly the margins of the pillows. The massive regions, which could therefore represent large pillows, are never longer than 2-3 m in the core (dimension along the core axis) and are often surrounded by or found close to mafic intrusions, which confuses the interpretation.

In thin section, up to 2% vesicles can be seen, filled with quartz and typically 200-300 μm across. The varioles were not visible in any of the sections taken. The groundmass is mostly irresolvable although 60% feldspar can be seen.

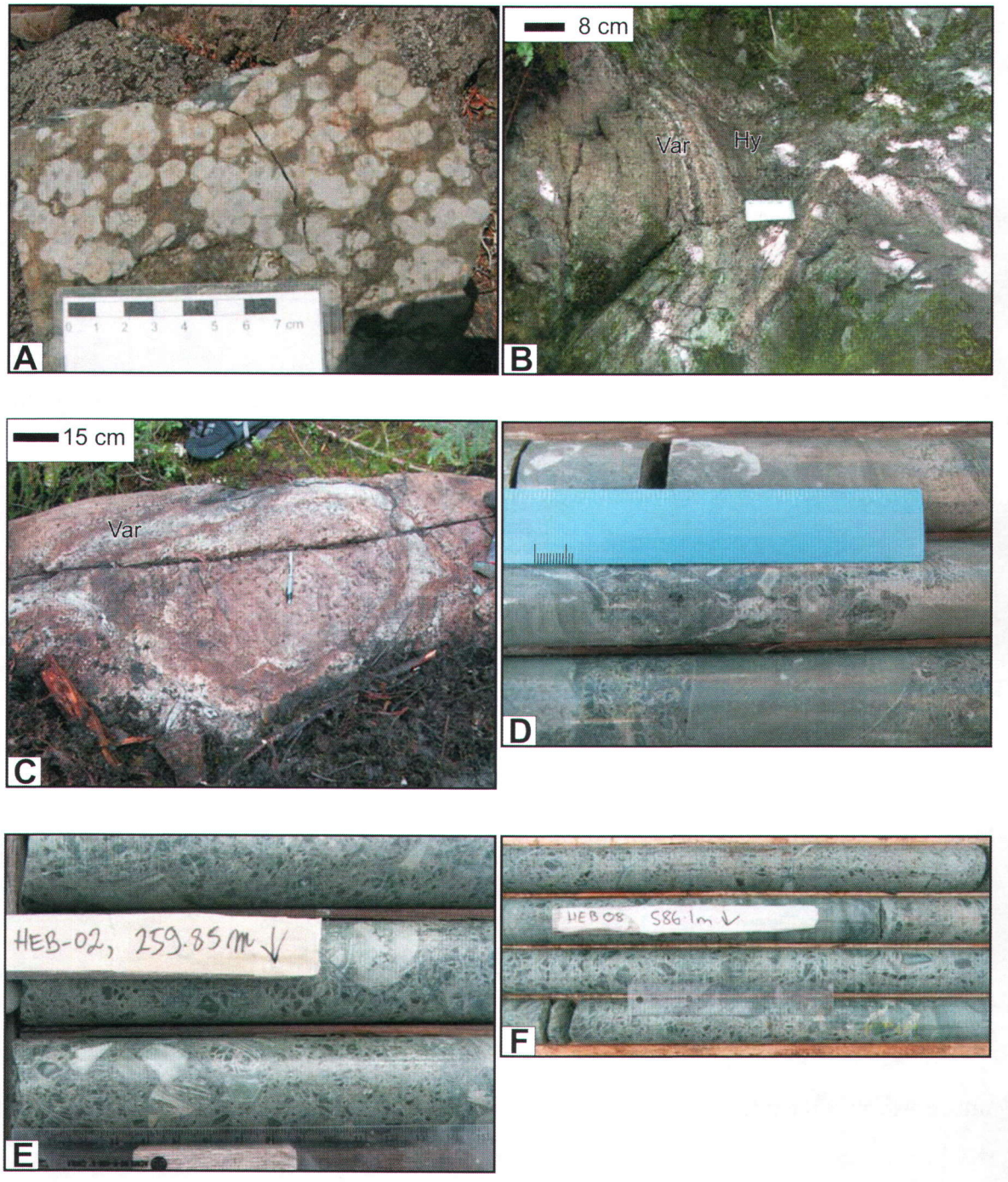

Fig. 3.5: Photographs of the uppermost occurrence of the Hébécourt basaltic andesite. (A) Massive facies displaying a high concentration of varioles. Scale is graduated centimeters. (B) Triple junction in the pillow facies with interstitial hyaloclastite (Hy). Varioles (Var) are abundant in the pillow margins. (C) A complete pillow with an increase in concentration of varioles and vesicles towards the margin. (D) Pillow breccia facies in drill core, comprising in situ fragmented hyaloclastite and larger clasts most likely representing pillow fragments. The ruler is graduated in centimeters and millimeters. (E)-(F) Hyaloclastite facies in drill core, displaying in situ fragmentation and small, chloritized clasts. In both cases the scale is a 15 cm plastic ruler with increments in millimetres.

3.2.2.2 Pillowed facies. The pillow lavas (Figs. 3.5b and 3.5c) young to the SE and represent the majority of the Hébécourt basaltic andesite between the main rhyolite and the upper rhyolite. The pillows are formed of aphyric, fine-grained rock that is medium to dark gray, sometimes greenish, on fresh surface. Vesicles, which generally vary from absent to 1-2%, are typically filled by quartz, calcite or chlorite, and increase in abundance (sometimes up to 5%) towards the pillow margins. The vesicles are typically 1-2 mm in diameter, and in some localities there is an increase in vesicle size in addition to increasing abundance towards the margins, up to 5 mm. The most striking aspect of the pillow margins is the varioles, which make up to 90% of the rock in the pillow margins and can be up to 2 cm in size with a decrease in size toward the centre of the pillow. In some cases, the varioles decrease in abundance toward the pillow centre, while in others the varioles appear to coalesce toward the centre until no individual variole is discernible.

Between the pillows, there is typical hyaloclastite formed of angular clasts with a jigsaw fit texture; the fragments are typically up to 1-2 cm in size. Most of the fragments are completely chloritized and may have sericite rims, but a number are completely epidote-altered. The cement of the hyaloclastite consists of quartz and occasionally sericite. Locally there can be very small varioles, less than 1 mm, visible in the clasts.

In the thin section from the pillows, a quench texture is seen similar to that in the Hébécourt basalt, but it is much less clear, often with only elements of it present. There are 1-2% vesicles visible, 300-400 μm across, predominantly quartz-filled, sometimes associated with opaque minerals. This is a separate species of vesicles to those seen in hand sample. Chlorite is sometimes seen filling the vesicles. The groundmass is very fine-grained, with details difficult to resolve, however in places feldspar microphenocrysts can be seen.

3.2.2.3 Fragmental rocks. The final two facies observed are the pillow-free hyaloclastites (Figs. 3.5e and 3.5f) and the pillow breccias (Fig. 3.5d). In the former, the angular fragments are completely chloritized, with a jigsaw-fit aspect and a quartz cement, very similar to what is seen interstitially in the pillow facies. However, there is often an

increase in the clast size up to 4 cm, a greater abundance of the cement between the fragments and in many cases there is 1-2% disseminated pyrite.

In thin section, the clasts of the hyaloclastite display a clear jigsaw-fit pattern (Figs. 3.4c and 3.4d), showing in situ fragmentation from the contact of lava with seawater. The larger clasts, >500 μm across, have chloritized centres, with a thin rim (<100 μm) of epidote around the margins, and an even thinner band of irresolvable material around that (Figs. 3.4e and 3.4f).

The pillow breccia facies is often gradational upward from the pillow facies. The transition is marked by an increase in the thickness of the hyaloclastite intervals between pillows and a decrease in the size of the pillows until the rock consists of hyaloclastite containing clasts of pillows. Pillow clasts typically range from 5-10 cm in diameter although fragments up to 25 cm across have been seen. These pillow clasts have round to fluidal forms with chilled margins in some cases; locally they contain varioles and/or vesicles which often display a concentration towards the margins. There are also angular clasts, 2-3 cm across, that do not display a jigsaw fit texture and are of the same material as the pillow fragments. The angular fragments also display complete chilled margins but the concentrations of vesicles and varioles are more random, and not located mainly toward the margins of the fragments as in the pillow fragments. In some cases, the matrix of the pillow breccia is sericitised where there is no quartz cement.

3.2.2.4 Thickness and facies variations; mode of emplacement. The following observations are from the youngest intercalation of basaltic andesite only. Field and core observations are considered here (Fig. 3.6), but much more information is available from drill cores, since the entire unit (base to top) can be observed in four separate drill holes. This unit thins from east to west, from 132 m to 56 m, until it eventually pinches out westward beyond DDH HEB-08 (Fig. 3.1). The pillow facies dominates proportionally in each of the drill holes. By averaging the measurements taken through each drill hole, a dramatic decline in pillow size towards the west is seen, from pillows averaging 90-100 cm (DDHs HEB-01, -02 and -03) to an average size of 40 cm in the west (DDH

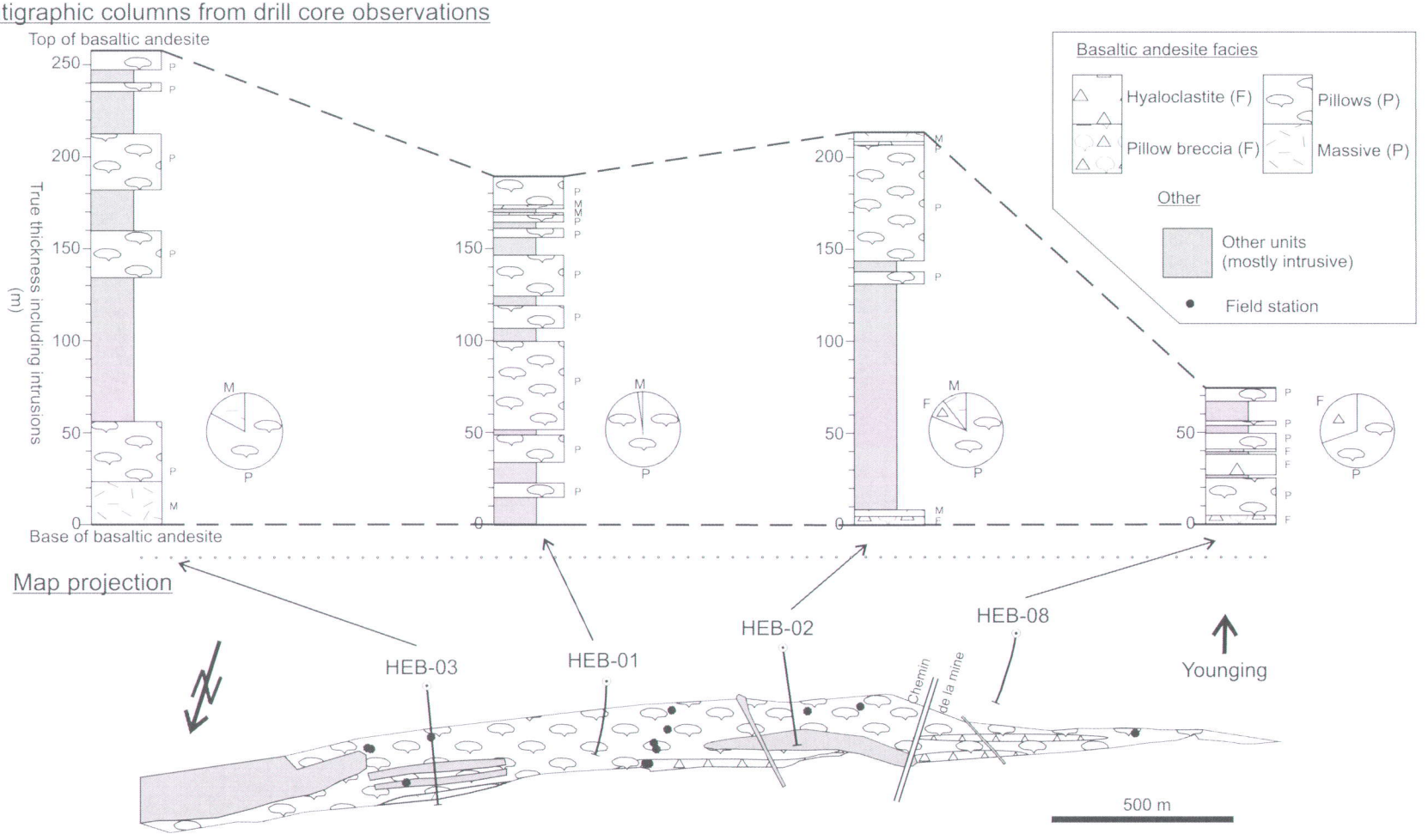

Fig. 3.6: Volcanic facies variations in the uppermost occurrence of the Hébécourt basaltic andesite. Top: Graphic logs of the four DDHs in which this unit is seen. All logs are on the same scale, which represents the true thickness of the units after inflation by intrusions. Thicknesses with intrusions removed are: HEB-03, 127 m; HEB-01, 132 m; HEB-02, 85 m and HEB-08, 56 m. Pie charts summarize the proportion of each volcanic facies within each DDH. Bottom: A map displaying the facies variations, integrating surface observations and drill core observations projected along the inferred 72° S bedding plane. The map has been rotated to show the correct way-up, and does not have the same orientation as figure 3.1.

HEB-08). The volume of fragmental rocks within the unit increases towards the west, from absent in DDH HEB-03 to 30% dispersed through the unit in DDH HEB-08 (Fig. 3.6). The massive facies, by contrast, is absent in DDH HEB-08 and is thickest in DDH HEB-03. These facies variations overall are typical of submarine lavas (see Chapter 2). The basaltic andesite unit consists of several stacked lava flows, which collectively define the facies variations and point to an effusive centre in the eastern part of the unit, near DDH HEB-03.

3.2.3 Geochemistry of the mafic tholeiitic rocks of the Hébécourt Formation

Four geochemical samples were taken from the Hébécourt basalt; three of these are from the upper 770 m of the mafic flows below the Hébécourt main rhyolite and one occurs above the Hébécourt main rhyolite. The four samples are clearly basalts on the SiO_2 vs. Zr/TiO_2 diagram (Fig. 3.7a) and plot as a compact group in the basalt/andesite field on the Zr/TiO_2 vs. Nb/Y diagram (Fig. 3.7b). All samples are tholeiitic, as shown by the Zr vs. Y, La vs. Yb and Th/Yb vs. Zr/Y diagrams (Figs. 3.8a, 3.8b and 3.8c).

The extended multi-element diagrams show flat profiles and small negative Ti anomalies for the basalt (Fig. 3.9a). The first three elements (Th, Nb, and Ta) are slightly depleted relative to the others, as is typical of normal mid-ocean ridge basalts (N-MORB). The N-MORB profile is shown for comparison. However, the samples from the Hébécourt basalt are more enriched in these elements (especially Th) than N-MORB, suggesting these basalts may be from a back-arc environment where the influence of a subduction zone is weakly present, hence the elevated Th (Jenner, 1996).

Twenty samples from the Hébécourt basaltic andesite were analyzed: five from outcrops and fifteen from drill cores. Two of the samples were taken below the Hébécourt main rhyolite and the rest immediately above. All of these samples plot within the lower half of the andesite/basaltic andesite field on the SiO_2 vs. Zr/TiO_2 diagram, although there is some scatter as a result of major element mobility (Fig. 3.7a). On the Zr/TiO_2 vs. Nb/Y diagram, all the samples cluster tightly in the andesite field (Fig. 3.7b). This unit has a tholeiitic affinity shown by the cluster in the tholeiitic field of the La vs. Yb diagram and

the Th/Yb vs. Zr/Y diagram (Figs. 3.8b and 3.8c). Although on the Zr vs. Y diagram (Fig. 3.8a) the samples straddle the tholeiitic-transitional boundary, the tight clustering on the other two graphs in addition to the shape of the extended multi-element plot confirm the tholeiitic affinity. On the extended multi-element diagram (Fig. 3.9b), the tightly grouped samples display very flat profiles with negative Ti anomalies. There is also a depletion of the first three elements like in the Hébécourt basalt, suggesting a common tectonic environment and evolution from the same magma chamber or magma source (Kerrich and Wyman, 1996).

3.3 Felsic tholeiitic rocks in the Hébécourt Formation in Québec from DDH HEB-04 eastward

3.3.1 Hébécourt main rhyolite

The Hébécourt main rhyolite, with a maximum true thickness of 495 m (with the thickness of the intrusions removed), occurs towards the top of the Hébécourt Formation and is invaded by a number of sub-concordant mafic intrusions (Fig. 3.1). The main rhyolite has been shown as a single undivided unit on the maps of the Ministère des Ressources naturelles et de la Faune du Québec, but exploration companies have historically divided it into two subunits using a variety of apparently independent criteria such as the presence or absence of phenocrysts, TiO_2 contents, SiO_2 contents, or the Zr/Y ratio (Fraser, 1991; Cashin and Fraser, 1992; Martin, 1994; Bambic, 1998; Carignan and Lafrance, 2008). In this study, the main rhyolite is again divided into two subunits (Fig. 3.10a) based on their TiO_2 contents that correlate with the presence (or absence) of phenocrysts and the Zr/Y ratios: a low-Ti rhyolite, and a high-Ti rhyolite.

During this study, the main rhyolite was observed at 21 field stations and in four drill holes, allowing the identification of a massive and a fragmental facies in both subunits. Since there is no significant difference in facies characteristics between the low-Ti and the high-Ti subunits, these facies characteristics are described together for the two subunits, except for the petrographic aspects.

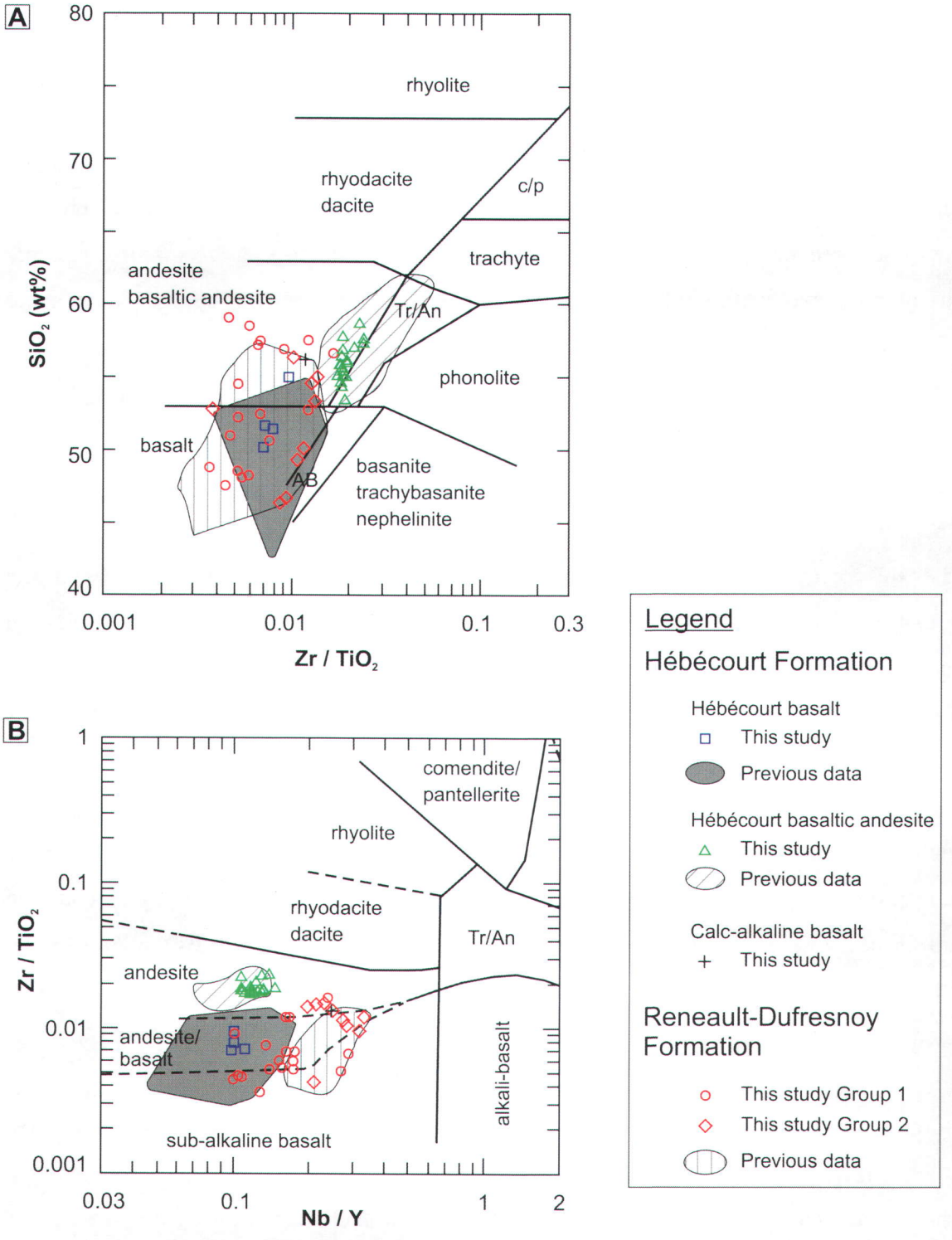

Fig. 3.7: Geochemistry of mafic to intermediate volcanic rocks in the study area. (A)-(B) Classification diagrams from Winchester and Floyd (1977). Analyses illustrated by symbols on all geochemical figures were obtained from Activation Laboratories Ltd. in Ancaster, Ontario using fusion ICP-AES for major elements, and fusion ICP-MS for the trace elements shown. The compiled data plotted as fields here and on figures 3.8, 3.13 and 3.14 was provided by Cogitore Resources Inc., with additional unpublished data from the Geological Survey of Canada (courtesy of E. Grunsky).

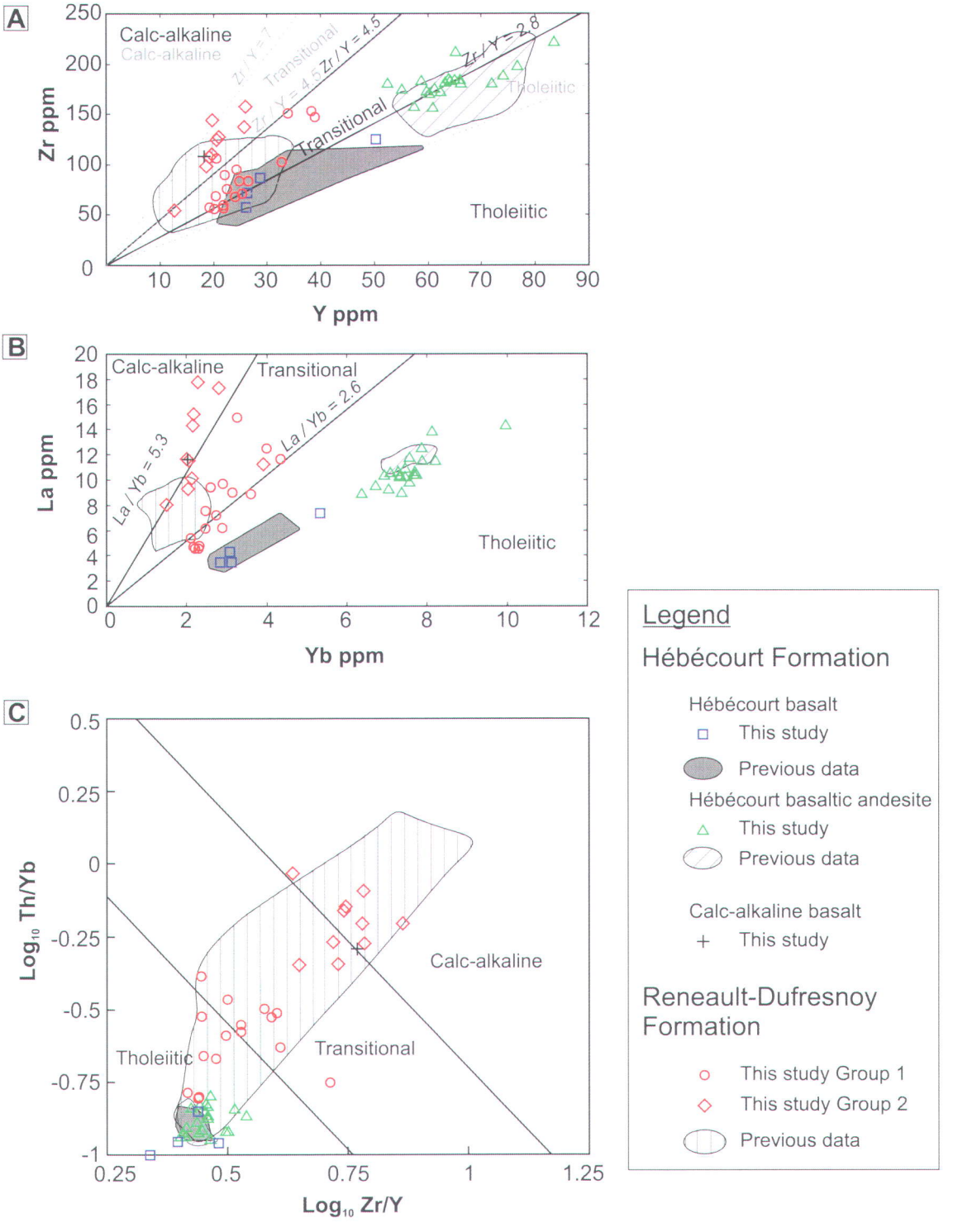

Fig. 3.8: Geochemistry of mafic to intermediate volcanic rocks in the study area. (A)-(C) Magmatic affinity diagrams from Ross and Bédard (2009). (A) Also includes the affinity boundaries from Barrett and MacLean (1999) as grey dashed lines.

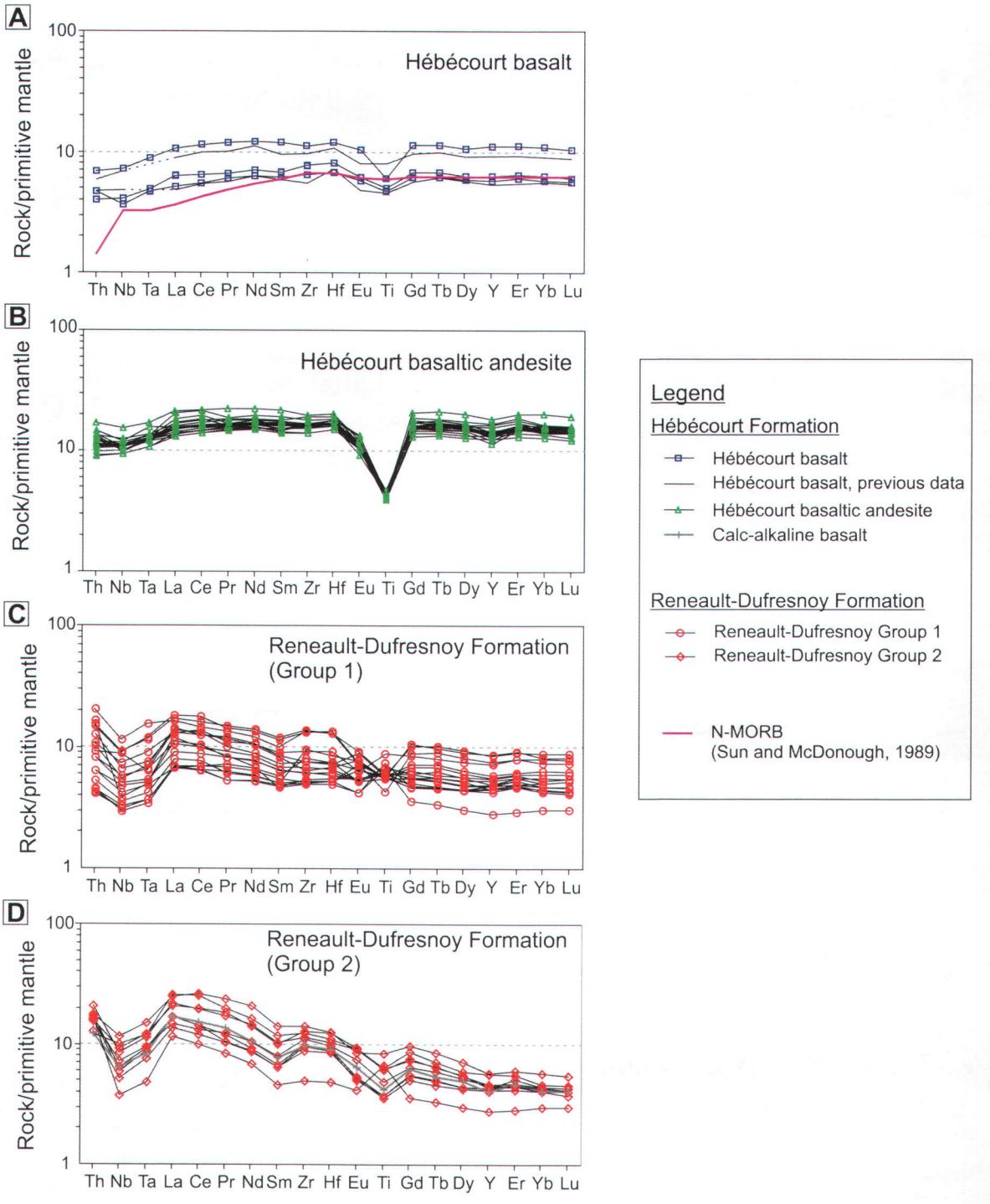

Fig. 3.9: Extended multi-element plots for mafic to intermediate volcanic rocks in the study area: (A) Hébécourt basalt; (B) Hébécourt basaltic andesite; (C) Reneault-Dufresnoy Formation, Group 1; (D) Reneault-Dufresnoy Formation, Group 2, and a calc-alkaline basalt from the Hébécourt Formation. Primitive mantle normalization values and normal MORB composition are from Sun and McDonough (1989). Two unpublished analyses of the Hébécourt basalt (no Ta determined) were supplied by E. Grunsky.

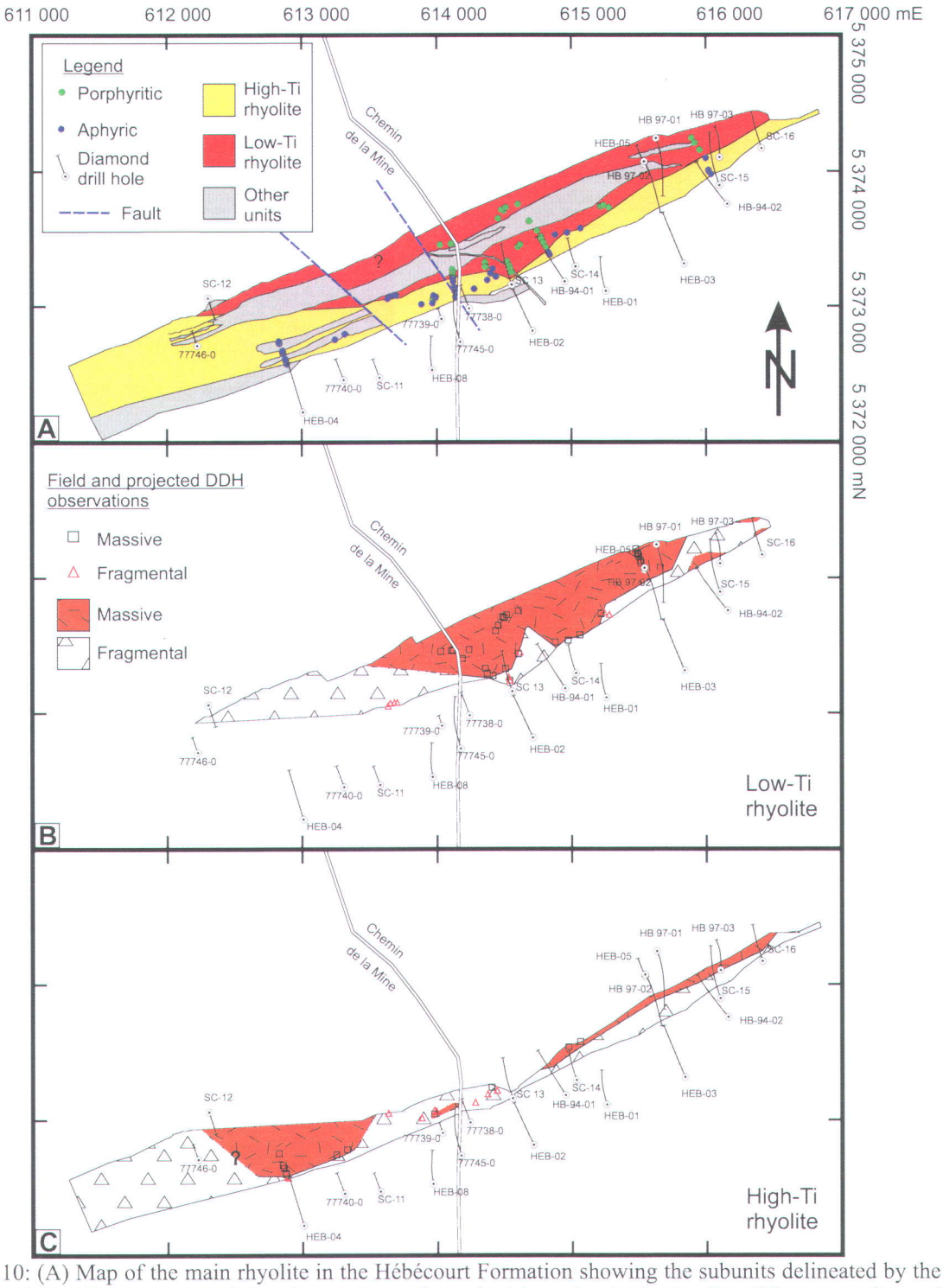

Fig. 3.10: (A) Map of the main rhyolite in the Hébécourt Formation showing the subunits delineated by the high- and low-Ti samples, and the observations of porphyritic and aphyric rhyolite. Where samples and observations are from drill core, they have been projected to the surface using the regional dip of 72°S and a strike perpendicular to S_0. (B) Map showing the distribution of facies in the low-Ti rhyolite based on new drill core and surface observations, plus historical drill core logs from the Ministère des Ressources naturelles et de la Faune (Québec) mining exploration files. The shape of the breccia above the central massive region is defined from drill core and three outcrops; it may not be an accurate representation of the facies on surface, as the breccia in drill core is seen at depth. Only the compiled DDHs are shown on the figure. (C) Map showing the distribution of facies in the high-Ti rhyolite, based the same data sources.

3.3.1.1 Massive facies. The massive rocks in the Hébécourt main rhyolite are medium to fine-grained and medium gray in fresh surface (Fig. 3.11a). Many of the massive regions display flow banding, highlighted or defined by various dominant minerals. The presence of vesicles varies from nil to 3%, and the vesicles can be filled with calcite, chlorite or most commonly quartz and are typically 1-2 mm in size. A sugary texture is sometimes visible on a weathered surface giving the rock a siliceous look. There can also be seen locally a micro-spherulitic texture, with spherules that are less than 1 mm across. A macroscopic spherulitic texture is also observed in places, although not with the micro-spherulitic texture, consisting of white, gray or beige, circular to irregular spherules up to 1 cm across that do not coalesce, which is common in the spherulitic textures of the felsic units yet to be described. The spherules range from widely spaced and less than 1% to up to 90%, where they are present at all. As mentioned above, the presence or absence of phenocrysts is a way of distinguishing between the low-Ti and high-Ti sub-units. The phenocrysts observed in the field consist predominantly of 1-2% quartz 1-2 mm across, with rarer, smaller feldspar phenocrysts.

In thin section, the massive samples from the low-Ti rhyolite contain both quartz and feldspar microphenocrysts (Figs. 3.12a and 3.12b). The quartz microphenocrysts range between 1% and 5% in abundance, with an average of 3%. As they are between 200 and 300 μm across, they are a different generation than that seen in hand sample. In many cases they have overgrowths of quartz. The feldspar is in the form of microphenocrysts (<200 μm), averages less than 2% and these crystals are not seen in every sample. Both types of microphenocrysts have subhedral to euhedral shapes, although euhedral feldspar microphenocrysts are rare. In contrast, thin sections of massive high-Ti rhyolite are typically aphyric, although in one case there are <1% quartz microphenocrysts which are <200 μm across. The groundmass for both subunits appears to be predominantly formed of quartz and feldspar, although it is very fine-grained and it is difficult to resolve further details. Rhyolite alteration is described in Chapter 4.

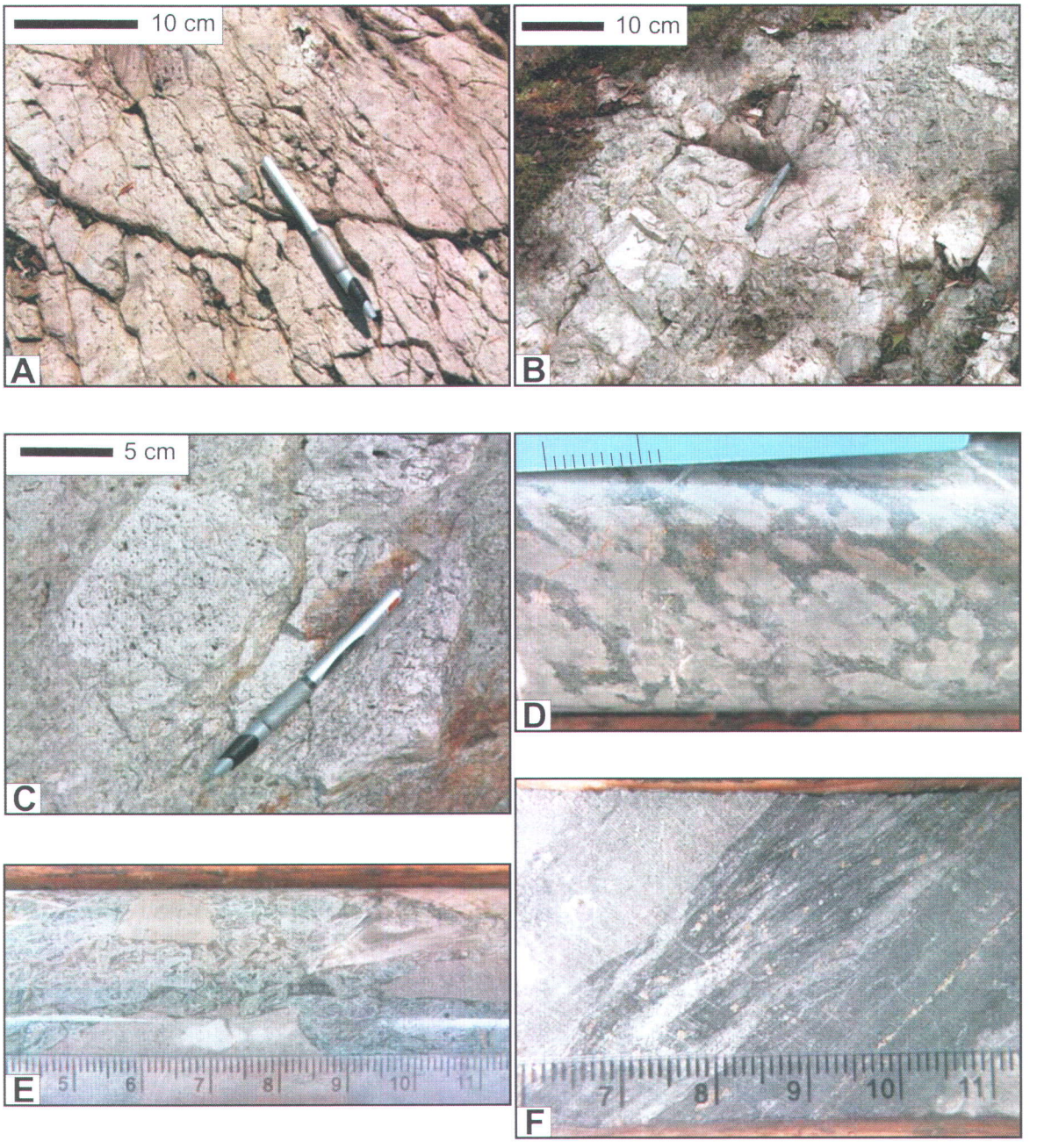

Fig. 3.11: Photographs of felsic rocks in the Hébécourt Formation. (A) Massive facies in the low-Ti subunit in the main rhyolite, with hairline sericite veins and 1-2 mm "quartz eye" phenocrysts. (B) Breccia facies of the low-Ti rhyolite, clearly matrix-supported with large clasts. (C) Breccia facies of the high-Ti rhyolite. (D) Massive facies of the upper rhyolite, with coalescing, irregularly shaped spherules. (E) Lapilli-tuff facies of the upper rhyolite, with angular fragments. The smaller clasts are epidote-altered and the larger clasts display a micro-spherulitic texture. (F) Interbedded finely laminated tuff and argillite from the boundary between the first and second volcanic episodes of the upper rhyolite. Where the ruler is used as a scale the increments are in millimetres.

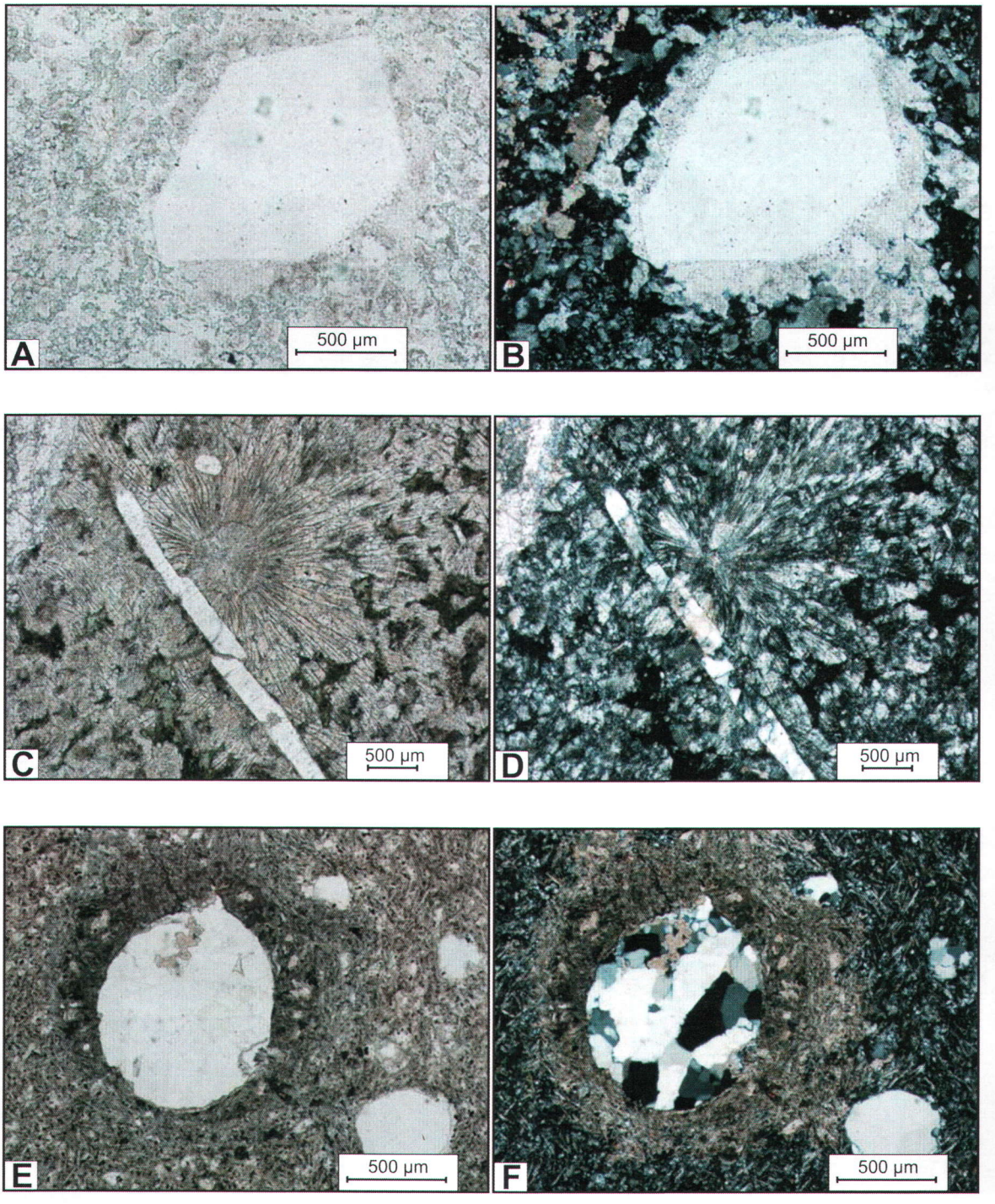

Fig. 3.12. Photomicrographs from the felsic units of the Hébécourt Formation. PPL=Plane Polarised Light, CPL=Cross Polarised Light. A) Quartz phenocryst in the low-Ti rhyolite in PPL. B) The same as A, but in CPL. C) Radial fibres in a spherule in the upper rhyolite in PPL. D) Same as C but in CPL. E) Quartz-filled vesicles in the Calc-alkaline basalt in PPL. F) Same as E but in CPL.

3.3.1.2 Fragmental facies. The most common variety of the fragmental facies consists of monomictic volcaniclastic rocks (Fig. 3.11b and 3.11c) with a wide range in rhyolite clast sizes, from 1 mm to 35 cm. Therefore in terms of grain-size, these volcaniclastic rocks consist of tuff-breccias, lapilli-tuffs and tuffs, with tuff-breccias being the most abundant. Bedding is typically absent, but has been seen in one location. Normal grading has been only been observed in some of the lapilli-tuffs with clasts less than 2 cm in size. The clasts are mostly angular to sub-rounded, generally equant in shape and randomly orientated. Rounded clasts are rarer and when the rock displays rounded clasts, they are 2-5 cm in size forming a matrix-supported lapilli-tuff. Clasts displaying flow banding are extremely common. The monomictic volcaniclastic rocks are usually cemented with quartz, although sericite, chlorite and epidote alteration of the matrix is not uncommon. These fragmental rocks are interpreted as in situ to remobilized hyaloclastite (part of lava domes and lava flows) due to their structures and textures, and due to their intimate association with massive rocks of the same geochemical composition (see facies variations and geochemistry below).

Typical hyaloclastite is sometimes present, with small angular fragments (≤1 cm) and a quartz cement. This is different from the most common variety of the fragmental facies, due to smaller clasts and a jigsaw-fit aspect. The clasts of the typical hyaloclastite intervals are mostly chlorite-altered, although sometimes there is additional epidote.

3.3.1.3 Thickness and facies variations; mode of emplacement

Low-Ti rhyolite. The low-Ti subunit is thickest in its centre (Fig. 3.1; 490 m with the thickness of the intrusions removed) and thins both westward and eastward (the thickness patterns are not known in the third, now subvertical, dimension) (Fig. 3.2). The central region is characterized by massive lava and there is a change to fragmental rocks laterally and towards the top (Fig. 3.10 b). There are other less important massive areas on the flanks to the east; however these were noted in historical drill core descriptions only and may represent large coherent lobes within fragmental rocks.

The facies variations seen in this unit can be explained using the subaqueous lava dome model of McPhie et al. (1993): the massive regions in the low-Ti rhyolite represent the coherent core of that model, whereas the largely unbedded monomictic volcaniclastic rocks with coarse, angular to sub-rounded rhyolite clasts are typical of in situ to slightly remobilized hyaloclastite. This unit most likely represents a lava dome rather than a lava flow because of its symmetrical shape and the central location of the coherent rocks, however without the location of the feeder dykes the interpretation can only be based on a two dimensional representation. The dome could be the result of more than one eruptive event however; because of the large distance between the control points and the discontinuous nature of the exposure in the field, there could be several regions of hyaloclastite that have been overlooked.

The low-Ti rhyolite dome is most likely fully extrusive rather than a cryptodome. Although the internal facies variations are very similar in cryptodomes and extrusive domes, the former are more common in mixed volcano-sedimentary environments (McPhie et al., 1993) whereas the study area is a volcanic-dominated environment; also extrusive domes contain more fragmental deposits. The low-Ti lava dome was presumably emplaced on a paleo-horizontal surface formed by mafic lavas since it appears symmetrical (at least in two dimensions), and the model allows a prediction that the vent would be in the region of DDH HEB-02, just east of Chemin de la Mine (Fig. 3.10b).

High-Ti rhyolite. Facies variations are less clearly defined for the high-Ti subunit due to fewer control points, but the inferred origin is similar due to similar facies characteristics and facies variations: felsic lava flows or domes. The high-Ti rhyolite appears to be thinner where the low-Ti unit is thickest (Fig. 3.10c). The high-Ti rhyolite consists predominantly of fragmental rocks, with dispersed regions of massive rock (Fig. 3.10c). Again, using the model of McPhie et al. (1993), the large massive regions would represent the coherent cores of lava flows, with the fragmental rocks representing in situ hyaloclastite or resedimented hyaloclastite. In this model, the smaller massive regions would represent individual lobe structures or collections of lobes. The large massive

regions are not located near the proposed vent area of the underlying low-Ti rhyolite, suggesting that the two subunits do not share the same effusive centre. Given the location of the massive regions and the thickness variations within the high-Ti rhyolite, it could have come out of two separate vents, one on each side of the Chemin de la Mine (Fig. 3.10c). The eastern vent may have been located between DDHs HEB-01 and HEB-02, although the vent location is difficult to ascertain. The western vent may correspond to the poorly defined massive region in the vicinity of DDH HEB-04. The high-Ti rhyolite appears to become thicker westward from this presumed western vent, possibly because this was the down-slope direction at the time of extrusion. The western termination of the high-Ti rhyolite is not known.

3.3.1.4 Geochemistry. All of the samples from the Hébécourt main rhyolite (n=29 including the two subunits) plot in the rhyolite fields of the SiO_2 vs. Zr/TiO_2 and Zr/TiO_2 vs. Nb/Y diagrams, if alteration effects are accounted for (Figs. 3.13a and 3.13b). On a diagram of TiO_2 versus Zr (Fig. 3.14c), an arbitrary horizontal line can be drawn at TiO_2 = 0.16%; this separates the low-Ti and high-Ti subunits. The distribution of these two rhyolite subunits fits closely the quartz-phyric (low-Ti) and aphyric (high-Ti) occurrences on the map (Fig. 3.10a). Trying to define rhyolitic subunits based on their Ti/Zr ratios (e.g., Barrett and MacLean, 1999) instead of TiO_2 contents does not produce such well-behaved map units and a consistent relationship with quartz crystals.

Further, the two subunits defined on TiO_2 values and quartz crystals plot separately (with a minor overlap) on a Zr vs. Y diagram (Fig. 3.14a). These TiO_2-discriminated groups have been statistically shown to have different mean Zr/Y ratios at the 95% significance level (t-tests for independent samples, assuming unequal variances, on a compiled database of 217 samples from the main rhyolite consisting of 113 samples from the low-Ti subunit and 104 samples from the high-Ti subunit). The Zr vs. Y diagram shows that both subunits have a transitional to tholeiitic affinity using the boundaries of Ross and Bédard (2009), but a tholeiitic affinity using the boundaries of Barrett and MacLean (1999). The Th/Yb vs. Zr/Y diagram (Fig. 3.14d) shows both groups predominantly within the tholeiitic field, with only two samples from the high-Ti rhyolite within the

transitional field. The extended multi-element plots for the two subunits (Fig. 3.15a and 3.15b) both have relatively flat profiles, with significant negative Ti anomalies.

As expected, the high-Ti rhyolite has a shallower Ti anomaly than the low-Ti rhyolite. As in the Hébécourt basalt and Hébécourt basaltic andesite, the first three elements (Th to Ta) are slightly depleted relative to the rest of the profiles, suggesting a similar, or presumably common source.

3.3.2 Hébécourt upper rhyolite

The 45-75 m-thick upper rhyolite forms the top of the Hébécourt Formation in the eastern part of the field area. The facies of the upper rhyolite were mainly defined by drill core intersections and this unit was only observed at two small outcrops on the shore of Lake Hébécourt (Fig. 3.1).

3.3.2.1 Massive facies. The massive rocks of this unit are medium gray in color and are predominantly spherulitic (Fig. 3.11d). There are two types of spherulitic texture: the first consists of discrete white spherules, up to 2 mm across, circular to slightly irregular in shape, which do not coalesce; the second comprises coalescing spherules 1-2 cm across, and there are intervals of completely coalesced spherules. In the second spherulitic texture, radial fibers are sometimes present within the spherules, and in thin section the radial fibers are clearly seen (Fig. 3.12c and 3.12d). Locally there are traces of quartz phenocrysts, typically less than 1 mm across but they can be up to 2 mm. Smaller (400-600 μm) feldspar phenocrysts can be seen in thin section. Locally there can be 2-3% quartz- or more rarely chlorite-filled vesicles, which are typically 1-2 mm across and circular to irregular in shape. There is epidote and sericite alteration locally, and more rarely patches of chlorite alteration or chlorite replacement of mafic minerals.

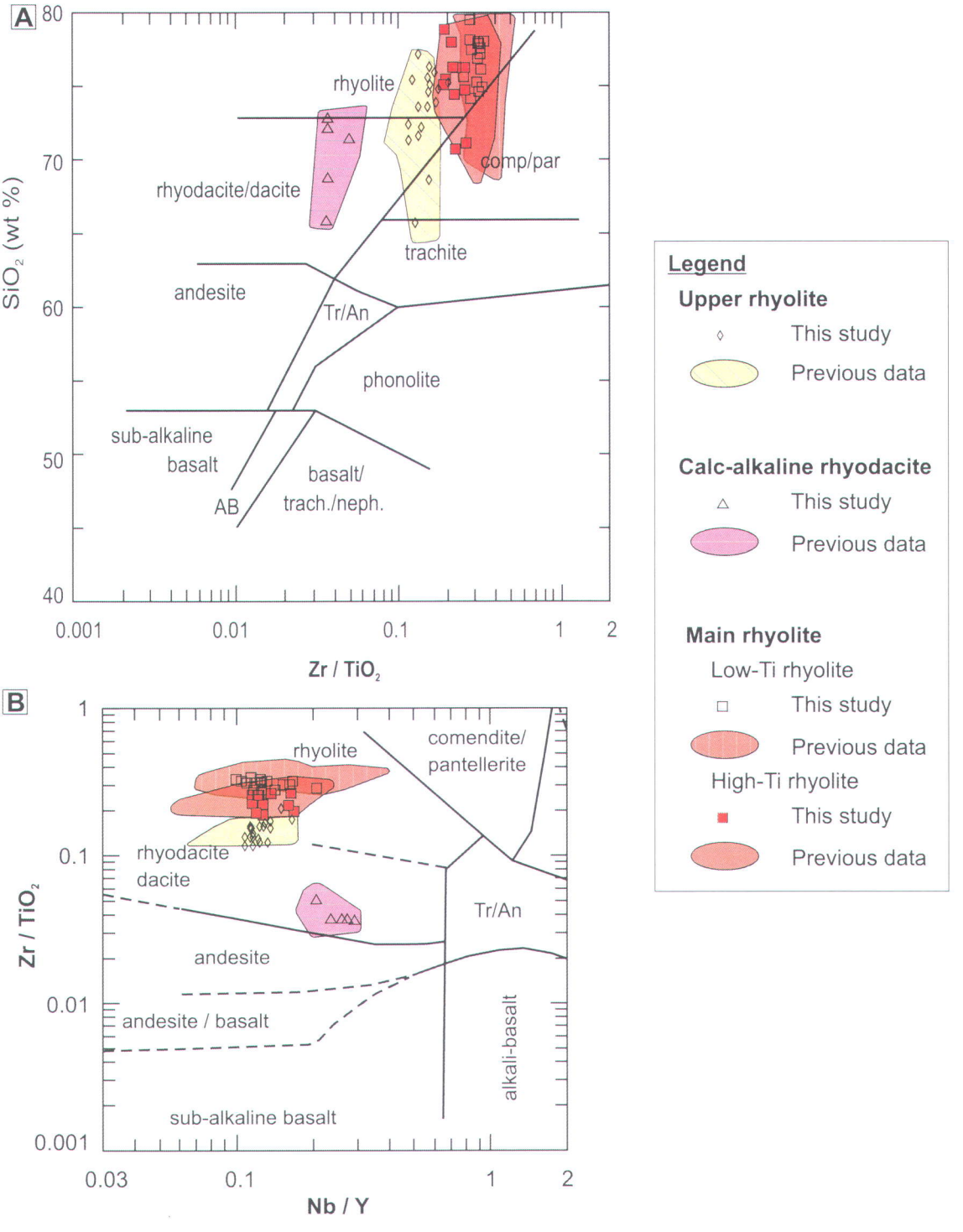

Fig. 3.13: Geochemistry of felsic volcanic rocks from the Hébécourt Formation in the study area. (A)-(B) Classification diagrams from Winchester and Floyd (1977) for all units east of DDH HEB-04.

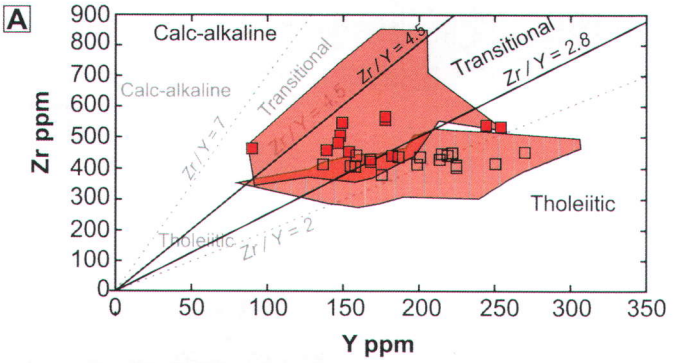

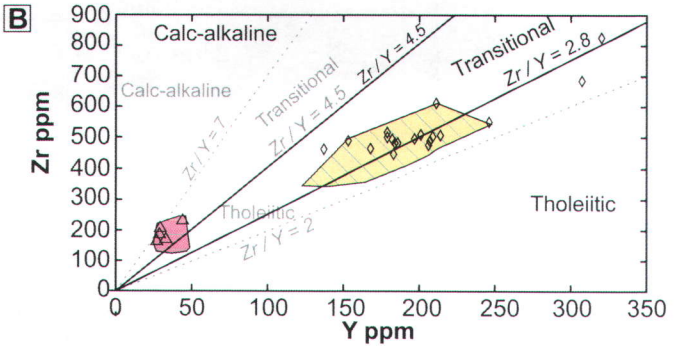

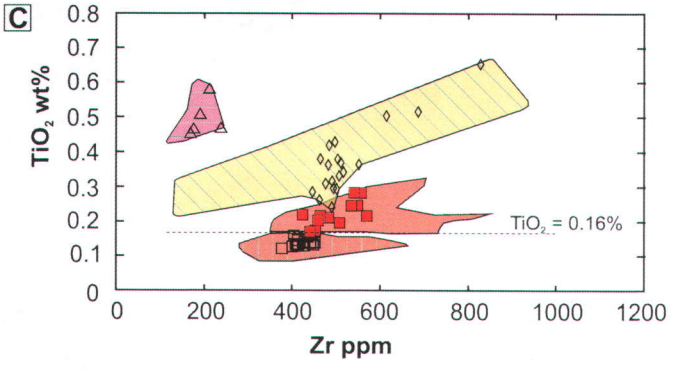

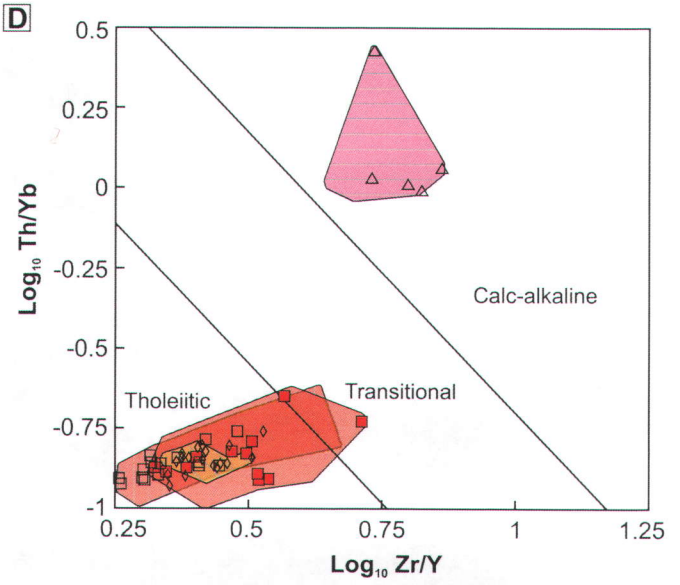

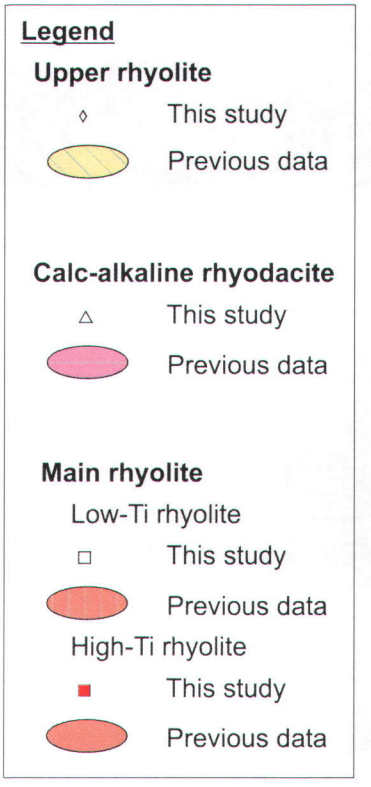

Fig. 3.14: Geochemistry of felsic volcanic rocks from the Hébécourt Formation in the study area. (A)-(B)-(D) Magmatic affinity diagrams from Ross and Bédard (2009): (A) for the two sub-units of the main rhyolite; (B) for the upper rhyolite and the calc-alkaline rhyodacite ; (D) for all units. (C) Graph of TiO_2 vs. Zr for all units.(A) and (B) both also include the affinity boundaries from Barrett and MacLean (1999).

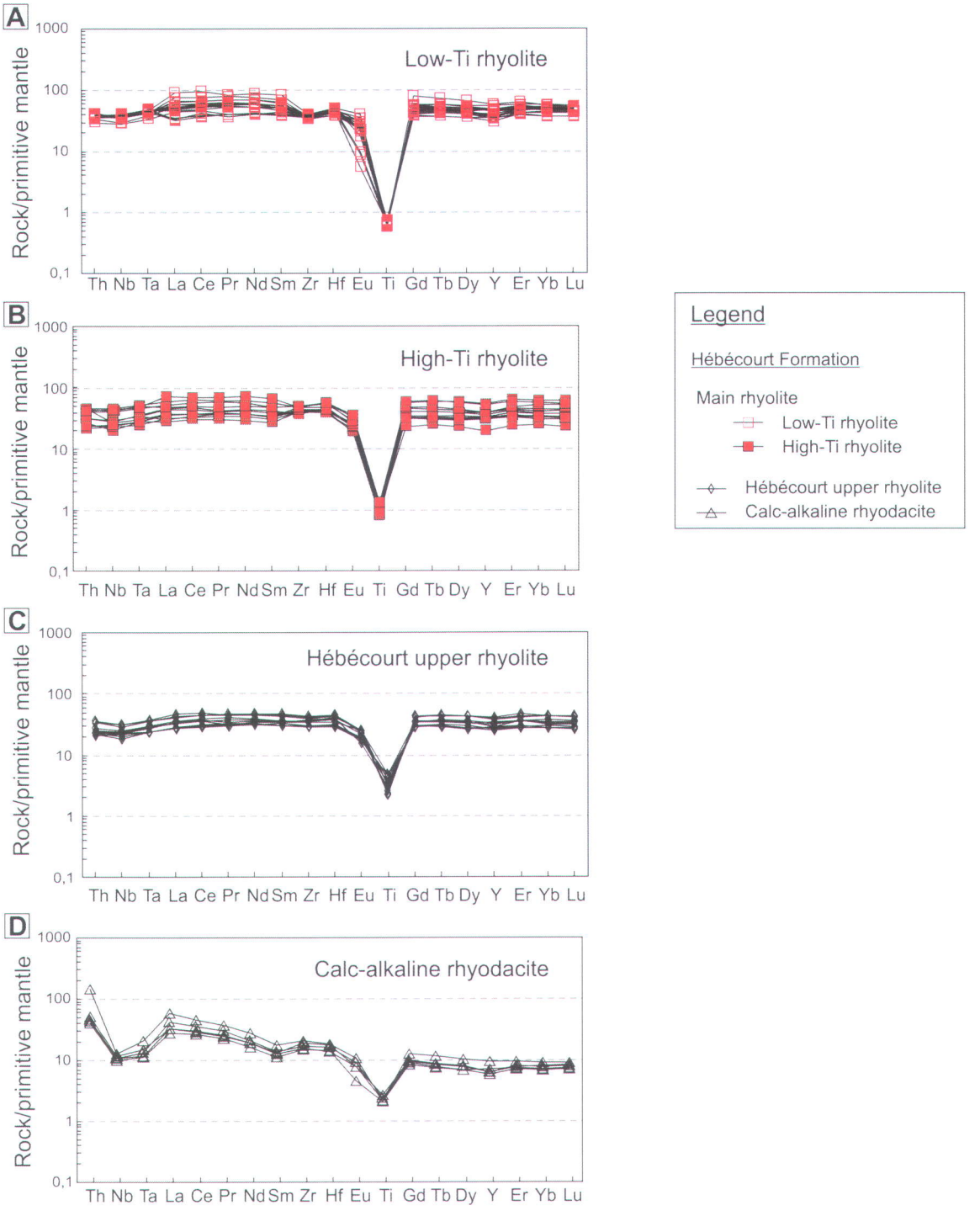

Fig. 3.15: Extended multi-element plots normalized to the primitive mantle for felsic volcanic rocks from the Hébécourt Formation in the study area: (A) low-Ti rhyolite; (B) high-Ti rhyolite; (C) upper rhyolite; (D) calc-alkaline rhyodacite. Normalization values from Sun and McDonough (1989).

3.3.2.2 Fragmental facies. The fragmental facies is much more affected by alteration than the massive facies, often to the extent that the primary texture is difficult to recognize. There are three types of fragmental rocks within this unit: (i) typical hyaloclastite; (ii) angular fragment lapilli-tuff; and (iii) rounded fragment tuffs and lapilli-tuffs, some of which are stratified. The most abundant are type (ii) and (iii).

Type (i) volcaniclastic rocks consist of typical non-bedded in situ hyaloclastite with angular clasts, 0.5 cm across on average, and a jigsaw-fit texture; the fragments are strongly chloritized and locally epidote-altered, with a silica cement.

Type (ii) volcaniclastic rocks are not bedded, contain angular fragments (Fig. 3.11e), are of lapilli-tuff grade and typically matrix-supported with a fine-grained matrix, although locally the rocks are clast-supported where the clasts are larger. The lapilli are typically up to 1-2 cm across, although they can be up to 5 cm. Within the lapilli there is often a spherulitic texture visible, with white spherules up to 1 cm in size, and sometimes epidote alteration spots. The tuffaceous matrix and many of the lapilli are typically chloritized, epidote-altered and there is complete silica replacement in places. Some of the fragments are individual quartz crystals. These angular fragment lapilli-tuffs likely represent resedimented hyaloclastite with the clast-supported sections possibly still being in situ.

Type (iii) volcaniclastic rocks are the only type that ever shows stratification, medium-thickness bedding with occasional normal grading, but it is not typical. They consist of very coarse tuffs and lapilli-tuffs containing rounded to sub-rounded clasts averaging 2 mm, although where there is normal grading the clasts at the base can be 1-2 cm. Clasts are typically green or white in color, with the white fragments being predominantly formed of siliceous rhyolite while the green fragments consist of epidotized rhyolite. Some of the clasts are chloritized but it is not as common as in the type (ii) volcaniclastic rocks. The type (iii) lapilli-tuffs and tuffs probably represent resedimented volcaniclastic rocks, judging by the rounded fragments, bedding and grading.

3.3.2.3 Interbedded material. In addition to the three types of felsic volcaniclastic rocks described above there are also fine felsic tuffs, which form finely laminated to thickly bedded intervals, and in HEB-08 they are interbedded with argillite (Fig. 3.11f) and fine mafic tuffs. However, due to the necessarily wide spacing of the whole rock geochemistry sampling and the difficulty in distinguishing between altered felsic and mafic tuffs without geochemistry, the relative proportions are unknown. The finely laminated tuffs and argillites often have high concentrations of pyrite associated with them. These finely laminated tuffs are likely from a very distal source, while the argillite will be the result of background sedimentation from the water column. These intercalations represent a pause in the proximal felsic effusive magmatism within the upper rhyolite.

3.3.2.4 Facies and thickness variations; mode of emplacement. The Hébécourt upper rhyolite contains mostly felsic rocks, but they are interbedded with finely laminated tuffs of a mafic tholeiitic composition, as well as argillite, as indicated above. This indicates that the rhyolite was formed by several different volcanic episodes.

The older volcanic episode formed the thickest deposits, which thin towards the west, from 70 m in DDHs HEB-01 and HEB-03 to 40 m in DDHs HEB-02 and HEB-08 (Fig. 3.16). The upper rhyolite in DDH HEB-01 consists entirely of massive lava with increasing amounts of fragmental rocks to either side, suggesting that the older volcanic episode formed a felsic lava or dome, with the vent location in the vicinity of DDH HEB-01. Bedded fragmental rocks with rounded clasts in DDH DDH-03 (type (iii) volcaniclastic rocks) likely represent remobilized volcaniclastic debris on the flank of the dome or in the distal part of a lava flow.

The younger rhyolitic volcanic episode is seen only in DDH HEB-08 (Fig. 3.16), and consists predominantly of fragmental rocks with angular clasts (type ii volcaniclastic rocks). There are also intersections of massive rhyolite in this DDH, and these likely represent lobes within the fragmental rock. The absence of this younger episode in the other DDHs suggests that the vent is to the west and is not the same as the vent for the older episode.

3.3.2.5 Geochemistry. The analyzed Hébécourt upper rhyolite samples (n = 19) plot within the rhyolite field on the SiO_2 vs. Zr/TiO_2 diagram (Fig. 3.13a), although they do extend down to the rhyodacite/dacite field, which may at least partly be a result of major element mobility. On the Zr/TiO_2 vs. Nb/Y diagram (Fig. 3.13b) the samples straddle the boundary between the rhyolite and rhyodacite/dacite fields.

The main distinction between the Hébécourt upper rhyolite and the main rhyolite is the Zr/TiO_2 ratio (Fig. 3.14c), which is smaller in the upper rhyolite mainly due to higher TiO_2 contents. The Zr/Y diagram (Fig. 3.14b) shows that the Hébécourt upper rhyolite straddles the tholeiitic-transitional boundary of Ross and Bédard (2009), but is within the tholeiitic boundaries of Barrett and MacLean (1999). The Th/Yb vs. Zr/Y diagram (Fig. 3.14d) shows clearly that this unit has a tholeiitic affinity. The tholeiitic affinity can also be seen by the flat profile on the extended multi-element plot (Fig. 3.15c). Again the first three elements, Th to Ta, are slightly depleted, suggesting petrogenetic links with MORB-like magmas or rocks.

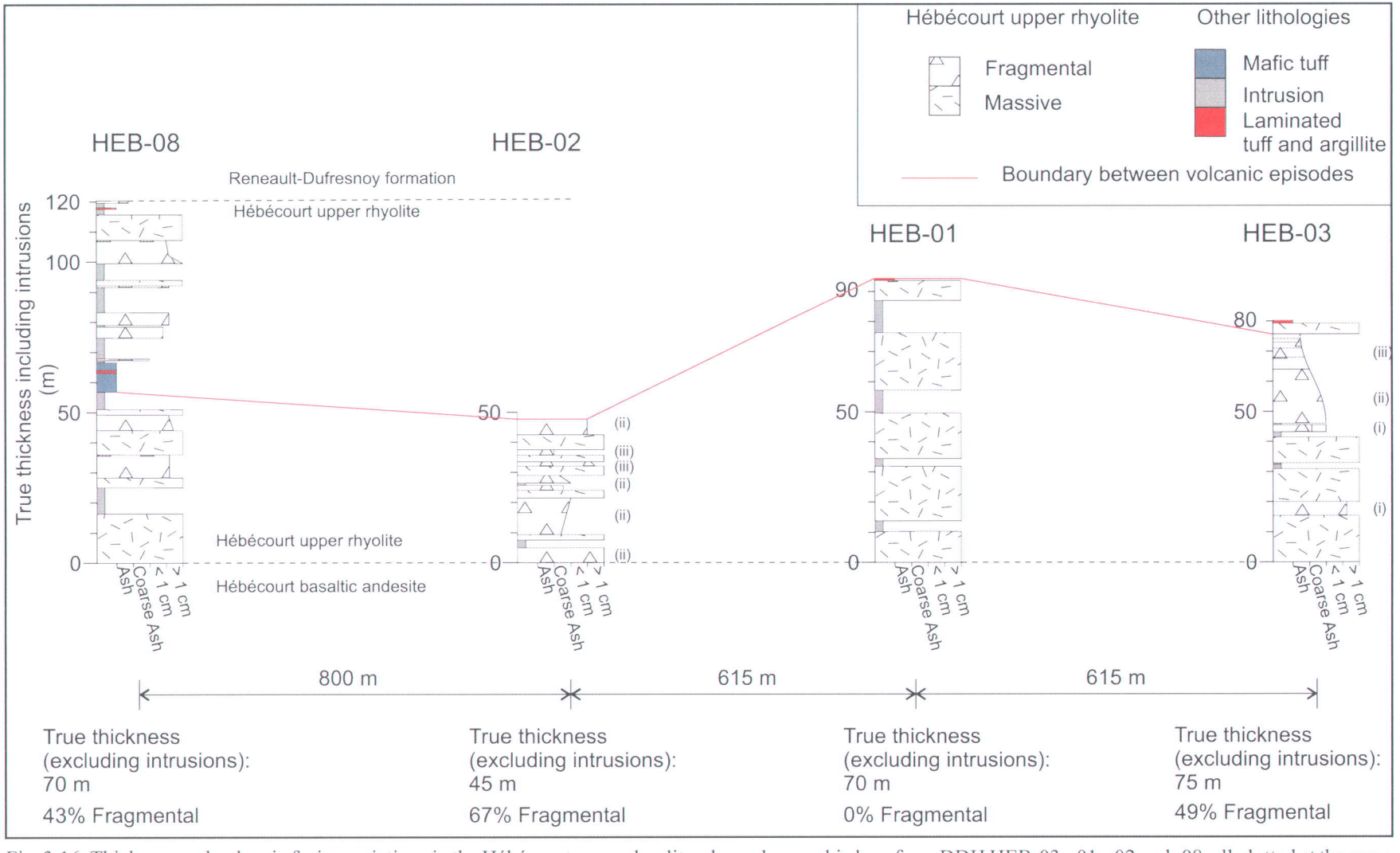

Fig. 3.16: Thickness and volcanic facies variations in the Hébécourt upper rhyolite, shown by graphic logs from DDH HEB-03, -01, -02 and -08, all plotted at the same vertical scale. The horizontal axis is a grain-size scale. The red line is believed to represent the boundary between two volcanic episodes in the Hébécourt upper rhyolite, marked by finely laminated ash and argillite, and in HEB-08 a thicker unit of mafic tuff.

3.4 Calc-alkaline intercalations in the Hébécourt Formation in Québec

Although the Hébécourt Formation is overwhelmingly tholeiitic, this study has identified minor intercalations of calc-alkaline eruptive products occur at various stratigraphic levels in the easternmost part of the study area (DDH HEB-03 and HEB-01). There are four main calc-alkaline intercalations known, three being formed of rhyodacite and one of basalt. The calc-alkaline rocks are located between the main rhyolite and the upper rhyolite.

3.4.1 Rhyodacite

The calc-alkaline rhyodacites include massive and volcaniclastic rocks. The massive facies only occurs in DDH HEB-03, in which three massive occurrences, with a maximum true thickness of 20 m, are separated by lapilli-tuffs and tuffs of the same composition, as well as by mafic dikes.

3.4.1.1 Massive rhyodacite. The massive facies is fine-grained to aphanitic, medium to dark gray in fresh surface and contains 1-2% white spherules, up to 2 cm across. The rock also contains 1-2% quartz amygdales 2-3 mm across, with irregular shapes. In thin section it can be seen that there are additional small amygdales filled with chlorite, and that many of the quartz-filled amygdales also contain chlorite around the margins. In one of the massive occurrences, the rock has 1-2% feldspar phenocrysts that are up to 2 mm across.

3.4.1.2 Fragmental rhyodacite in DDH HEB-03. There are two types of volcaniclastic rocks composed of calc-alkaline rhyodacite in DDH HEB-03. The most common type is a matrix-supported lapilli-tuff with white or gray, rounded to sub-rounded felsic clasts 3-5 cm across. There are quartz amygdales within some clasts. The tuffaceous matrix is green in fresh surface. The less common type of volcaniclastic rock consists of typical in situ hyaloclastite with ≤1 cm felsic fragments. The fragments are often chloritized but can instead have epidote alteration or no apparent alteration.

3.4.1.3 Fragmental rhyodacite in DDH HEB-01. In DDH HEB-01, the 21 m-thick calc-alkaline rhyodacite is entirely volcaniclastic. Two types of volcaniclastic rocks are distinguished. The first type forms several 2-3 m-thick normally graded beds. At the base of such graded beds, there is lapilli-tuff with 3-4 cm fragments in a matrix-supported rock, where the matrix is siliceous and contains 3-4 mm fragments in addition to the larger clasts. Each graded bed has coarse tuff at the top with average grain size of 1-2 mm. The coarse tuff contains rounded to sub-angular, predominantly chloritized clasts which sometimes display a jigsaw-fit aspect.

The second type of calc-alkaline rhyodacitic volcaniclastic rock in DDH HEB-01 consists of lapilli-tuff, similar to the coarsest lapilli-tuff in the graded beds, but containing white fragments not seen elsewhere. At the base of these lapilli-tuffs intervals the angular white fragments are the only fragments and they are 4-5 cm in size, but they decrease in size and abundance up stratigraphy, until at the top of these units there are 3-5% angular white clasts which are 1-2 cm across on average.

3.4.1.4 Mode of emplacement of the calc-alkaline rhyodacite. The presence of multiple graded beds and rounded fragments in volcaniclastic rocks from the calc-alkaline rhyodacite intercalations suggests lateral transport within density currents on the seafloor. This texture excludes any possibility that these intercalations are intrusive in origin and requires near-simultaneous extrusion of both abundant tholeiitic and very minor calc-alkaline magmas to form the Hébécourt Formation, likely from different volcanic vents. The calc-alkaline vent was likely located to the east of where these rocks have been encountered as there is a greater thickness of calc-alkaline rhyodacite the east and a higher proportion of tuff to the west.

3.4.2 Basalt

The calc-alkaline basalt, only present in the east (DDH HEB-03), has a thickness of 12 m and is formed of pillow breccia. The pillow breccia consists of pillow fragments in typical hyaloclastite. The aphyric pillow fragments have fluidal shapes, are up to 15 cm across and also have chilled margins. The typical hyaloclastite is made of 0.5-1 cm fragments

which are angular and chloritized with a jigsaw-fit aspect and chilled margins up to 2 mm-thick. A thin section of one of the clasts has shown 4-5% 700-800 μm quartz- (Fig. 3.12d and 3.12e) and carbonate-filled vesicles, although some of the quartz-filled vesicles have sericite mixed in the centre. There is a second generation of predominantly quartz-filled vesicles, 100-200 μm across and representing 1-2% of the rock. There are varioles in the pillow fragments, up to 1 cm in size and a beige-whitish color, and they coalesce locally. Again, pillow breccias demonstrate an extrusive, rather than intrusive, origin for the calc-alkaline intercalations.

3.4.3 Geochemistry

Five samples of calc-alkaline rhyodacite were analyzed: three from the fragmental facies and two from the massive facies. The samples plot mostly in the upper part of the rhyodacite/dacite field on the SiO_2 vs. Zr/TiO_2 diagram (Fig. 3.13a) despite some alteration as evidenced by the vertical scatter. On the Zr/TiO_2 vs. Nb/Y diagram, all of the samples cluster in the lower part of the rhyodacite/dacite field (Fig.3.13b). The calc-alkaline affinity is shown clearly on the Zr vs. Y and Th/Yb vs. Zr/Y diagrams (Figs. 3.14b and 3.14d). The extended multi-element profiles (Fig. 3.15d) are comparatively steeply inclined, with high Th, Nb-Ta troughs, Zr-Hf plateaus and negative Ti anomalies, typical of arc magmas (Jenner, 1996).

The calc-alkaline basalt plots with Group 2 of the Reneault-Dufresnoy Formation (defined below) on every diagram shown (Figs. 3.7 and 3.8). The extended multi-element profile (Fig. 3.9d) is also the same as that seen for Group 2 of the Reneault-Dufresnoy Formation (see below). This suggests that arc-type calc-alkaline volcanism began earlier than previously believed, within the time period which produced the overwhelmingly tholeiitic Hébécourt Formation. Since two different tectonic environments cannot have been present simultaneously in the same relatively small area, it appears likely that some of the trace element variations in the Blake River Group result from effects such as crustal contamination and/or different melting depths/sources rather than a constantly changing tectonic environment.

3.5 Stratigraphy of the Hébécourt Formation in Ontario and west of DDH HEB-04 in Québec

Outcrop west of DDH HEB-04 in Québec and in the Ontario part of the study area is extremely limited, and so is DDH information, so overall the geology is poorly known, but the little that is known is described here. There are three Cogitore DDHs in the Ontario part of the study area: MD-01, MD-02 and MD-03.

3.5.1 Geological outline

The oldest unit in both Québec and Ontario is the Hébécourt basalt, and the Hébécourt Formation is overlain in both provinces by the Reneault-Dufresnoy Formation, but the order of the felsic units is not the same; the low-Ti rhyolite contains phenocrysts, as opposed to its aphyric nature in Québec; thin tholeiitic basalts occurs above the felsic package in Ontario; and west of DDH HEB-04 a new felsic unit, the McDiarmid dacite, appears. In Ontario, the oldest felsic unit known is the high-Ti rhyolite (Fig. 3.3); however it is unclear whether or not this unit directly overlies the Hébécourt basalt since DDH MD-02 does not display the required mafic-felsic contact in the north. Within the high-Ti rhyolite, there are at least two intercalations of the upper rhyolite, however the youngest of these is seen at the top of two DDHs, MD-01 and MD-02, with no information between, so it may either by very thick or have one or more intercalations of other units within it (Fig. 3.3). There is another occurrence of the high-Ti rhyolite above the upper rhyolite, which is overlain by the McDiarmid dacite. Within the McDiarmid dacite there is a thin intercalation of the low-Ti rhyolite. The McDiarmid dacite is then overlain by another unit of Hébécourt basalt at the top of the formation (Fig. 3.3). Given the distances involved and the differences in the stratigraphic order of the units, it is unlikely that felsic rocks in Ontario share a vent with those in Québec.

3.5.2 Hébécourt basalt

In Ontario, the Hébécourt basalt is seen in DDH MD-01, where it occurs above the felsic rocks, directly beneath the Reneault-Dufresnoy Formation, and above all other units in the Hébécourt Formation (Fig. 3.3). In this position, all three of the facies seen elsewhere are present: pillow lava, massive lava and pillow breccia. In MD-01, the Hébécourt basalt contains very common varioles, white to pale green in colour, 0.5 cm to 2 cm in size and

very frequently concentrating at the pillow margins. A vent location cannot be estimated as this unit is only seen in one DDH, so the variations in the facies cannot be established.

Chemically the Ontario and Québec samples of Hébécourt basalt are similar, and the samples from Ontario plot within the fields generated by the new samples from Québec and the previous data (Figs. 3.17 and 3.18).

3.5.3 Main rhyolite

3.5.3.1 Low-Ti rhyolite. The low-Ti rhyolite is seen in DDH MD-01, and only has a true thickness of 15 to 16 m. It is massive, coherent, dark grey and is quartz- and feldspar-phyric. There are 3-4% quartz phenocrysts that are less than 2 mm across. The 5% feldspar phenocrysts are euhedral to subhedral and 2 mm across.

3.5.3.2 High-Ti rhyolite. The high-Ti rhyolite in Ontario displays the massive facies and the fragmental facies, both of which are very similar to those seen in Québec. The fragmental facies is interspersed within the massive facies, but only in thicknesses of up to a meter, and the generally rounded fragments have a maximum size of 20 cm and a fine ash minimum. There is no stratification anywhere in the fragmental facies. A major difference between the high-Ti rhyolite seen here and that in Québec is a greater abundance of both quartz and feldspar phenocrysts, typically 4-5% of each type although locally up to 10%, and 2-3 mm across.

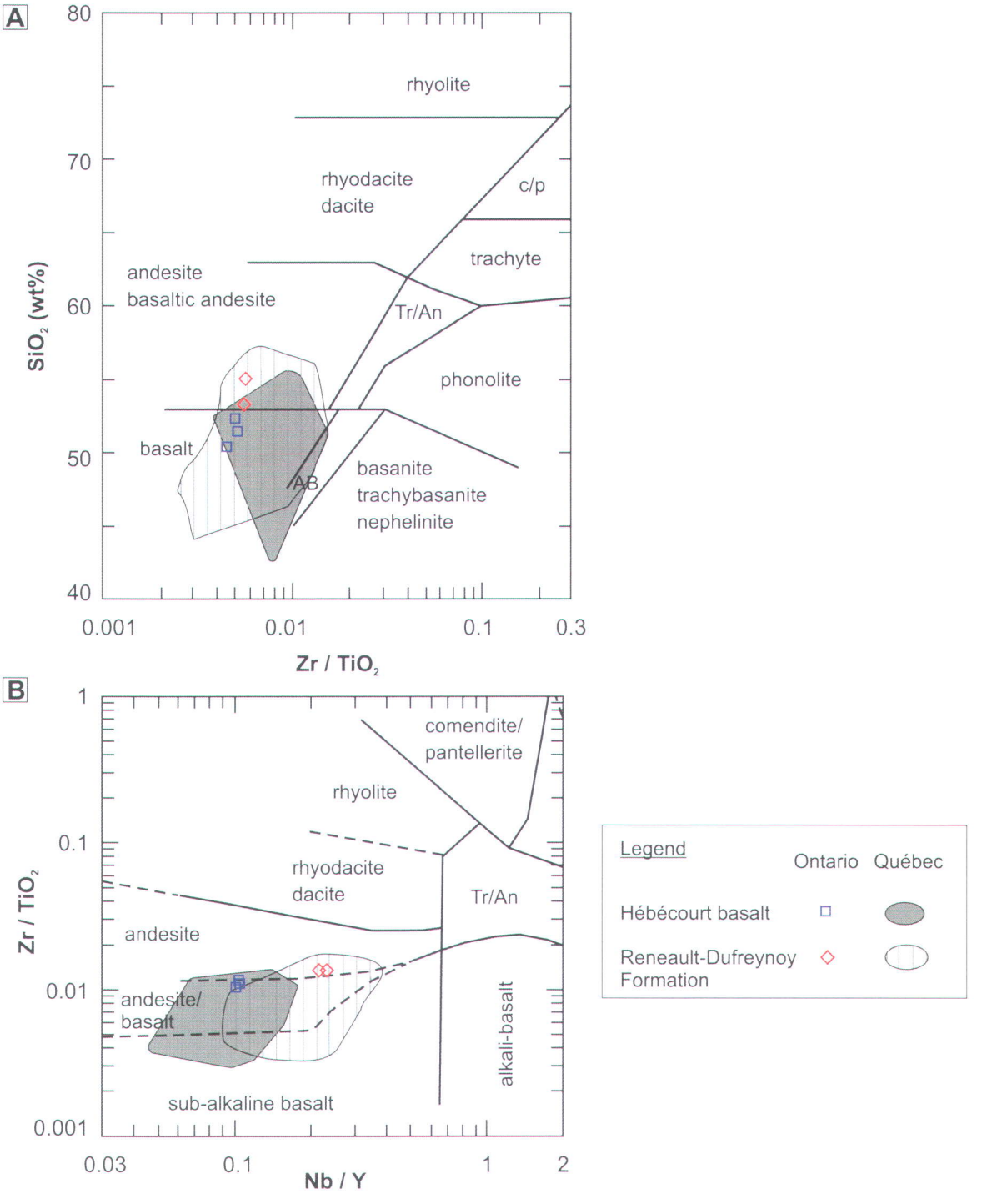

Fig. 3.17: Geochemistry of mafic to intermediate volcanic rocks in the study area. (A)-(B) Classification diagrams from Winchester and Floyd (1977) showing samples taken from west of DDH HEB-04 plotting with a field formed by samples from east of DDH HEB-04 .

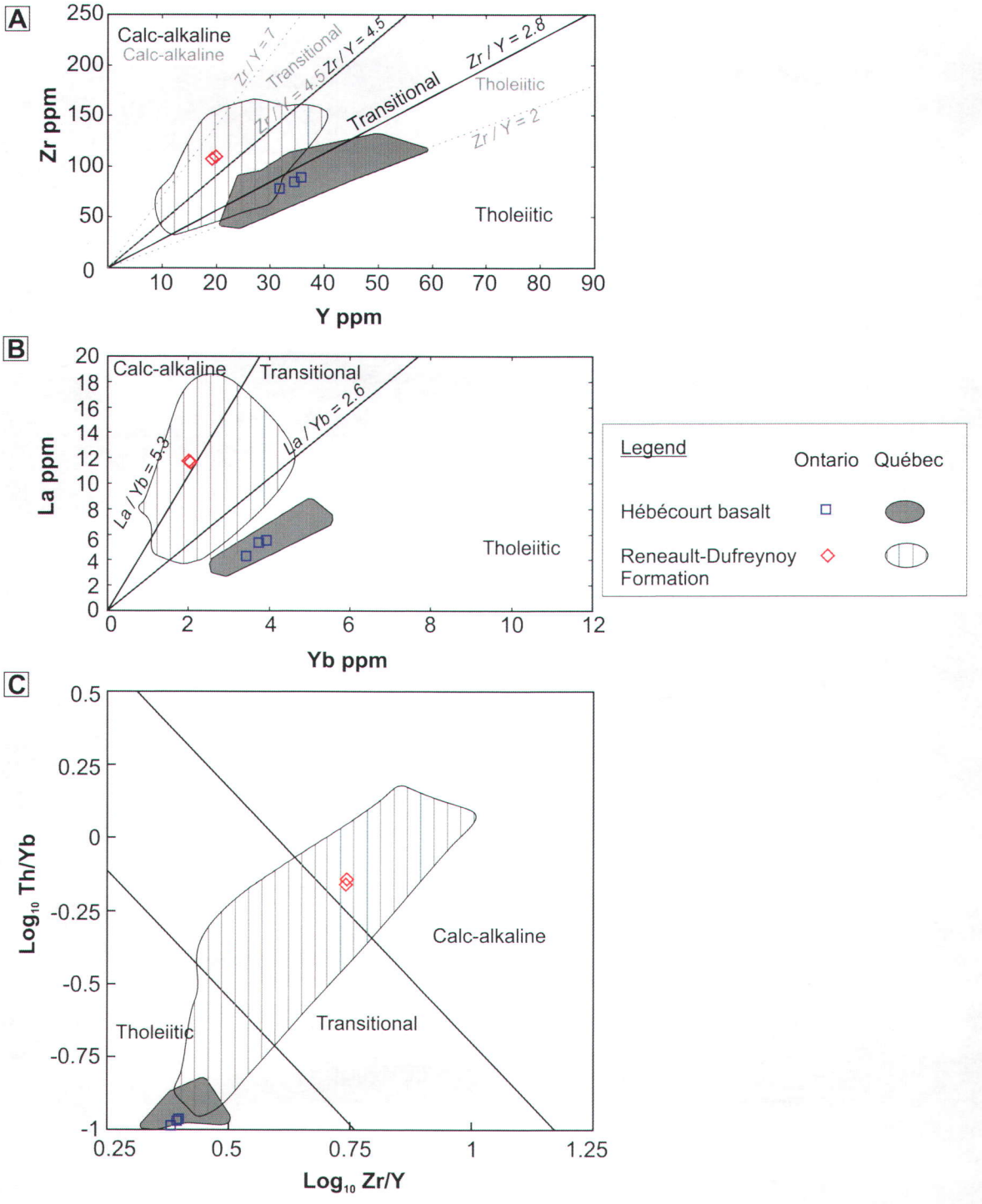

Fig. 3.18: Geochemistry of mafic to intermediate volcanic rocks in the study area. (A)-(C) Magmatic affinity diagrams from Ross and Bédard (2009). (A) Also includes the affinity boundaries from Barrett and MacLean (1999). All graphs show samples from west of DDH HEB-04 plotted with a field formed of samples from east of DDH HEB-04. The field for the Renealt-Dufresnoy Formation also includes samples from south of the study area.

Therefore, despite the same geochemical composition, the low-Ti rhyolite in Ontario is not directly correlatable with that in Québec, as also shown by the different stratigraphic position.

3.5.3.3 Geochemistry of the main rhyolite. Chemically, the samples taken in Ontario for both subunits of the main rhyolite plots with the fields defined in Québec on the Winchester and Floyd plots (Fig. 3.19) and the magmatic affinity diagrams (Zr vs. Y, La vs. Yb and Th/Yb vs. Zr/Y) (Fig. 3.20).

3.5.4 Upper rhyolite

The upper rhyolite in Ontario is much thicker than in Québec and consists of several different occurrences separated by other units, compared to the single thin unit in Québec. The facies observed in the upper rhyolite in Ontario include a massive and a fragmental facies. The massive facies is dominant, and the fragmental facies does not contain any stratification, but is finer-grained than in Québec.

Chemically the unit plots within the field formed by the samples from the upper rhyolite in Québec on all diagrams (Figs. 3.19 and 3.20).

3.5.5 McDiarmid dacite

The McDiarmid dacite, defined in this study, extends from Ontario where it is seen in DDH MD-01 into Québec where it is seen in DDHs HEB-04 and HEB-09. In Québec it overlies the high-Ti rhyolite. In Ontario it is seen in several occurrences within the felsic package (Fig. 3.3).

3.5.5.1 Massive facies and lobate facies. The massive facies of the McDiarmid dacite is a medium grey color and fine-grained. The presence of phenocrysts is variable, in places there are 2-3% quartz phenocrysts and 2-3% feldspar phenocrysts while elsewhere there is less than 1% phenocrysts or they are absent. Where they are present, they can range in size from less than 1 mm to 3 mm. The rock is also variably spherulitic, with two types of

spherulitic texture observed. The first type consists of very small spherules <1 mm, which are white and siliceous, and this type does not coalesce.

The second type consist of larger spherules, up to 2 cm across, white to green in color and they do coalesce; radial fibers have been seen in this type. The abundance of both types of spherules ranges from absent to 90%.

In DDH HEB-09, there are short intervals of in situ hyaloclastite, which are never longer than 10 cm of core and separate 2-3 m lengths of coherent rock with a similar texture to the massive facies described above. The hyaloclastite contains angular clasts that are 0.5-1 cm across. The coherent domains separated by hyaloclastite are interpreted as felsic lobes.

3.5.5.2 Volcaniclastic facies. In addition to the in situ hyaloclastite of the possible lobe facies, there are other fragmental intervals in the McDiarmid dacite, consisting of lapilli-tuffs and very minor tuffs.

The monomictic lapilli-tuffs are formed of angular rhyolite clasts which range in size from 2 mm to 30 cm, with an average of 5 cm. Some of the lapilli display the spherulitic textures seen in the massive intervals. The lapilli-tuffs commonly exhibit the well sorted aspect of typical in situ hyaloclastite, but just as often are matrix-supported in a tuffaceous matrix.

The tuffs are present in DDHs HEB-09 and HEB-04, where they have true thicknesses of 15 cm and 8 cm respectively; they are absent from MD-01. The tuffs are very fine-grained and finely laminated. The tuff in HEB-04 forms part of a normally graded bed with lapilli-tuff. In HEB-09, the tuff is interbedded with fine laminations of argillite.

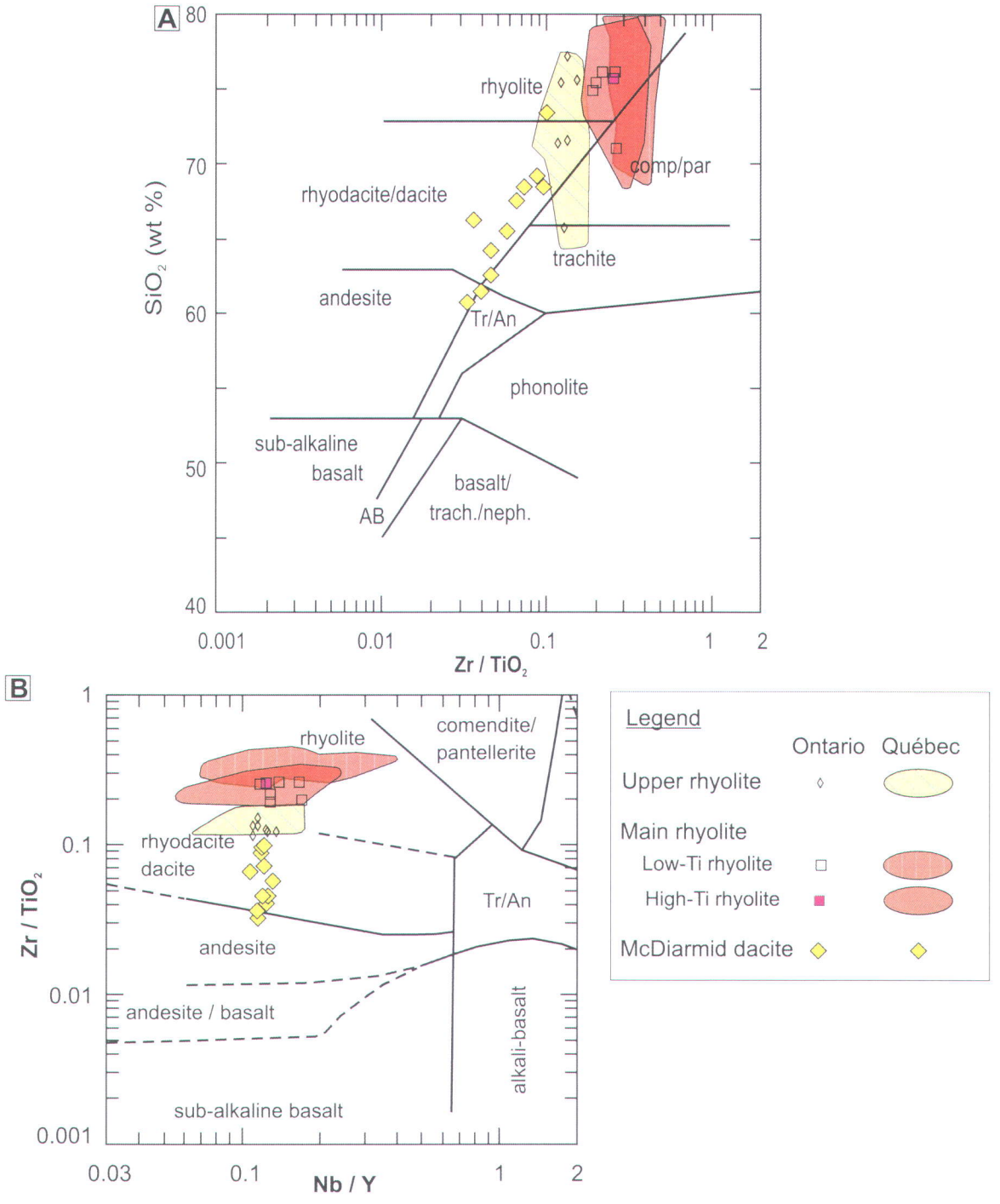

Fig. 3.19: Geochemistry of felsic volcanic rocks from the Hébécourt Formation west of DDH HEB-04. Both plots are classification diagrams from Winchester and Floyd (1977). The graphs show a good correlation between the samples west of DDH HEB-04 and the fields formed by the samples taken east of DDH HEB-04 for the upper rhyolite and the main rhyolite. In addition the composition of McDiarmid dacite throughout the study area is shown.

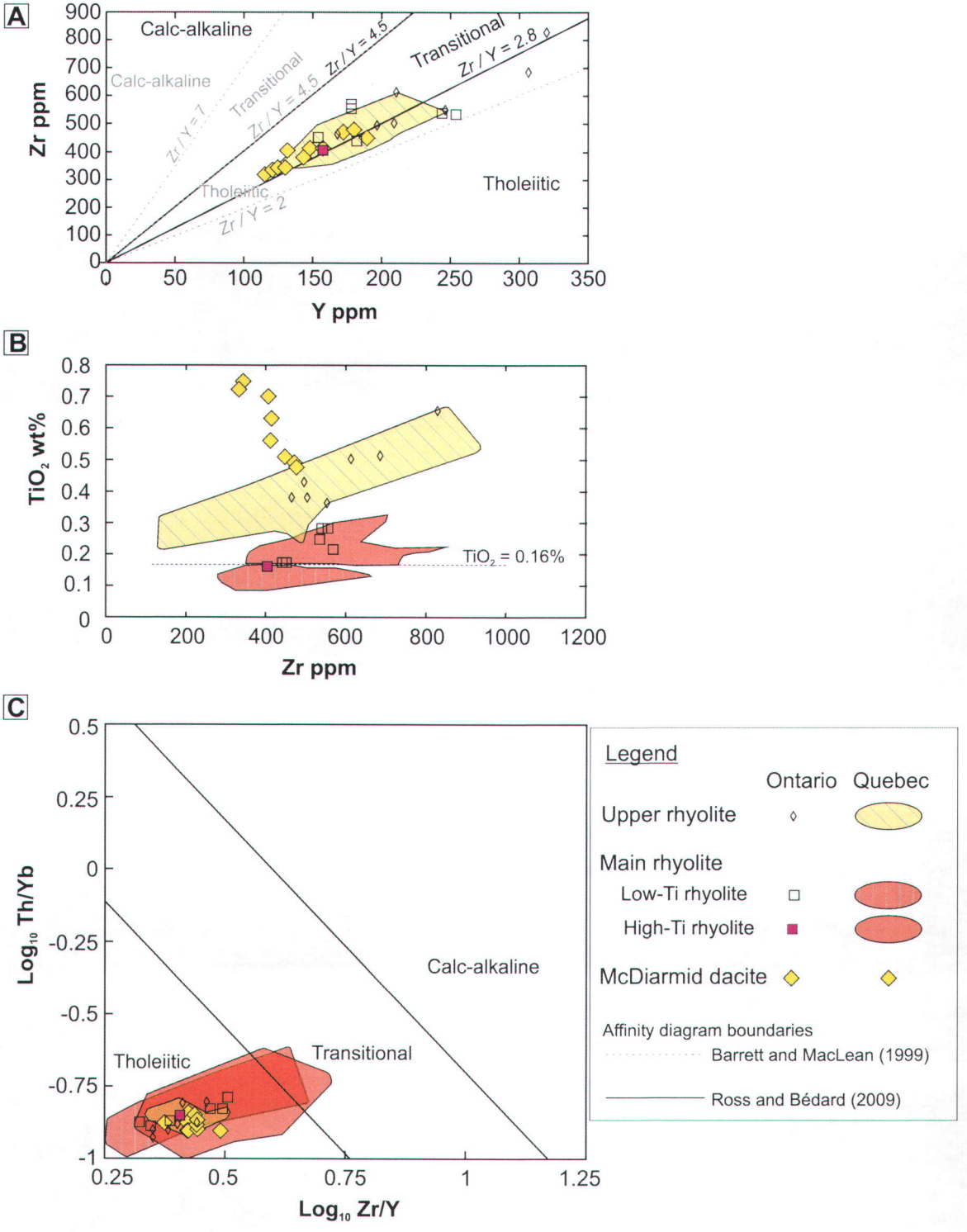

Fig. 3.20: Geochemistry of felsic volcanic rocks from the Hébécourt Formation west of DDH HEB-04. (A) Zr vs Y diagram for the samples west of DDH HEB 04 plotted on fields formed by the samples from east of DDH HEB-04. (B) Graph of TiO_2 vs. Zr for all units west of DDH HEB-04 plotted on fields formed by the samples from east of DDH HEB-04. (C) Magmatic affinity diagram from Ross and Bédard (2009)

3.5.5.3 Facies variations. The McDiarmid dacite in MD-01 is dominated by massive intervals, with the only fragmental facies being very small intervals of typical hyaloclastite. In HEB-09, the next DDH east of MD-01 (but with 2.8 km in between), the base of the interval is predominantly massive with two 3-4 m intervals of the monomictic lapilli-tuff, above which is a sulphide-bearing stratified horizon (see Chapter 5). Above this horizon there is a small massive interval, followed by finely laminated tuff, interbedded with which is one argillite lamination. The lobe facies is above this.

In HEB-04, the easternmost DDH in which this unit is present, there are still significant thicknesses of massive rock, but the thickness of the fragmental intervals are thicker than seen in the other two DDH. The base of the unit consists of a massive interval at the base, three massive intervals in total separated by two intervals of lapilli-tuff, and the youngest massive interval is overlain by a normally graded interval, from lapilli-tuff to finely laminated tuff.

A reliable interpretation from the facies variations in this unit is much less likely than for the units east of DDH HEB-04 because: 1) the distances between the drill holes is much greater than that to the east (Fig. 3.1) and 2) there are no surface observations of this unit.

In general, the proportion of massive facies decreases to the east and the proportion of fragmental facies increases, with lobe facies seen in the central DDH only, suggesting a proximal to distal variation from west to east (see Chapter 2). However, the presence of the sulphide bearing horizon and the other argillite lamination in DDH HEB-09 clearly divides the unit in this hole into three separate events, and which of these events correlates to what is seen in the other holes is unknown.

Whether the observed units in all three holes shared a vent, whether the three separate events seen in DDH HEB-09 were from the same vent, how the three separate events in DDH HEB-09 relate to the other holes, the number of vents and the location of the vents are all questions that cannot be answered at present.

3.5.5.4 Geochemistry. On the Winchester and Floyd (1977) diagrams, the McDiarmid dacite plots within the rhyodacite/dacite field, but with a lot of scatter, even extending into the andesite field (Fig. 3.19a and 3.19b). The Zr vs. TiO_2 plot shows that this unit is distinct from the other felsic units in the study area, but also shows more of a fractionation pattern than an alteration pattern (Fig. 3.20b), suggesting that with more information available the McDiarmid dacite may become divisible into several subunits. The unit straddles the tholeiitic-transitional boundary of Ross and Bédard (2009) but is clearly tholeiitic as shown by the boundaries of Barrett and MacLean (1999) on the Zr vs. Y diagram (Fig. 3.20a) and the Zr/Y vs. Th/Yb diagram (Fig. 3.20c).

3.6 Reneault-Dufresnoy Formation in Québec and Ontario

The Reneault-Dufresnoy Formation is the youngest stratigraphic unit in the study area. Only the base of the formation was documented in this study (the first 250-300 m in Québec and 30-40 m in Ontario). The mafic to intermediate lavas are pillowed to massive, with fragmental rocks contributing only a small proportion of what was seen in this study, although Ross et al. (2008a) describe larger volumes of mafic to intermediate volcaniclastic rocks further south, near the Monsabrais Pluton (Fig. 3.1). The Reneault-Dufresnoy Formation in the Monsabrais area, just south of the Hébécourt Formation, is interpreted as a south-facing tilted volcano (Ross et al., 2008a; submitted a).

3.6.1 Massive facies

The massive facies has more variety in grain-size, from medium- to very fine-grained, than the pillowed facies. The massive rocks are green to medium gray in color, and have up to 2% carbonate or chlorite filled vesicles, which are up to 2 mm in diameter. In thin section, the variation in grain size is also visible, but in all cases the groundmass is formed of randomly orientated laths of feldspar surrounded by irresolvable dark brown material.

3.6.2 Pillowed facies

The pillows are formed of aphyric, fine-grained lava that is a medium gray to green color on fresh surfaces. The pillows are typically less than a meter across with a minimum size

of 70-80 cm, although they can be up to 2 m in size locally. There are typically 2-3% vesicles, but locally up to 20%, 1-3 mm in diameter and filled by quartz (sometimes rose quartz) and chlorite. In some cases, the vesicles concentrate towards the pillow margins, but this is not as common as seen in pillow facies of the Hébécourt Formation. In thin section, there is a greater proportion of vesicles seen (4-5%) than in hand specimen since many are smaller than 1 mm. The vesicles seen in thin section are predominantly filled of quartz, although about a quarter of them are filled with calcite, and in some cases both. The vesicles range in size from 20 μm to 70 μm, and in drill core the largest are seen in portions from lower down in the stratigraphy. The pillow margins are occasionally variolitic; the varioles are less than 0.5 cm across and coalesce rapidly towards the centre and are indistinguishable after 4-5 cm. There is evidence of silica and chlorite veining, with patchy epidote alteration locally. Typical hyaloclastite is seen between the pillows, with chlorite- and epidote-altered, angular fragments that are 3-4 mm across and can be up to 1 cm. In many cases, there is pyrite and pyrrhotite associated with the inter-pillow hyaloclastite.

3.6.3 Volcaniclastic rocks

The fragmental rocks mainly consist of pillow breccia, although there are rare occurrences of tuff. The pillow breccia comprises pillow fragments within typical hyaloclastite. There is up to 10% massive and vesicular basalt pillow fragments that are greater than 15 cm. These pillow fragments have fluidal shapes, chilled margins and vesicles concentrated around the margins. In some cases, there are varioles visible on some of the pillow fragments. The hyaloclastite has angular, chloritised, jigsaw-fit fragments that are 2-4 mm across and held together with quartz and chlorite cement.

3.6.4 Geochemistry

There were 28 geochemical samples taken in this unit (for both provinces together), including 26 from drill core. All of these samples are from the lower 250-300 m in the Reneault-Dufresnoy Formation in Québec and the lower 30-40 m in Ontario. In addition, figures 3.7 and 3.8, display a compiled field of samples from a wider geographic region (extending further south, i.e. stratigraphically upward). Despite some major element

mobility, all of these samples plot as basalts and andesites on the Winchester and Floyd (1977) diagrams (Figs. 3.7a and 3.7b). Two groups have been defined based on magmatic affinities (Figs. 3.8) and trace element patterns (Figs. 3.9c and 3.9d). Although rocks from both groups are not always found together, rocks from the first group (Group 1) are systematically located stratigraphically below the rocks of the second group (Group 2). Ross et al. (submitted a) also noted that there are variable magmatic affinities within the mafic to intermediate rocks of the Reneault-Dufresnoy Formation further south.

The samples from Group 1 are tholeiitic to transitional, whereas the samples from Group 2 are transitional to calc-alkaline in magmatic affinity, suggesting a general change to more calc-alkaline magmatism with time in the first 250-300 m of the Reneault-Dufresnoy Formation. On extended trace element diagrams, Group 1 profiles have gentle to moderate overall slopes, shallow Nb-Ta anomalies, small Zr-Hf plateaus, and small negative (sometime positive) Ti anomalies. In contrast, Group 2 profiles are more steeply inclined, have deeper Nb-Ta troughs, more pronounced Zr-Hf plateaus and deeper Ti anomalies. These profiles resemble those of modern oceanic arc magmas (Jenner, 1996).

3.7 Intrusions

The intrusions observed in the study area were predominantly mafic with a felsic intrusion only observed at one outcrop. There are predominantly two types of mafic intrusions. The first type forms thick intrusions which can be represented on the map. Description of the first type of mafic intrusions is based on the intrusion observed in the centre of the felsic package in Québec (Fig. 3.1). It is medium grey, massive and homogenous, with a grain size of up to 2 mm in the centre but finer to aphanitic towards the margins, with sharp contacts. The rock is locally feldspar–phyric, typically 2-3% with occasionally up to 10% when the texture is glomeroporphyritic. This intrusion and others like it are typically parallel to the stratification observed in the surrounding volcanic rock.

The second type of mafic intrusion, which is likely of the same generation as the first type, forms thin intrusions. These intrusions were seen in drill core, and although they are too thin to be shown on the map, they do significantly contribute to the thickness of the

volcanic sequence. This type ranges in scale from centimetres to metres and is typically fine to medium grained, although the grain size sharply decreases towards the margins. Chilled margins can sometimes be observed at the contacts with the surrounding rocks, but not in every case. They are typically medium grey to green in colour, not magnetic, aphyric, and homogenous.

The first and second types are believed to be mostly syn-volcanic in origin. There is a another generation of mafic intrusions cutting the stratification of the volcanic rocks, and these are believed to be much later although they were not observed directly during this study and no emphasis was given to the intrusions generally in this study.

The felsic intrusion observed at outcrop only is massive with visible quartz phenocrysts 1-2 mm, but with an otherwise fine grain size.

3.8 Chapter summary

This chapter has subdivided the geology of the Hébécourt and Reneault-Dufresnoy Formations in the study area on a chemo-stratigraphic basis. In summary, the Hébécourt Formation east of DDH HEB-04, where the chemo-stratigraphy is firmly established, consists of the Hébécourt basalt, Hébécourt basaltic andesite, the main rhyolite (low-Ti), the main rhyolite (high-Ti) and the upper rhyolite. The facies within each of these units has been described and the variations of the facies within some of these units have been interpreted to reconstruct a most likely mechanism of emplacement. The whole succession is interpreted as the product of bimodal submarine effusive volcanic activity: mafic rocks form massive, pillowed and fragmental lavas, whereas felsic units form massive to fragmental lavas and extrusive domes. There are no obvious pyroclastic rocks in the succession.

Using the mechanisms of emplacement and facies variations, the location of the effusive centers for these units could be predicted (Fig. 3.21). The proposed vent location for the low-Ti subunit from the main rhyolite is in the vicinity of DDH HEB-02. For the high-Ti subunit, two vents are proposed: one in the vicinity of DDH HEB-04 and one between

DDHs HEB-01 and HEB-02. Two vents are also predicted for the upper rhyolite; one in the vicinity of DDH HEB-01 and one west of DDH HEB-04 (not shown).

The Hébécourt basaltic andesite vent is predicted to be east of DDH HEB-03, and no predictions were made for the Hébécourt basalt or the Reneault-Dufresnoy Formation, which overlies the Hébécourt Formation.

While the same geochemical units can be observed in Ontario and west of DDH HEB-04 in Québec, the stratigraphic order of the units is very different, and this along with the distance between the control points in both provinces makes it unlikely that they shared any vents, at least for the felsic rocks. The information available west of DDH HEB-04 was not sufficient to constrain facies variations or predict vent locations.

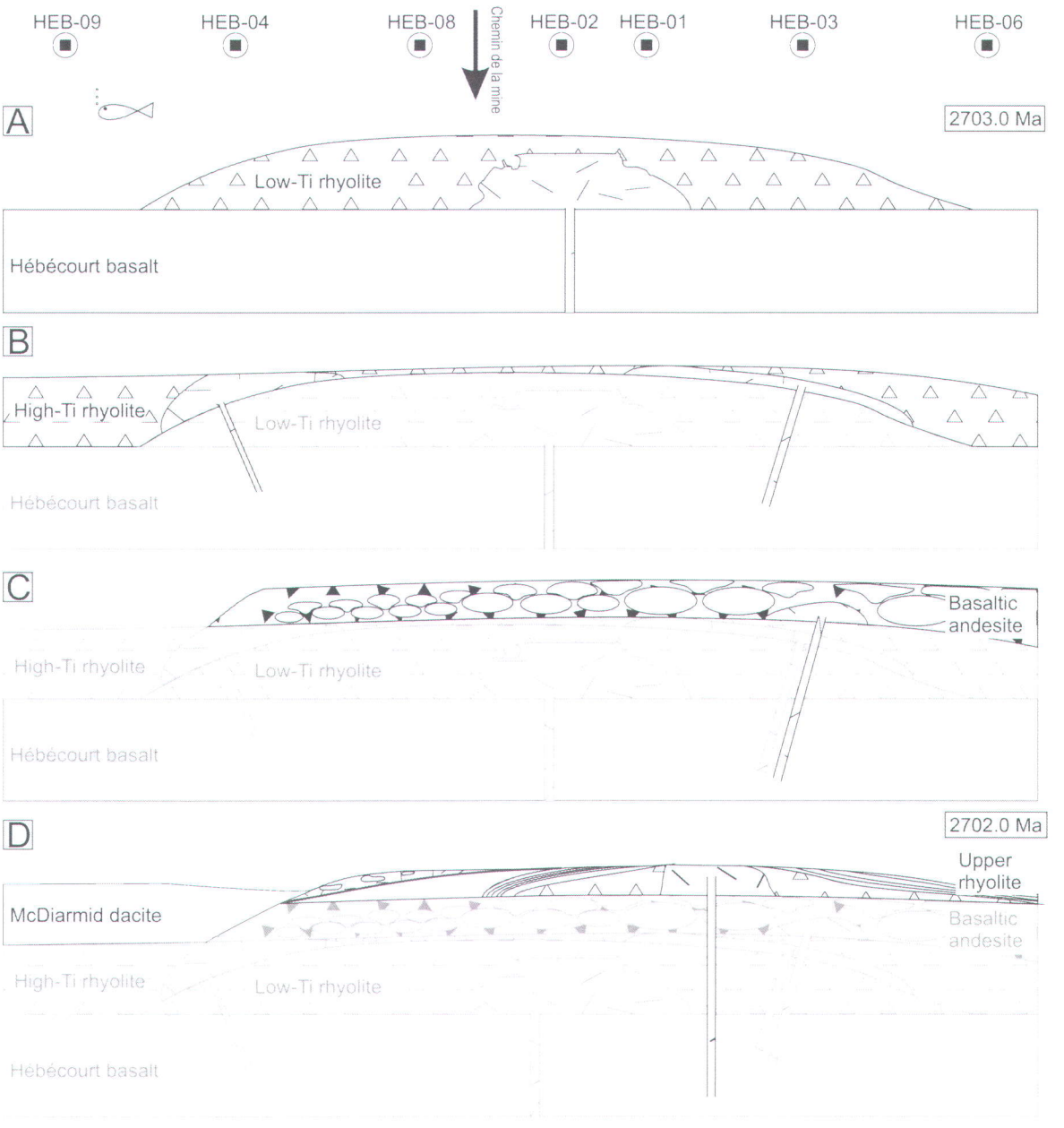

Fig. 3.21: Geological history of the study area, focusing on the top part of the Hébécourt Formation, illustrated by schematic sections (not to scale). (A) Deposition of the low-Ti subunit of the main rhyolite. Triangles represent the fragmental facies and randomly orientated dashes represent the massive facies. (B) Eruption of the high-Ti subunit of the main rhyolite, from two separate vents.(C) Eruption of the youngest intercalation of the Hébécourt basaltic andesite. Filled triangles represent hyaloclastite and the pillows decrease in size to the west. (D) Eruption of the upper rhyolite from the easternmost vent, as the western vent is unknown. Also shown is the McDiarmid dacite, erupted from an unknown vent.

4. Alteration and mineralization

The top of the Hébécourt Formation in the area between the Ontario-Québec border and Lake Hébécourt, including the two rhyolites described in chapter 3, has historically been recognized as a potentially fertile area for VMS-type mineralization since the discovery of zinc in this area in the early 1970s. Since then, exploration has focused mainly on the main rhyolite east of the Chemin de la Mine (Fig. 3.2). Other areas may also have potential for VMS mineralization, as shown in subsequent chapters. The current chapter describes the alteration using alteration indices, describes the distribution of the alteration using thematic maps of the alteration indices and describes the alteration minerals seen in hand sample and thin section. In addition the historical mineralization is described here.

4.1 Alteration

4.1.1 Alteration indices

The alteration box plot (Large et al., 2001; Gifkins et al., 2005) consists of two alteration indices ranging from zero to 100, the Ishikawa index (AI: Ishikawa et al., 1976) and the chlorite-carbonate-pyrite index (CCPI). The AI is a good indicator of chlorite and sericite alteration as well as plagioclase destruction, white the CCPI is able to distinguish between chlorite and sericite while also identifying carbonates and pyrite. The two combined indices can further be used to identify possible diagenetic assemblages such as epidote+calcite±albite and albite+chlorite, as well as fresh rocks, which then plot in certain boxes depending on their geochemical composition.

The alteration box plot shows that the mafic volcanic rocks in the study area are predominantly fresh (Fig. 4.1a), suggesting that the minor to moderate chlorite and sericite observed in hand samples and thin sections of mafic rocks are metamorphic minerals. The felsic rocks, by contrast, show several alteration assemblages including hydrothermal assemblages. The hydrothermal alteration assemblages are chlorite±pyrite±sericite and sericite+chlorite+pyrite, perhaps with some carbonate alteration. There is also an albite+chlorite diagenetic assemblage, as well as an epidote+calcite±albite diagenetic assemblage (Fig. 4.1b). The alteration assemblages

suggested by the box plot can be confirmed by drill core and petrographic observations on felsic rocks, with some limitations, as explained below.

4.1.2 Distribution of alteration

Thematic maps of the AI were created to locate the most altered regions. Values below 20 are indicative of diagenetic assemblages, fresh rocks have AI values between 20 and 60-65, and rocks with higher values are increasingly more altered (Gifkins et al., 2005). AI values were calculated for compiled datasets of historical and new surface samples (Fig. 4.2a) and drill core samples (Fig. 4.2b). Figure 4.2a shows that the low-Ti rhyolite is much more significantly altered than the overlying high-Ti rhyolite near the Chemin de la Mine. The differing degrees of alteration of the main rhyolite subunits were also seen in drill cores further east (Fraser, 1991; Martin, 1994; Bambic, 1998), as shown on figure 4.2b. The samples having suffered diagenesis are located to the west of the Chemin de la Mine in the high-Ti rhyolite, in the proposed region of the western vent for this unit (Chapter 3).

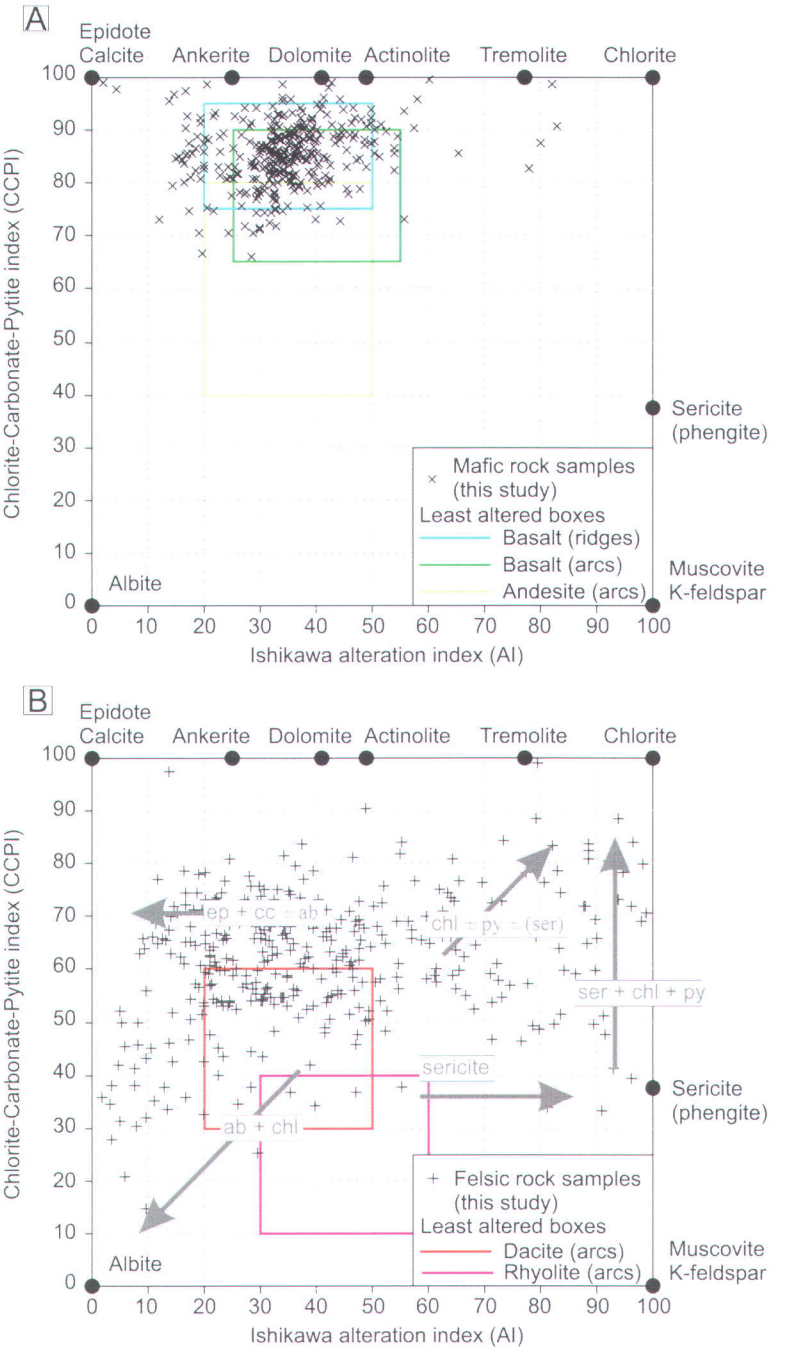

Fig. 4.1: Hydrothermal alteration in the study area. (A)-(B) Alteration box plots of AI vs. chlorite-carbonate-pyrite index (CCPI) (Large et al., 2001; Gifkins et al., 2005) for mafic and felsic samples, respectively. The geochemical analyses used are from this study and a compiled data set supplied by Cogitore Resources Inc. The box of unaltered basalts from young submarine ridges has been compiled from the GEOROC database (http://georoc.mpch-mainz.gwdg.de/georoc/, 274 samples with outliers excluded), whereas the four other boxes for unaltered young arc rocks are taken from Gifkins et al. (2005).

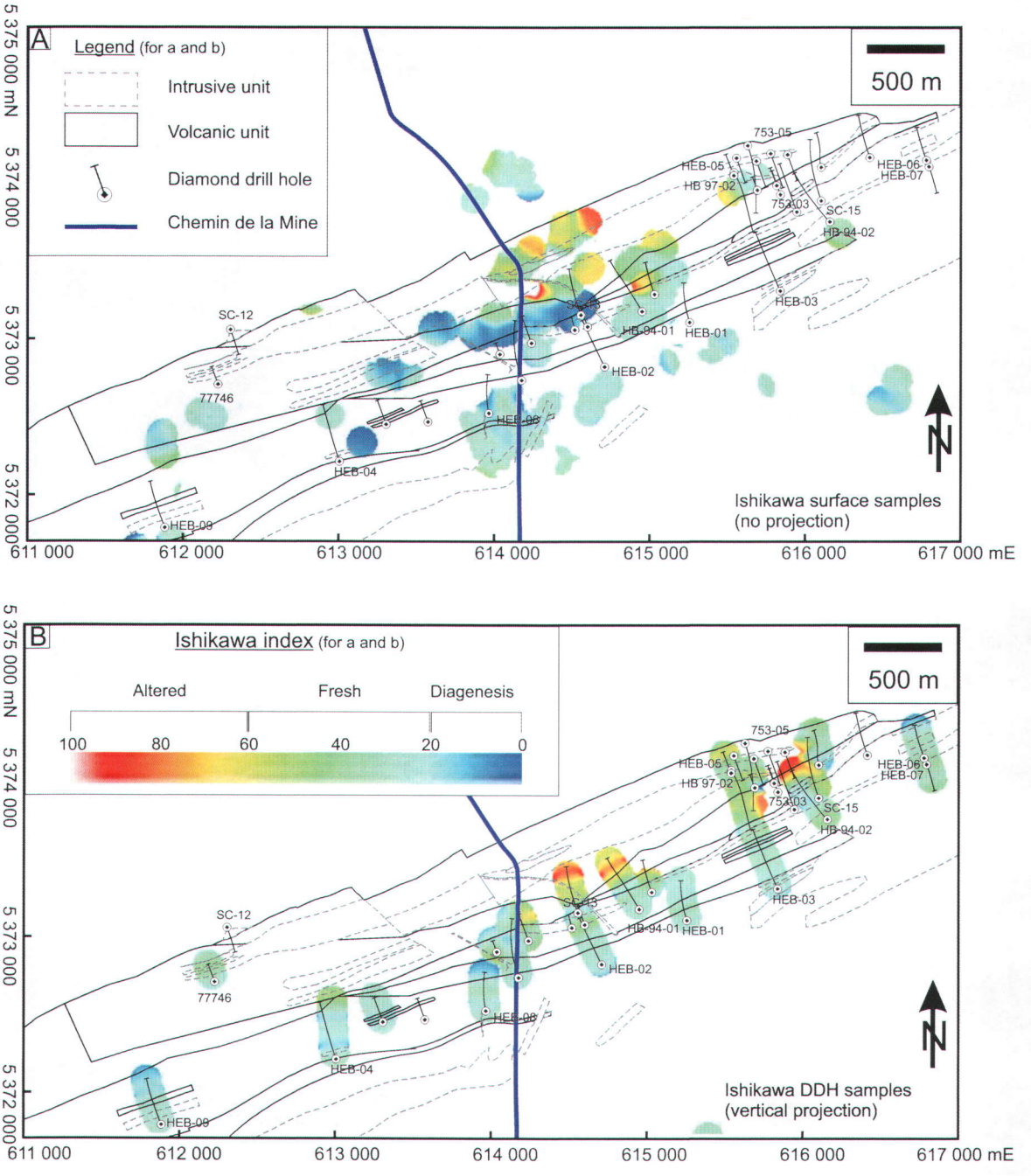

Fig. 4.2: Hydrothermal alteration in the study area. (A)-(B) Maps of the Ishikawa alteration index (AI) (Ishikawa et al., 1976) for surface samples and drill core samples, respectively. Geological boundaries are provided for reference. Note that for simplicity, core samples are projected vertically from variable depths and likely do not project to the right geological unit at surface (recall the 72°S dip of strata). The 10 m AI grids were produced by interpolation between samples with a search radius of 100 m and a minimum of two samples per grid point.

4.1.3 Alteration observations

The observed alteration minerals and textures will now be described, as seen in hand sample and thin section. However, when sampling for this study, the focus was on least-altered samples for both geochemical and thin section samples, to improve the chemo-stratigraphy of the study area and study primary volcanic textures. Also, the DDHs in which the most altered rocks occur were not available for sampling. As a result, highly altered samples were not selected, and the following descriptions likely do not reflect the most intense alteration in the study area. Only felsic rocks are described in this section since mafic rocks are predominantly fresh (secondary minerals are mentioned in Chapter 3 for mafic rocks).

4.1.3.1 Low-Ti rhyolite. The low-Ti rhyolite is the most altered unit in the Hébécourt Formation. There is silica, epidote, sericite and chlorite alteration, with variable intensity. In drill core, the alteration is more intense in the fragmental units, with silica often cementing the fragments. The fragments themselves are often altered by chlorite, sericite and epidote, although these alterations also affect the matrix. In the massive intervals, the alteration is more often vein-controlled and although sometimes the alteration can be intense enough to obscure the primary texture, the alteration is generally weaker in the massive intervals than in the fragmental rocks. In addition, carbonate and iron carbonate alteration have been observed in the field, although this was always vein controlled.

In thin section, the sericite is seen predominantly replacing the groundmass of fragments in volcaniclastic rocks or the groundmass of massive lavas (Fig. 4.3a and 4.3b), although vein-controlled alteration and replacement of feldspar phenocrysts has been seen. In addition, the sericite alteration is more intense toward the base of the low-Ti rhyolite than the top of the unit. The chlorite alteration has a similar pattern to the sericite, with greater intensity at the base of the unit than the top, and the alteration predominantly affecting the groundmass. Silicification is not very common in thin section, but where it is seen, it is predominantly within vesicles, and forming overgrowths on the quartz phenocrysts.

4.1.3.2 High-Ti rhyolite. The alteration in the high-Ti rhyolite is less intense than that in the low-Ti rhyolite, but is still formed of chlorite, epidote, silica and sericite. Again, similar to the low-Ti rhyolite, the alteration predominantly affects the fragmental units. Alteration occurs in both the matrix and the clasts, but is more concentrated in the matrix. Epidote is only present in the massive units, forming spots. Silicification is much less common than the other types of alteration, generally vein-controlled and associated with an intensification of the other types of alteration. Often where silicification is present, the primary texture is completely obscured (Fig. 4.3e). Weak but pervasive carbonate alteration is only present in the westernmost DDH.

In thin section, the same alteration minerals are seen; chlorite, sericite and very minor epidote. These alterations are predominantly replacing the groundmass, although sericite in particular is also associated with veins. Silica alteration is only present in vesicles, as the samples selected to make thin sections were in the least-altered rocks.

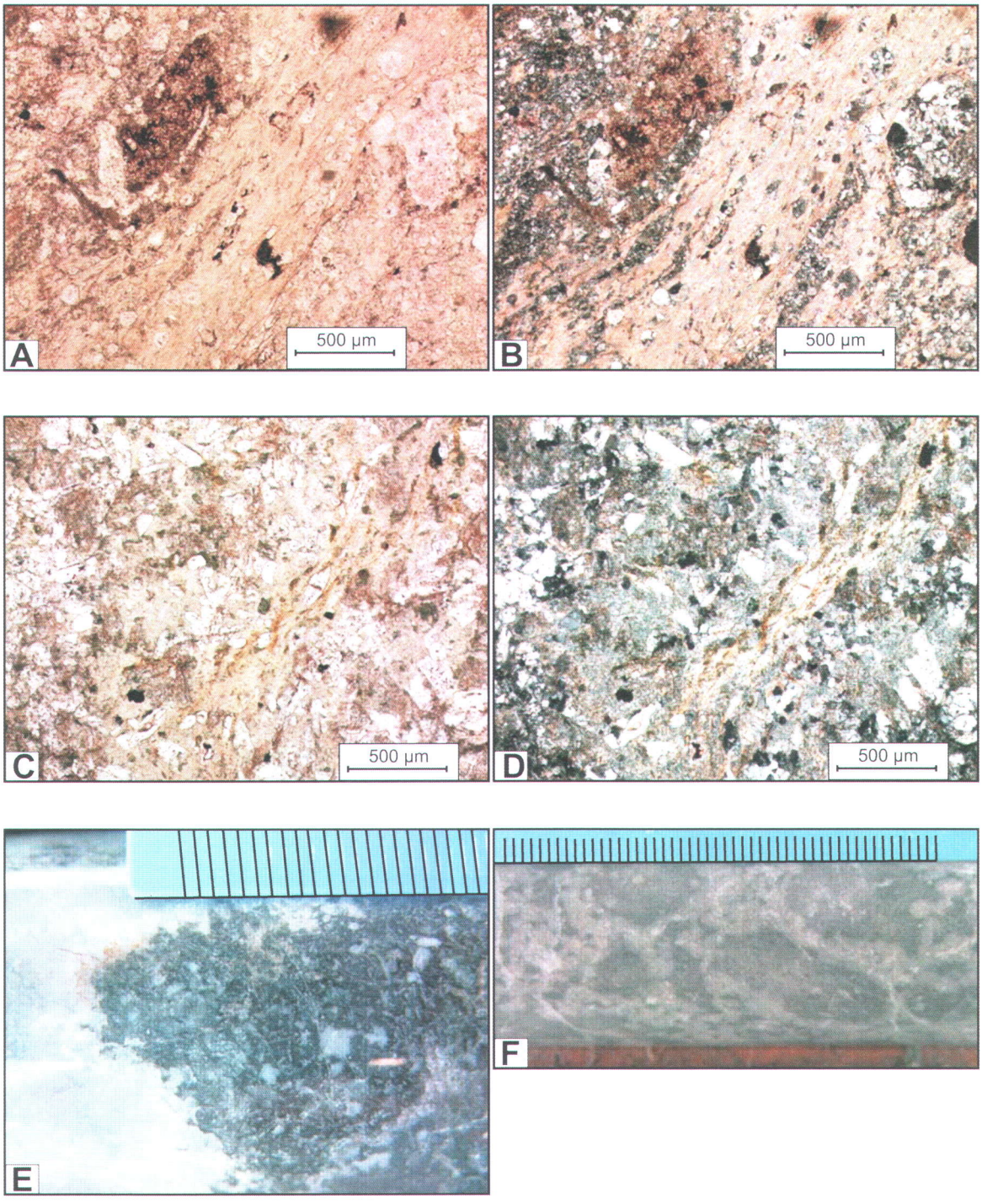

Fig 4.3. A) Plane polarised light photomicrograph of sericite alteration of the groundmass, from a field sample of the low-Ti rhyolite. B) The same as A but in cross polarised light. C) Plane polarised light photomicrograph of sericite veinlets with selvages of sericite alteration, from the upper rhyolite in DDH HEB-02. D) The same as C but in cross polarised light. E) Alteration almost completely obscuring primary texture, predominantly silica in this case, from the high-Ti rhyolite in DDH HEB-04. F) A false fragmental texture formed by silica alteration, from the upper rhyolite in DDH HEB-01. Where the ruler is used as a scale the increments are in millimetres.

4.1.3.3 Upper rhyolite. The upper rhyolite is the least altered felsic unit examined, but still affected by epidote, sericite, silica and chlorite. The alteration varies in intensity, but is concentrated in the matrix of the fragmental units. However the alteration does affect the coherent intervals, in one instance the combination of all four alteration types, with silica predominant, in distinct regions forms a false fragmental texture (Fig. 4.3f) and where the unit is spherulitic, the spherules are highlighted by weak to moderate chlorite alteration. Carbonate alteration is a very minor component seen sporadically throughout the unit but is never more than weak.

In thin section, the same minerals are again visible, chlorite, sericite and epidote predominantly affecting the groundmass. Sericite is also seen altering feldspar phenocrysts, although this is a lesser factor than the alteration of the groundmass (Fig. 4.3c and 4.3d). The sections from the lapilli-tuffs show much more intense sericite and chlorite alteration that the sections from coherent rocks. The chlorite alteration is also more intense where the rock is spherulitic, although it is not known whether this is preferential alteration or if the alteration is more visible even in thin section. Silicification is a very minor component, and where present is concentrated in the groundmass, although in a few cases it is seen filling vesicles.

4.2 Mineralization in the main rhyolite

Copper and zinc contour maps were created based on the available assay data (Fig. 4.4). Note that large search radii were used to interpolate between drill holes and samples, and that depth of mineralization or anomalies was not taken into account when creating these maps. The purpose was simply to visualize where the copper and zinc values were relative to geological unit and alteration patterns.

Based on these rough Cu and Zn contour maps, mineralization and anomalous metal values occur in two zones, informally called zone A (Fig. 4.4a) and zone B (Fig. 4.4b). Zone A is located in the central region of the main rhyolite (mostly within the high-Ti subunit) and is dominated by anomalous Zn, with almost no Cu. The highest values for Zn (6.17% over 0.1 m) are in DDH SC-13 and represent semi-massive bands or stringers

of pyrite and sphalerite (Cloutier, 1975; Martin, 1994; Bambic 1998). There are lesser values south of this area and to the east and west. Slightly to the west, in DDH 77738, Zn occurs in pyrite-rich disseminations and thin, fracture-controlled stringers. In DDH SC-14 to the east, the mineralization consists of pyrite and sphalerite stringers associated with quartz.

Zone B, which is characterized by higher grades than zone A, is located in the north-east corner of the study area (Fig. 4.4b). It consists of up to 40 m-long mineralized intersections within a zone of chlorite and sericite alteration (Cloutier, 1975; Bambic, 1998). Copper and zinc values come from both disseminations and sulphide stringers (Cloutier, 1975), with Zn more widely distributed than Cu. The disseminations of pyrite, sphalerite and chalcopyrite occur mostly in the westernmost region of zone B, whereas pyrite-dominated stringers are found in the eastern region (Cloutier, 1975). The highest Cu grades (0.19% Cu over 1.9 m) and the most altered rocks (AI = 80 to 95, due to both chlorite and sericite alteration) occur in DDH 753-07, where mineralization occurs in the matrix of a low-Ti rhyolite breccia containing angular fragments of an average size of 3-4 cm (Cloutier, 1975). This breccia is part of the east flank of the low-Ti dome. Much lower Cu-Zn values occur higher up in the high-Ti rhyolite. The best Zn intersection in zone B is 11.6% Zn over 1.1 m in DDH 753-01 (Cloutier, 1975).

It is interesting to remark that the most altered and mineralized rocks occur in rhyolite breccias and that mineralization probably formed by sub-seafloor replacement, given the textures (disseminations and stringers). This has implications for exploration in the area, as will be discussed in Chapter 6.

4.3 Chapter summary

This chapter has established that the mafic rocks are predominantly fresh and has outlined the types of alteration present in the felsic rocks of the study area. The low-Ti subunit of the main rhyolite is the most altered felsic unit, followed by the high-Ti and the upper rhyolite. All three units are affected by chlorite, sericite, silica and epidote alteration. It has also been shown that the regions with the highest base metal values are spatially

associated with the most altered areas, and as will be discussed in more detail in Chapter 6, these areas are spatially associated with the effusive centres identified in the previous chapter.

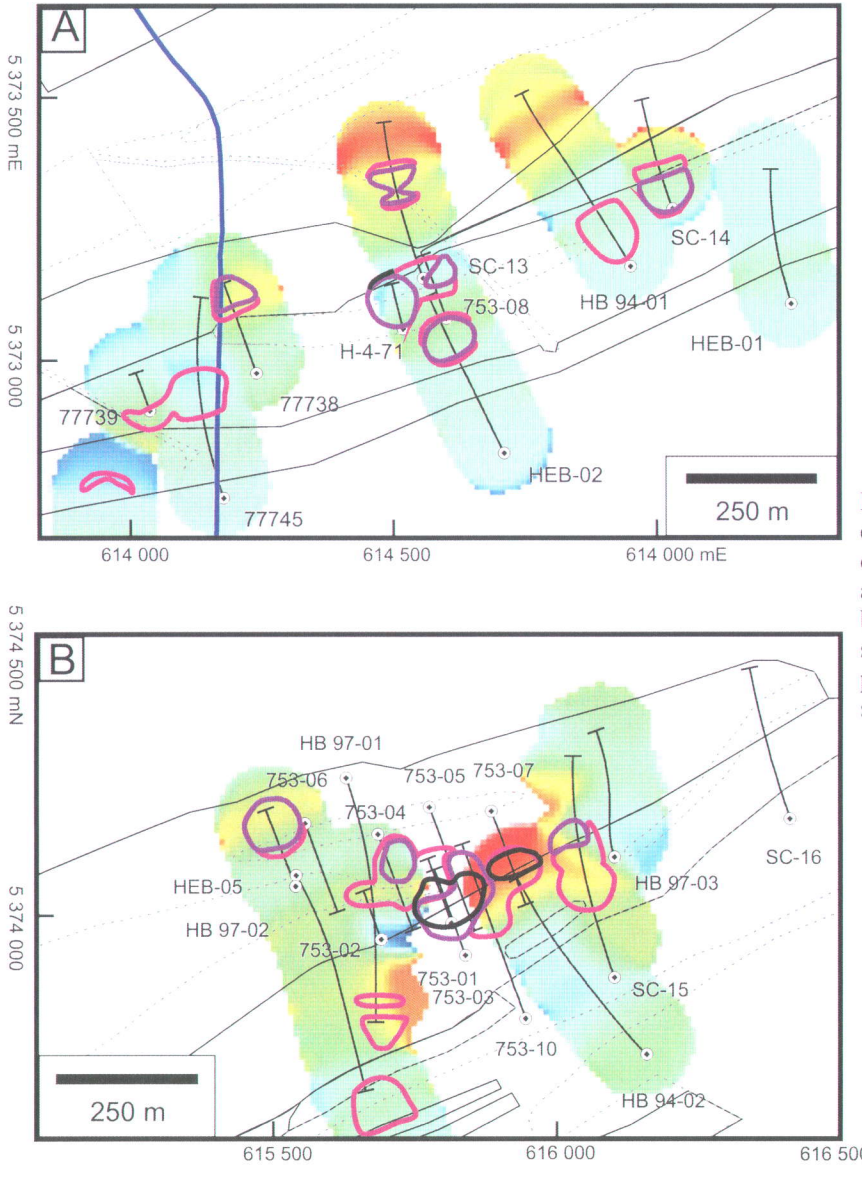

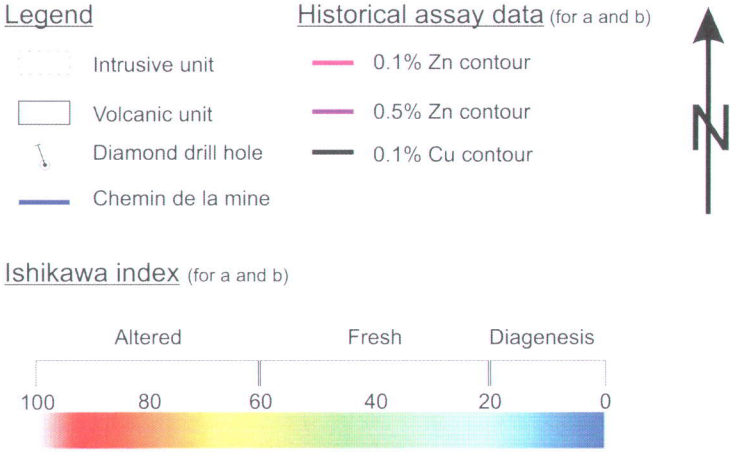

Fig. 4.4: Base metal mineralization in the study area. (A)-(B) Copper and zinc contours representing mineralized zones A and B, respectively (see text for descriptions), superimposed on a grid of the Ishikawa alteration index (Ishikawa et al., 1976) for drill core samples, prepared as in figure 4.2. The Cu and Zn contours are based on 5 m grids of drill core assays using interpolation between samples with a search radius of 50 m and a minimum of two samples per grid point. Samples were projected vertically from various depths to the surface for both alteration and assays, so the geological boundaries are provided for reference only.

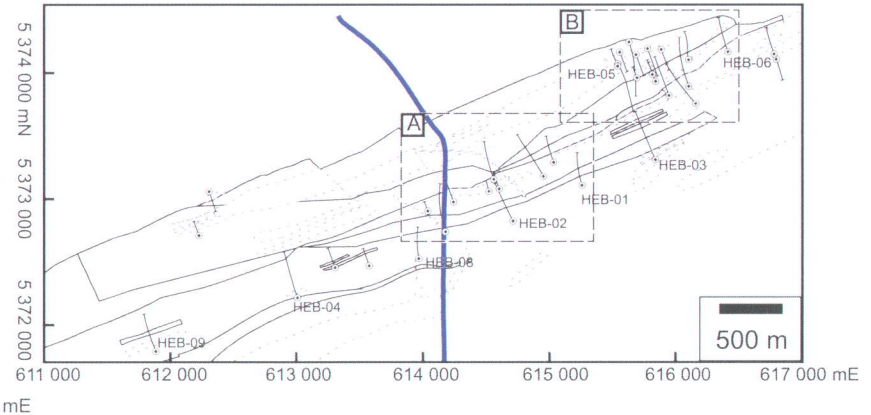

5. Sulphide-bearing stratified horizons, and their use in targeting hydrothermal up-flow zones

Two sulphide-bearing stratified horizons, historically believed to be exhalative in origin ("exhalites"), were previously identified at the contact between the main rhyolite and the youngest basaltic andesite in the Hébécourt Formation, and at the contact between the Hébécourt upper rhyolite and the Reneault-Dufresnoy Formation (Fraser, 1991; Carignan and Lafrance, 2008). Cogitore Resources Inc. has obtained Zn values up to 1.2% over core lengths of several decimeters for these horizons (Carignan and Lafrance, 2008). During the examination and sampling of these horizons in DDHs HEB-01 to HEB-09, it was noted that they do not always occur at the contacts mentioned above (see Figs. 5.1 and 5.2), and that the number of these horizons in a particular DDH ranges from one to three. A few horizons are actually found in the Reneault-Dufresnoy Formation (Figs. 5.1 and 5.2). In addition, it is inferred, due to observations explained below, that sulphides in these horizons have largely been introduced by sub-seafloor replacement rather than by precipitation and sedimentation from a hydrothermal plume in the water column (Fig. 5.3). Hydrothermal fluids rose up in fractures within coherent portions of the lava pile, or in the primary porosity of volcaniclastic deposits; when fluids encountered the pre-existing bedded tuffaceous to sedimentary horizons, they changed pathways to move laterally along these horizons, where they precipitated the sulphides. Therefore, sulphide-bearing stratified horizons are largely not exhalative in origin, but they can still be used in identifying possible hydrothermal up-flow zones. The idea is that high metal values in sulphide-bearing stratified horizons can indicate mineralized zones at deeper (or even possibly higher) stratigraphic levels, since metal-bearing fluids which introduced the sulphides in these horizons were moving mostly in a vertical direction before they permeated the stratified horizons. Some of the very fine-grained concordant pyrites may still be exhalative, as discussed below.

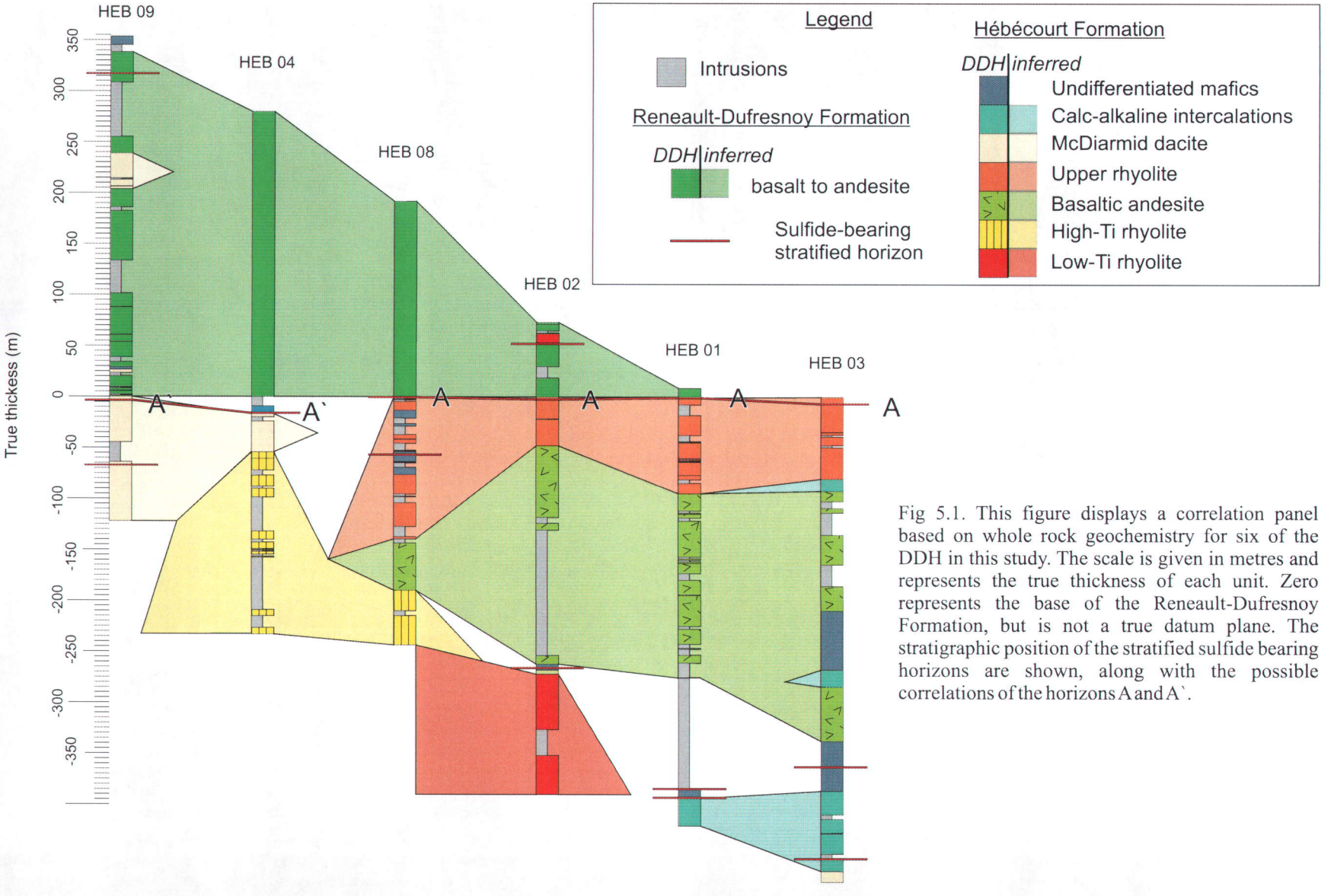

Fig 5.1. This figure displays a correlation panel based on whole rock geochemistry for six of the DDH in this study. The scale is given in metres and represents the true thickness of each unit. Zero represents the base of the Reneault-Dufresnoy Formation, but is not a true datum plane. The stratigraphic position of the stratified sulfide bearing horizons are shown, along with the possible correlations of the horizons A and A`.

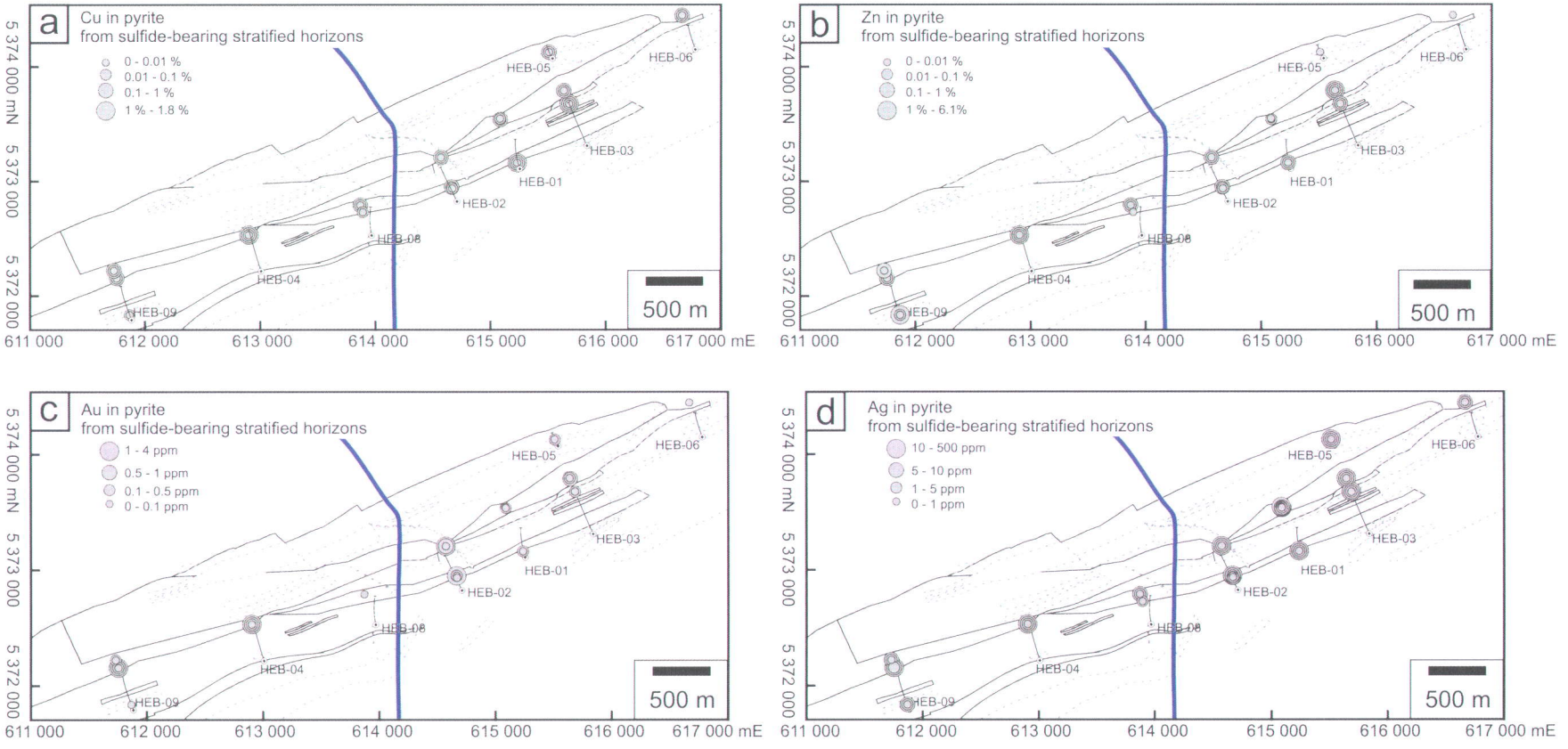

Fig. 5.2: Thematic maps for Cu (A), Zn (B), Au (C) and Ag (D) values in pyrites from sulfide-bearing stratified horizons in drill core, based on LA-ICP-MS measurements. The samples are projected to the surface using the regional dip of 72°S, so they plot at the correct stratigraphic position.

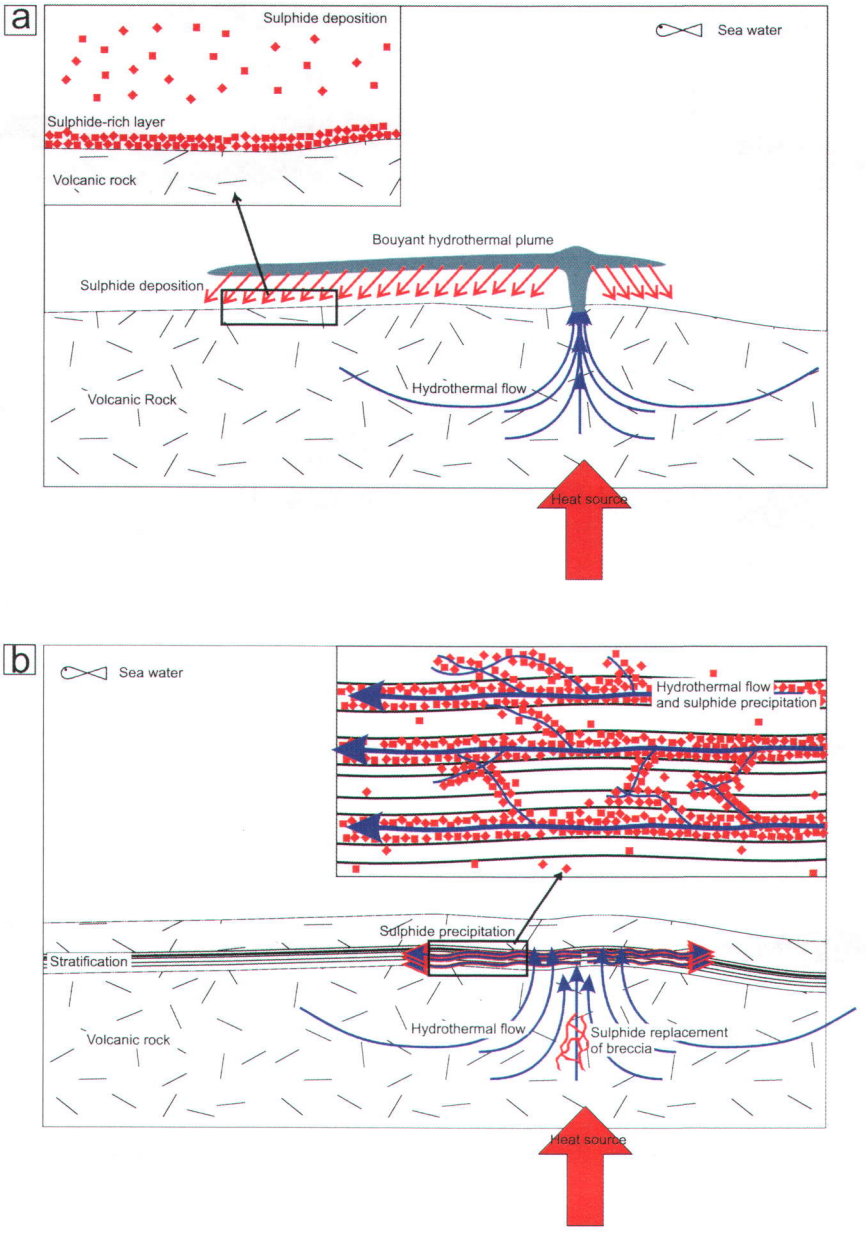

Fig. 5.3. (A) Mechanism of emplacement for a typical exhalite. Uprising hydrothermal fuids forming a bouyant plume vents into seawater, with precipitation and deposition of the sulphide from the plume. (B) Mechanism of sulphide emplacement believed to be active in the study area, hydrothermal fluid rose in a broad up-flow zone and spread along stratified horizons, with precipitation occuring within the existing stratigraphy.

5.1 General description of sulphide-bearing stratified horizons

Sulphide-bearing stratified horizons include (i) thinly laminated to thinly bedded intervals, 20 cm-thick on average (locally up to 50-60 cm-thick) consisting of alternating fine-grained volcanic ash, chlorite, argillite and very fine-grained pyrite (Figs. 5.4a, 5.4b and 5.4c), and (ii) generally thicker tuffaceous intervals, 60-70 cm thick on average, which typically lack internal stratification (Fig. 5.4d).

In the thinly laminated to thinly bedded intervals, which have an average thickness of 20 cm, individual layers range from 1-2 mm to 3-4 cm in thickness. The laminations containing fine-grained ($\leq$1 mm) pyrite, when present, are often the thinnest, <1 mm to 2 mm thick, and in many cases the pyrite is hosted by argillite. Chlorite veinlets are also observed, suggesting that the chlorite laminations represent replacement of tuff laminations.

The thicker tuffaceous units consist of tuffs and lapilli-tuffs (Fig. 5.4d). The larger clasts in these units, when present, are typically 2-3 cm across and are most commonly angular, although in some cases they are rounded. Grading is not a commonly observed feature. These volcaniclastic rocks are possibly the result of suspension deposition through the water column during time intervals representing gaps in the effusive activity.

In a few cases, the laminated intervals are disturbed, showing a progression from well-preserved lamina to syn-sedimentary folding and faulting (Fig. 5.4e), to clastic units where lamina can still be seen in many of the clasts. These intervals were likely formed from syn-sedimentary processes, such as slumping, sliding and dewatering.

Chalcopyrite and sphalerite were petrographically observed to be minor to trace phases in the sulphide-bearing stratified horizons, but the dominant sulphide mineral, occurring in all samples, is pyrite. Therefore pyrite was chosen for systematic investigation of its metal contents.

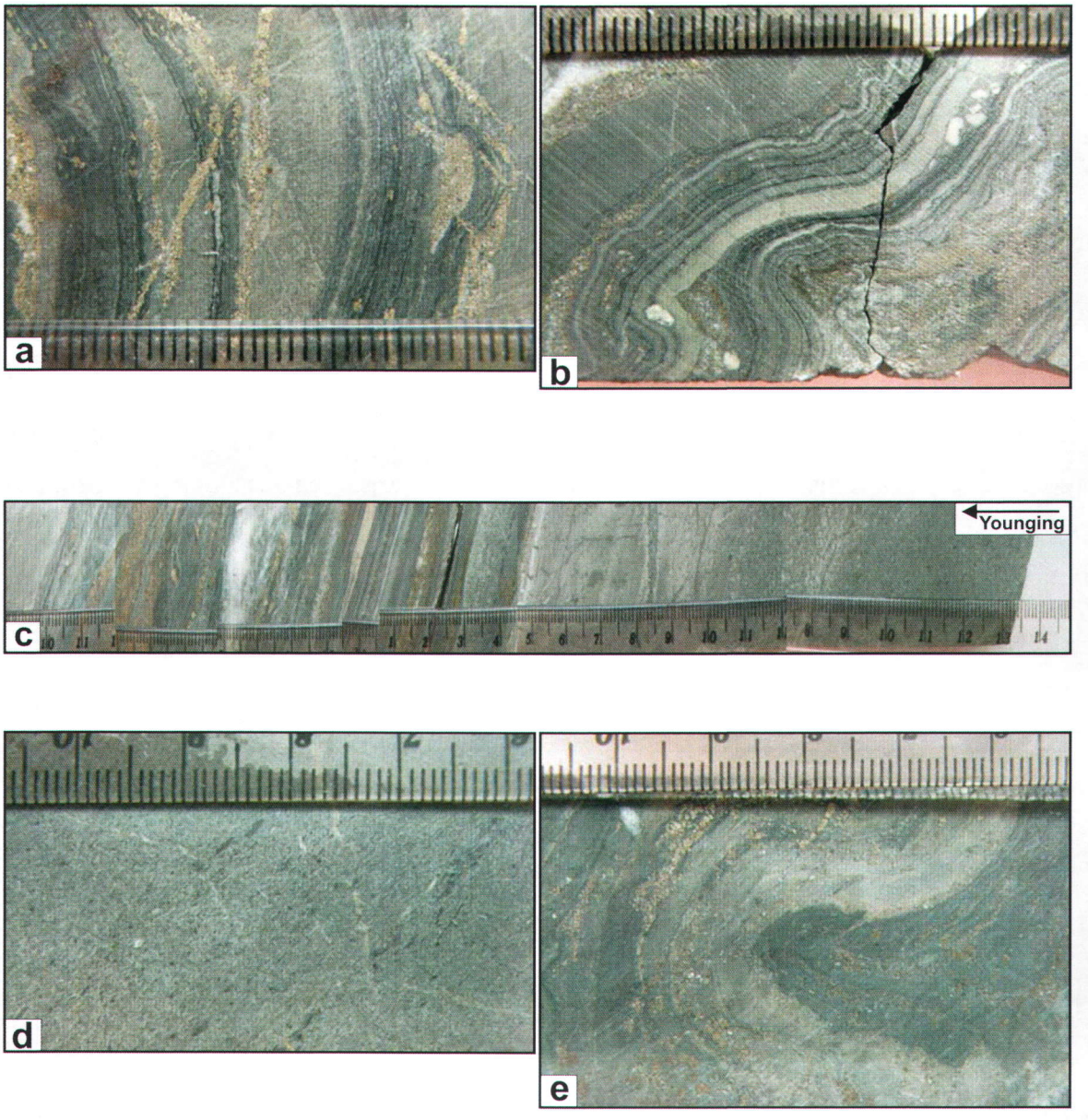

Fig. 5.4: Photographs of the sulphide-bearing stratified horizons. (a) Thinly laminated to very thinly bedded interval containing tuff and argillite. Pyrite is present in veinlets and in blebs between and within layers. (b) Thinly to thickly laminated tuffaceous interval showing syn-sedimentary deformation. Fine-grained concordant pyrite is associated with some laminations. (c) A composite image of the sulphide-bearing horizon in HEB-04 showing an upward progression form coarser tuff to finer and then finely laminated intervals which have high concentrations of pyrite. (d) An example of the tuffaceous intervals which form the thicker intervals between the sulphide-richer finely laminated intervals. (d) An example of the laminated fragments in some of the chaotic, disturbed sediments. Where the ruler is used as a scale the increments are in millimetres.

5.2 Pyrite occurrences and textures in the thinly laminated to thinly bedded intervals

Pyrite is most common in the thinly laminated to thinly bedded intervals, as opposed to the thicker tuffaceous units. The pyrite is typically fine-grained (<2 mm) and is often associated with particular laminations (Fig. 5.4a). In some cases, the abundance of pyrite is high enough to give the impression of sulphide laminations. Disseminations of pyrite spread evenly across several laminations are rare. There are occasions where the pyrite forms coarse blebs within a lamination or at the boundary between two.

Discordant pyrite veinlets can occur in any unit (Fig. 5.4a). In the veinlets, pyrite is typically associated with quartz, although in some cases the veinlets are entirely made of pyrite. The pyrite grains in the veinlets are typically coarser than those associated purely with laminations (Fig. 5.5b), and also in some cases better formed. In many cases, veinlets cut the laminations or connect with them, suggesting that at least some of the concordant pyrite has also been introduced by hydrothermal fluids after sediment deposition.

Small inclusions of other sulphide and silicate minerals within the pyrite are very common (Figs 5.5a-c). In contrast, euhedral coarser-grained pyrites (>2 mm) contain far fewer inclusions, probably as a result of metamorphic recrystallization (Chapman et al., 2008) (Fig. 5.5d).

Although the pyrite associated with the veinlets is typically well formed with few inclusions and that the pyrite associated with the laminations is inclusion rich, these are only general observations and there are inclusion-rich pyrites within the veinlets. In addition the veinlets are often seen connected to the laminations, which suggests that all pyrite in the sulphide-bearing stratified horizons was formed by the same hydrothermal system.

5.3 Stratigraphic position of the sulphide-bearing stratified horizons

As mentioned above, the stratigraphic position and lateral extent of the sulphide-bearing stratified horizons are variable from hole to hole. Figure 5.1 shows the position of these

horizons in relation to the stratigraphy. The majority of these horizons are in the Hébécourt Formation, but two are within the Reneault-Dufresnoy Formation: the uppermost in HEB-09 and HEB-02. A sulphide-bearing stratified horizon at the top of the upper rhyolite (horizon A) has been correlated between four DDHs consisting of HEB-03, HEB-01, HEB-02 and HEB-08. A second horizon (A') has been correlated at the top of the McDiarmid dacite to the west in DDHs HEB-09 and HEB-04. The two horizons are both at the base of the Reneault-Dufresnoy Formation although as the relative ages of the McDiarmid dacite and the upper rhyolite are unknown they cannot be firmly linked.

5.4 LA-ICP-MS analyses of pyrite

5.4.1 Samples

Thick sections (~100 μm thickness) were prepared for 19 representative samples of the thinly laminated to thinly bedded intervals from the sulphide-bearing stratified horizons. Each sulphide-bearing stratified horizon found during the study is represented by one or two thick sections. These were made in areas of the cores characterized by an abundance of pyrite, irrespective of the type of occurrence (e.g., pyrite veinlets vs. pyrite-rich laminations, fine or coarse grains, etc.).

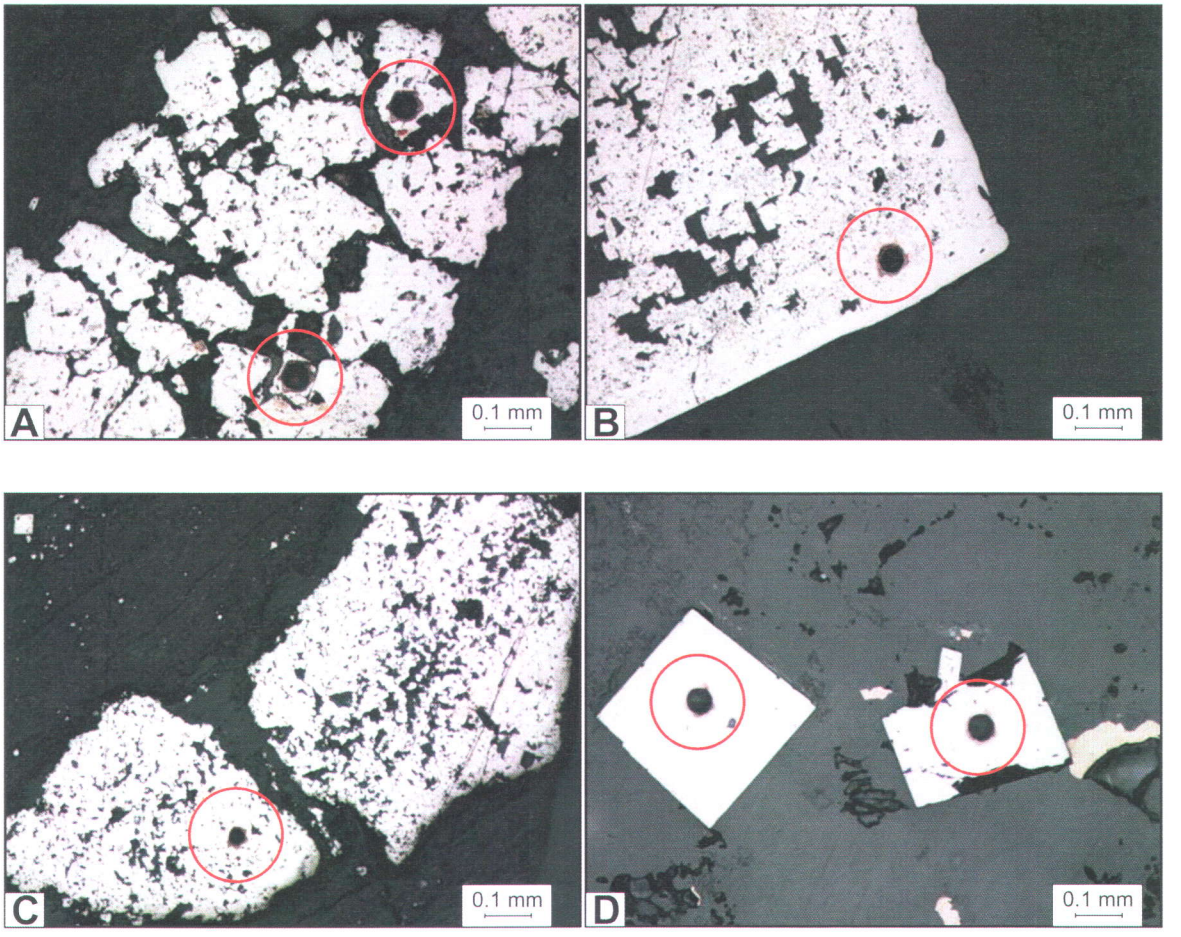

Fig. 5.5 Reflected light photomicrographs of the sulphide-bearing stratified horizons. (A) Fine-grained concordant pyrite. (B) Coarser veinlet-associated pyrite. (C) A pyrite grain extemely rich in sulfide and siicate mineral inclusions. (D) Euhedral pyrite crystals with almost no inclusions; both the lack of inclusions and the euhedral shape are likely the result of metamorphic recrystallisation. The pits in the surface are the result of laser ablation and are circled in red.

5.4.2 Methods

Laser Ablation Inductively Coupled Plasma Mass Spectrometry (LA-ICP-MS) analyses were performed on selected pyrite grains at Laurentian University in Sudbury, Ontario, using an ultra-violet laser beam from a NewWave Research 213 nm probe, coupled with a Thermo-Fisher XSeries 2 ICP-MS. The spots to be analyzed were first cleaned of possible surface impurities using a 2 s ablation with a 55 μm beam, and the actual analysis used a stationary 40 μm beam for 25 s. In five of the thick sections, the pyrite grains were too small and a 25 μm beam had to be used (same ablation time, following cleaning with a 2 s ablation using a 30 μm beam).

Between 10 and 20 spots were analyzed per thick section. Most pyrite grains are represented by one spot, although in the cases of larger grains, there may be two or more points to characterize possible metal zonations. Analyzed spots were chosen to obtain information on all pyrite types in the samples (concordant vs. discordant pyrite, with or without inclusions, etc.).

When selecting the integration interval for trace element calculations from the raw spectra, inclusions of other minerals in the pyrite grains, visible by spikes of elements such as Cu, Au and Zn in the spectra, were not excluded. These inclusions contain the bulk of the trace metals of interest in the pyrites, since these elements do not typically reside in the lattice (Huston et al., 1995; Abraitis et al., 2004). Iron in pyrite was used as the internal standard assuming stoichiometric proportions. The external standards used were the MASS1 synthetic polymetallic sulphide standard from the U.S. Geological Survey for most trace elements (Ag, As, Au, Bi, Cd, Co, Cr, Cu, Hg, Mn, Mo, Sb, Sn, V, Zn) and Standard Reference Material 612, a glass from the U.S. National Institute of Standards and Technology (NIST), for Ni, Pb, Sc, Ti, Tl, Th and U. Detection limits were calculated using the method from Heinrich et al. (2003).

5.4.3 Element residence

Trace elements can be hosted with pyrite grains in three sites; stoichiometric substitution within the lattice, non-stoichiometric substitution within the lattice and in inclusions of

other minerals (Huston et al., 1995; Abraitis et al., 2004). As mentioned above, spikes in the spectra inconsistent with the width of the iron spectra represent inclusions of other minerals in the pyrite grains. Three groups were determined from examination of the spectra; Ag, Au, Cd, Cu, Cr, Hg, Mn, Mo, Sb, Sc, Sn, Th, Ti, Tl, U, V and Zn (Group 1) (Fig. 5.6a) have spectra patterns that do not match iron in the overwhelming majority of cases, suggesting residence in inclusions; Ni (Fig. 5.6b) has spectra patterns which do match iron in the majority of cases, so this element must reside in the lattice; and As, Bi, Co and Pb (Group 2) (Fig. 5.6c) vary between matching iron and non-matching iron, implying variable residence sites.

These observations predominantly agree with published data for pyrites (e.g. Huston et al., 1995), with the exception of the elements Bi, Mo, Pb and Tl. Specifically, Bi and Pb are believed to mainly occur in inclusions in the literature but in this study they vary between the lattice and inclusions. In contrast, Mo and Tl are presented as occurring within the lattice in the literature, but in this study these elements are found predominantly in inclusions. The reason for these discrepancies could be a difference in the techniques used as there are few published cases of pyrite analyses using LA-ICP-MS, or a difference in the environment of pyrite formation between this study and others.

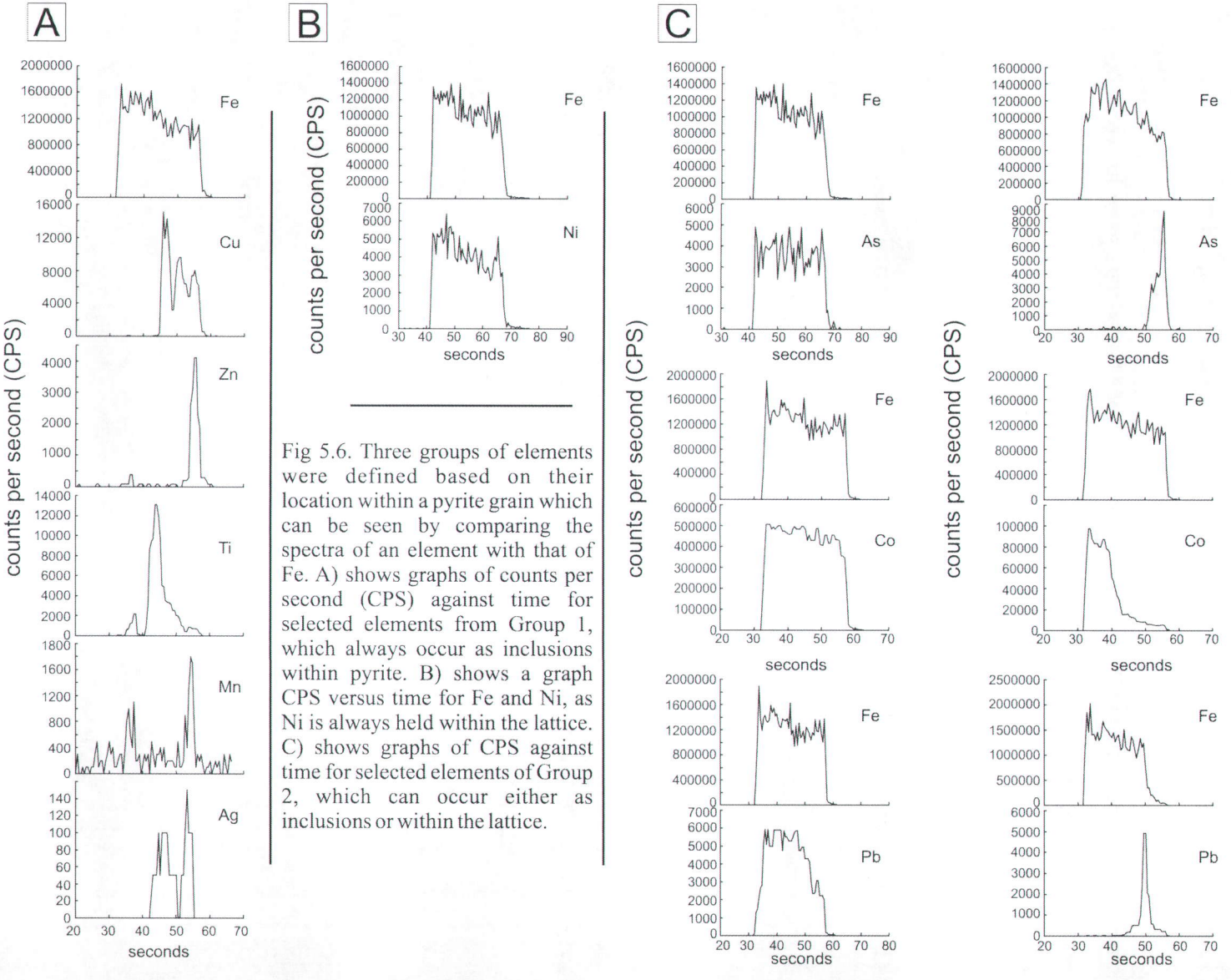

Fig 5.6. Three groups of elements were defined based on their location within a pyrite grain which can be seen by comparing the spectra of an element with that of Fe. A) shows graphs of counts per second (CPS) against time for selected elements from Group 1, which always occur as inclusions within pyrite. B) shows a graph CPS versus time for Fe and Ni, as Ni is always held within the lattice. C) shows graphs of CPS against time for selected elements of Group 2, which can occur either as inclusions or within the lattice.

5.4.4 Results

The determined trace element contents of pyrite are extremely variable, between samples and within samples, as found in similar studies performed elsewhere (e.g., Peter et al., 2003a; 2003b using electron microprobe; Chenery et al., 1995 and Chapman et al., 2008 using LA-ICP-MS). The distribution of values for Cu, Zn, Au and Ag are shown geographically as thematic maps on figure 5.2.

A pattern of where the highest values occur for the same elements can be visualized on a graph of metal contents vs. DDH lateral position (Fig. 5.7). For Cu, two peaks can be seen: a western one centered on HEB-04, and an eastern one in the region of HEB-02 to HEB-03, with a gap in between, clearly illustrated by the median and 90^{th} percentile curves (Fig. 5.7a). A similar pattern is seen for Zn, although the western peak is mainly visible in the median curve and the eastern Zn peak contains a "valley" at HEB-01 (Fig. 5.7b). This may reflect different fluid temperatures necessary to transport Cu and Zn. Au and Ag also display two peaks with pyrite from HEB-08 being depleted of trace metals (Figs. 5.7c and 5.7d). Similar patterns exist for As, Bi, Cd, Hg, Mn, Pb, Sb and Tl (not shown). These lateral variation patterns collectively suggest the existence of two distinct broad hydrothermal up-flow zones in the volcanic rocks of the upper part of the Hébécourt Formation: a western one in the HEB-09 to HEB-04 region, and an eastern one in the HEB-02 to HEB-03 region. Hydrothermal fluids also circulated within the lower levels of the Reneault-Dufresnoy Formation, as shown by high Cu and Zn in this formation within DDH HEB-09 (Figs. 5.2c, 5.2d).

The lateral element abundances for horizons A and A' are shown on figure 5.8. The Cu (Fig. 5.8a) has two peaks to the east and west with a trough in the centre, around HEB-08. The same pattern is seen for the other elements and matches the pattern shown on the multi-sample plots (Fig. 5.7), with the exception of Au (Fig. 5.8d) where none of the pyrites analyzed contained detectable gold. This good correspondence between patterns in trace elements for pyrites from a single, relatively continuous, sulphide-bearing stratified horizon (Figs. 5.1 and 5.8), with equivalent patterns for the whole dataset which includes multiple, mostly discontinuous horizons (Fig. 5.7), suggests that the hydrothermal up-

flow zones were long lived and infiltrated several horizons at different stratigraphic levels. The correlation between the patterns in multiple horizons and within a single horizon strongly suggests that the patterns are not statistical anomalies but reflect the presence of hydrothermal up-flow zones.

5.5 Chapter summary

The sulphide-bearing horizons sampled in this study vary greatly in character, but are formed of thicker units of tuff (60-70 cm) separating finely laminated intervals of finer-grained tuff and argillite. Sulphides are believed to have been added to these units by precipitation from hydrothermal fluids moving vertically and then spreading along permeable horizons. These horizons occur at multiple stratigraphic positions, and while two horizons, A and A', have been correlated, the rest likely represent horizons of limited lateral extent.

Trace elements within these pyrite grains can be hosted in two ways; within the lattice or within inclusions, but some elements vary between these types from grain to grain. The way in which the elements are hosted can be determined by examination of the spectra.

The location of the hydrothermal up-flow zones can be defined by the peaks in the trace element contents of the pyrite as analyzed by LA-ICP-MS, from the whole dataset at a particular lateral position and from the horizons that have been correlated. The data suggests that two hydrothermal up-flow zones, one in the east and one in the west, caused the trace element variations in the pyrites.

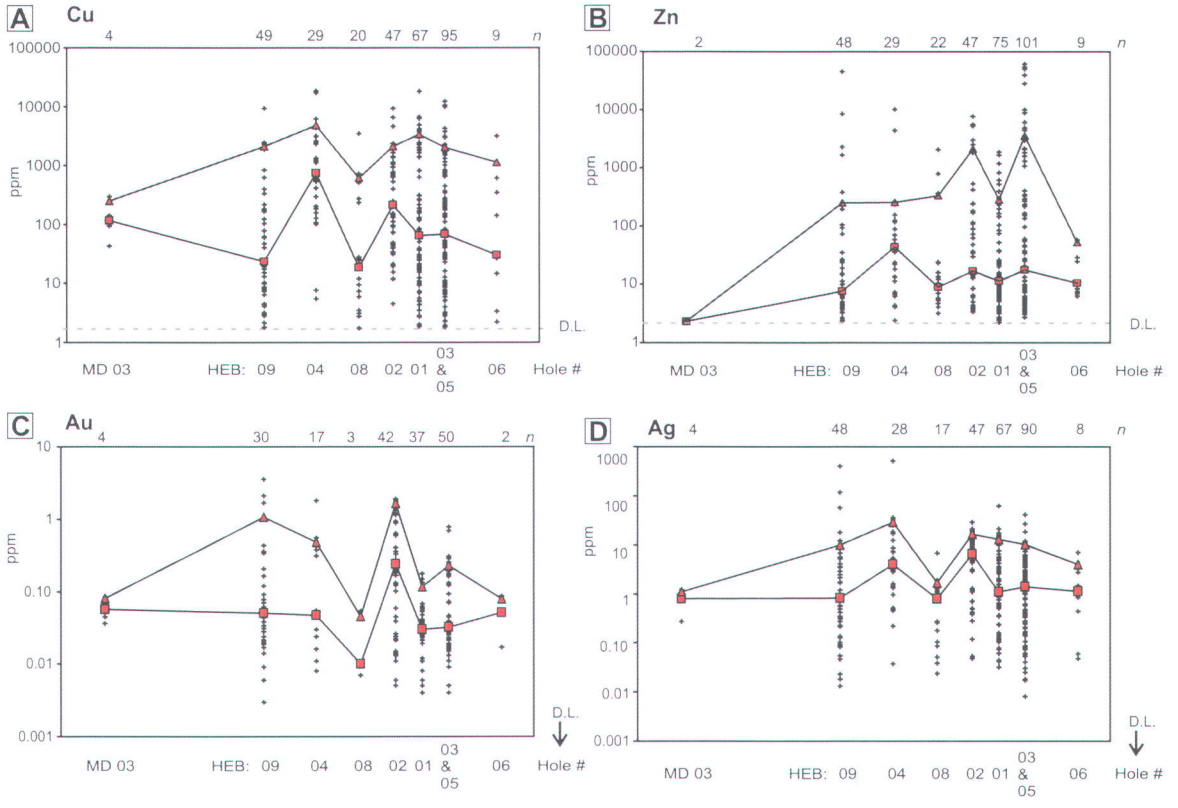

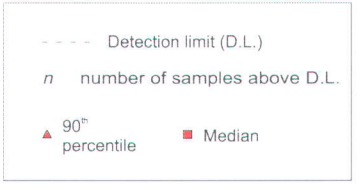

Fig. 5.7: Geochemical variations in pyrites from sulfide-bearing stratified horizons based on LA-ICP-MS analyses. Metal contents for individual analyses are plotted against the DDH in which the samples were taken, as a representation of lateral variations: (A) copper, (B) zinc, (C) gold and (D) silver.

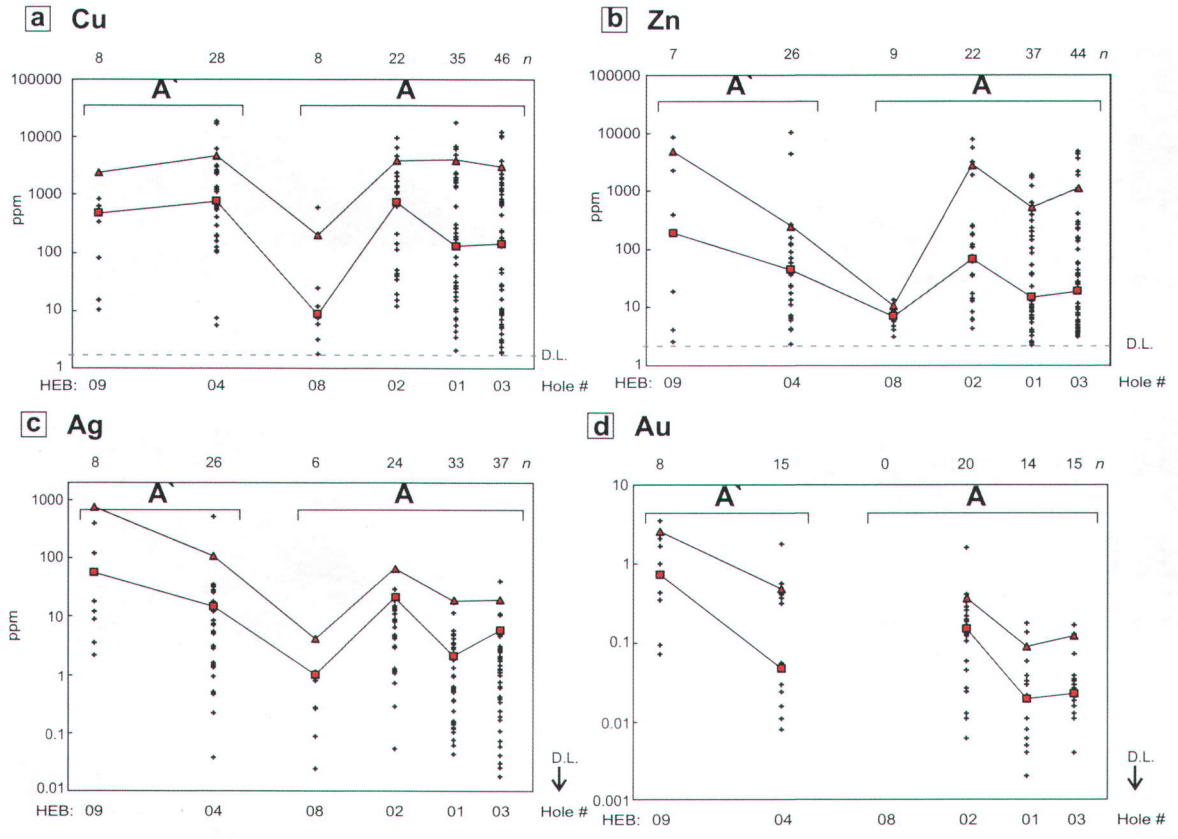

Fig. 5.8: Geochemical variations in pyrites, from sulfide-bearing stratified horizons A and A' identified on fig 5.1, based on LA-ICP-MS analyses. Metal contents for individual analyses are plotted against the DDH in which the samples were taken, as a representation of lateral variations: (A) copper, (B) zinc, (C) silver and (D) gold. None of the pyrites analysed from horizon A in HEB-08 had gold above the detection limit.

6. Discussion

This portion of the memoir will discuss the interpretations of the data presented in individual chapters in more depth than previously, and will also draw together the implications from different chapters to provide a comprehensive interpretation of the geological evolution of study area. The discussion will first provide an overview of the formations studied regionally, and then describe in more detail the interpretations of the physical volcanology for both the eastern and western areas. Following this will be a discussion of the mineralization and hydrothermal activity in the study area, as well as how this is associated with the volcanic centers identified by the physical volcanology. The applicability of these techniques in other areas will be mentioned. Finally, the rocks of the study area will be compared to the host rocks of the Horne VMS deposit due to the similarity in ages of the two areas, and clarification will be provided on the applicability of the term "exhalite".

6.1 Overview of the Hébécourt and Reneault-Dufresnoy formations in the study area and regionally

Regionally, the Hébécourt Formation is simpler than in the study area, as it consists largely of monotonous tholeiitic basaltic lavas interpreted as a lava plain (Dimroth et al., 1982) or overlapping scutulums. Felsic complexes are few and far between, and calc-alkaline intercalations have not been reported outside of the study area. The greater volumes of rhyolite in the region studied have no obvious explanation, but generation of more voluminous rhyolite may have been made possible by the development of a high-level magma chamber in the oceanic crust, or by local crustal extension generating a thermal anomaly (Franklin et al., 2005; Galley et al., 2007). Regardless of their mechanism of formation (e.g. differentiation from a tholeiitic basaltic magma or partial melting of a basalt), the tholeiitic rhyolites must have been generated at relatively shallow depths (Hart et al., 2004), which would have implied enhanced heat flow in the oceanic crust favoring hydrothermal activity. Following the emplacement of the Hébécourt Formation, magmas kept erupting in the same general areas and this lead to the

construction of a large shield volcano now exposed further south in the Reneault-Dufresnoy Formation (Ross et al., submitted a).

In summary, the Hébécourt Formation in the study area has been divided into six tholeiitic volcanic units: basalt; variably variolitic basaltic andesite; main rhyolite (comprising a typically quartz-phyric low-Ti subunit and a typically aphyric high-Ti subunit); upper rhyolite; and the McDiarmid dacite.

The stratigraphy east of DDH HEB-04 and the stratigraphy west of this DDH have a couple of points in common: (i) the Hébécourt basalt is the oldest unit in both successions and is intercalated with basaltic andesite and (ii) the transitional to calc-alkaline basalts and basaltic andesites of the Reneault-Dufresnoy Formation overlie the Hébécourt Formation in both successions. But while the felsic stratigraphy in both areas is composed of the same units, they have a different stratigraphic order (Figs. 3.1, 3.2 and 3.3), and the point at which the two felsic sequences could be expected to meet is not observed.

6.2 Chemo-stratigraphy and identification of volcanic vents

6.2.1 Eastern area

In the better exposed and well understood eastern area (east of DDH HEB-04), the Hébécourt main rhyolite directly overlies the Hébécourt basalt. However, tholeiitic basalt is also locally present in thin intercalations immediately above the main rhyolite. The Hébécourt basaltic andesite is also observed mainly below the main rhyolite, but a thick intercalation is present above it (Fig. 3.1). Finally, the formation ends with the upper rhyolite. Therefore, the bimodal Hébécourt Formation consists of two tholeiitic mafic-felsic cycles there, the second being significantly thinner than the first. The rhyolites are plausibly derived petrogenetically from the mafic magmas through crystal fractionation or they could be the product of partial melting of a mafic source.

The low-Ti subunit in the main rhyolite is interpreted as a lava dome extruded on a sub-horizontal basaltic seafloor surface from a single volcanic vent (or cluster of vents) in the vicinity of DDH HEB-02 (Figs. 3.10b, 3.21a). The core of the dome is formed of massive

rhyolite, with abundant volcaniclastic rocks on the top and flanks, as is typical of submarine felsic domes (e.g., Yamagashi and Dimroth 1985; Cas, 1992). The eastern flank of this dome contains most of the known Zn-Cu mineralization in the study area, likely formed by sub-seafloor replacement of the primary porosity in the volcaniclastic deposits (e.g., Doyle and Allen, 2003).

The high-Ti subunit in the main rhyolite is interpreted as composed of lava flows or domes. It has the opposite shape to that of the low-Ti rhyolite: it is thinner in the centre and thickest on each side (Fig. 3.10c). The shape of the high-Ti subunit and the distribution of volcanic facies within it suggest that it was not produced from a single effusive centre. There are two distinct massive regions which could represent individual vent areas, located to the east and west of the low-Ti rhyolite vent (Fig. 3.10c and 3.21b).

The thickness and facies distribution of the youngest intercalation of the Hébécourt basaltic andesite strongly suggests that the vent was located in the eastern part of the unit, in the same general area as the vent for the eastern part of the high-Ti subunit in the Hébécourt main rhyolite (Fig. 3.6 and 3.21c). The western vent for the high-Ti subunit, in contrast, does not appear to have been reactivated and used by mafic to intermediate tholeiitic magmas after the rhyolite eruptions.

Although thinner than each of the subunits in the main rhyolite, the Hébécourt upper rhyolite appears to have been formed from multiple vents in at least two episodes, with a hiatus in felsic effusive activity in between. The oldest and thickest of these episodes has the greatest proportion (100%) of massive rhyolite in DDH HEB-01, suggesting that this drill hole is located near the vent area (Fig. 3.16 and 3.21d).

In summary, the main rhyolite was initially produced from a central effusion point just east of the Chemin de la Mine (low-Ti subunit) (Fig. 6.1a), but subsequently two distinct felsic volcanic vents were active (high-Ti subunit), one on each side of the low-Ti dome (Fig. 6.1b). The overlying basaltic andesite was extruded from the east as well, and flowed westward (Fig. 6.1c). The effusive centre probably shifted slightly westward

(towards HEB-01) to produce the main part of the upper rhyolite (Fig. 6.1d). The facies variations documented in this study allow the presentation of the vent systems for the various units on a map, but this is only a two dimensional representation of a three dimensional system. Without seeing the feeder dikes, the exact position of the vent in the third dimension cannot be estimated.

6.2.2 Western area

The rocks west of DDH HEB-04 have far less surface exposure and fewer drill holes than in the east. While the stratigraphy is composed of the same units, the order is different. There are no intercalations of the basaltic andesite with the felsic package. It is presumed that the felsic package overlies the Hébécourt basalt, but this was not directly observed. The oldest observed felsic unit is the high-Ti rhyolite. There are two intercalations of the upper rhyolite within the high-Ti rhyolite, and the upper rhyolite is significantly thicker than in the east (Fig. 3.3). Above the high-Ti rhyolite is the McDiarmid dacite, which contains an intercalation of the low-Ti rhyolite, and is overlain by the Hébécourt basalt, at the top of the formation. Facies variations could not be determined for the majority of the units due to lack of control points.

6.3 Mineralization and hydrothermal up-flow

In the study area, there appears to exist at least a spatial link between the identified effusive centers, hydrothermal alteration zones, base metal mineralization, and metal concentrations in pyrites from sulfide-bearing stratified horizons (Fig. 6.1). Specifically, the proposed volcanic vent (effusive centre) for the last manifestation of the Hébécourt basaltic andesite is located immediately to the south of the known stringer-type mineralization (zone B) and most intense sericite-chlorite alteration in volcaniclastic rocks from the main rhyolite, lower down in the stratigraphy. This suggests that the basaltic andesite magmas used the same or nearby synvolcanic structures to get to the surface as the hydrothermal fluids which altered and mineralized the main rhyolite. Pyrites in sulphide-bearing stratified horizons from multiple stratigraphic levels and from a single correlated horizon in this area also contain appreciable Ag, Au, Cu and Zn, among others. The high metal values in such pyrites define a broad zone east of the

Chemin de la Mine (Figs. 5.7, 5.8 and 6.1) and therefore correspond overall to an area also containing the effusive centre for the low-Ti dome, the main volcanic vent for the upper rhyolite, and one of the vents for the high-Ti rhyolite, as well as the western weak Zn mineralization (zone A) from the historical assay data.

High metal values in pyrites from sulphide-bearing stratified horizons west of the Chemin de la Mine – as high as the values to the east of it – are not associated with known base metal mineralization and hydrothermal alteration further down in the stratigraphy. This may be the result of the very limited exploration in this area compared to further east, especially in the main rhyolite, rather than to an actual lack of alteration and mineralization. The western metal peak in the pyrites could potentially be associated with the proposed high-Ti rhyolite western vent in the region of DDH HEB-04 (see Figs. 3.10c, 5.7 and 5.8), or with other undefined volcanic vents and associated hydrothermal up-flow zones. This demonstrates the potential of using field mapping of volcanic facies and chemo-stratigraphy in parallel with trace element analysis of pyrite in defining vectors to ore in volcanic terrains.

The spatial link between volcanic vents and hydrothermal up-flow zones could be the result of both the magma and the hydrothermal fluids taking advantage of an existing weakness when developing a path to the surface, for example a syn-volcanic fault (Gibson et al., 1999; Galley et al., 2007). Although no syn-volcanic faults were clearly identified during this study, their presence could not be ruled out, because of the poor exposure in the region. An existing magma pathway would also explain why several volcanic centers would develop together spatially, and if the pathway were formed by a syn-volcanic fault it may also explain the lack of correlation between the eastern and western regions.

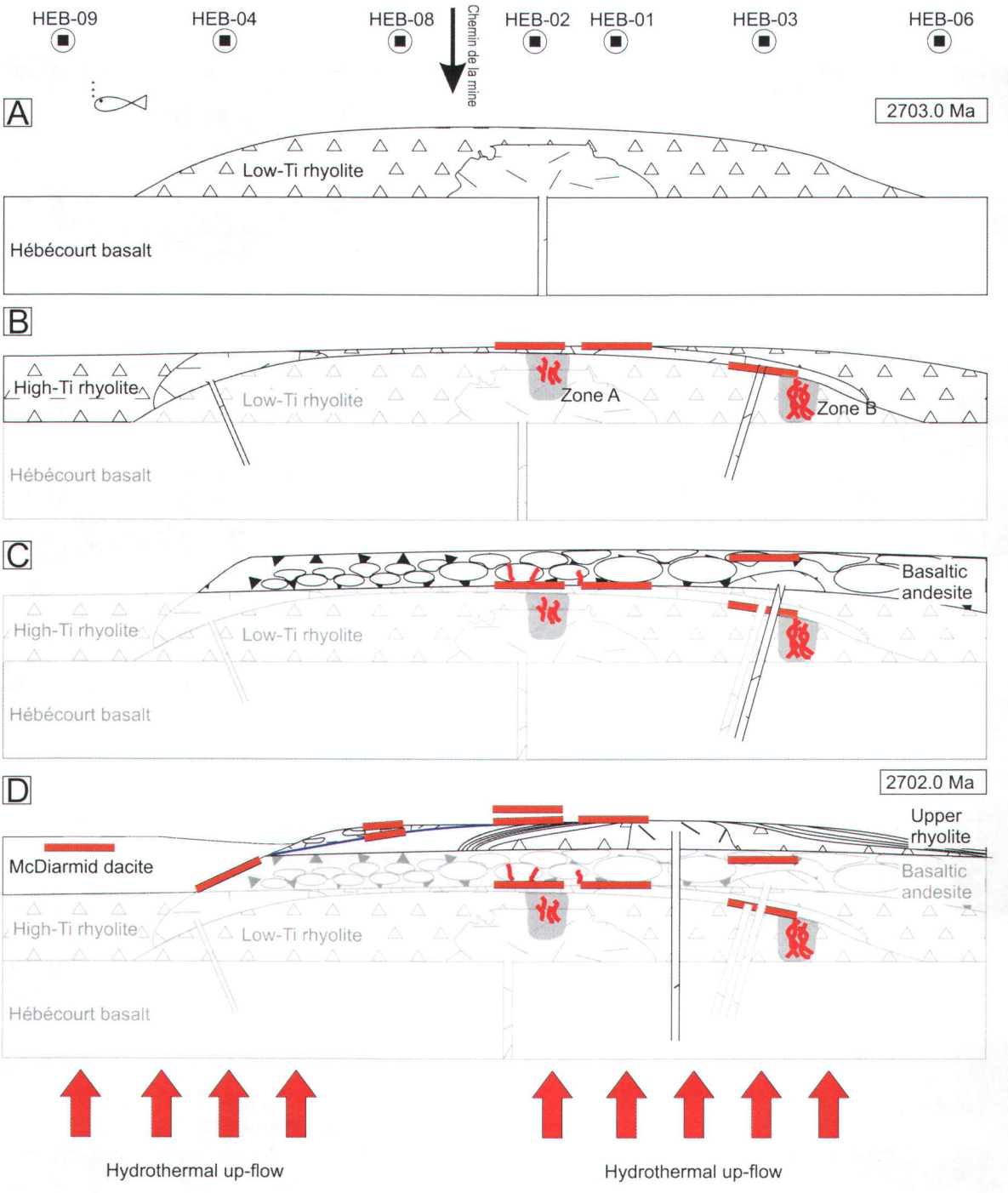

Fig. 6.1: Geological history of the study area, focusing on the top part of the Hébécourt Formation, illustrated by schematic sections (not to scale). Hydrothermal up-flow within volcanic units probably occurred more or less continuously during the time period shown. (A) Deposition of the low-Ti subunit of the main rhyolite. Triangles represent the fragmental facies and randomly orientated dashes represent the massive facies. (B) Eruption of the high-Ti subunit of the main rhyolite, from two separate vents. Also shown is the Zone A and Zone B alteration and mineralization. Thick orange lines represent the location of known sulphide-bearing laminated horizons (some may be more continuous than shown). (C) Eruption of the youngest intercalation of the Hébécourt basaltic andesite. Filled triangles represent hyaloclastite and the pillows decrease in size to the west. (D) Eruption of the upper rhyolite from the easternmost vent, as the western vent is unknown.

6.4 Implications for VMS exploration elsewhere

The combination of techniques used in this study could be applied elsewhere, within or outside VMS mining camps, and perhaps even in more highly metamorphosed and/or deformed greenstone belts. The combination of chemo-stratigraphy with physical volcanology is necessary to locate effusive centers, because the observations on facies variations cannot be utilized unless the variations are known to be contained within a single unit. For example, the interpretation of the facies variations in main rhyolite would have been very different without its division into two subunits. Further combining these data with trace element variations in sulphides from laminated horizons should help to identify hydrothermal up-flow zones, which can correspond to volcanic effusive centers.

6.5 Comparison between the Hébécourt Formation volcanism and the Horne block volcanism

6.5.1 Volcanology

As already mentioned, the rhyolites in the study area have the same age as the rhyolites hosting the Horne mine just north of Rouyn-Noranda (McNicoll et al., *submitted*). A comparison can be drawn between the Hébécourt main rhyolite in the study area and the 1340 member of the Main mine formation of the Horne sequence. This member consists of proximal lobe-hyaloclastite flows and resedimented hyaloclastite (Kerr and Gibson, 1993). Both the Hébécourt main rhyolite and the 1340 member are fragmental-dominated, proximal facies rhyolites. The abundant primary porosity of these rocks made them good hosts for replacement-type VMS deposits: this is certain at Horne (where 53.7 Mt of ore has been mined; Kerr and Gibson, 1993) and indicates potential for similar styles of mineralization in the Hébécourt Formation. However, the volcanological differences between the Horne sequence and the Hébécourt Formation are significant: the lowest member of the Horne sequence is dominated by products of explosive volcanism, while in the study area there are no proximal products of explosive volcanism. The Hébécourt Formation generally is dominated by mafic volcanism, and even in the study area contains significant volumes of basaltic andesite and basalt, while the Horne sequence is dominated by felsic volcanism (Kerr and Gibson, 1993). There are also thick mass-flow

deposits within the Horne sequence (Kerr and Gibson, 1993; Monecke et al., 2008), while these deposit types are not seen in significant volume in the study area.

Another difference between the Horne deposit host rocks and the Hébécourt rhyolites is that at Horne, there is an interpreted graben structure, clearly indicative of extension (Kerr and Gibson, 1993), whereas the Hébécourt region *may* have suffered extension, but syn-volcanic faults were not definitively proved by this study.

6.5.2 Geochemistry

The chondrite-normalized REE values for the rhyolites of the Horne mine produce profiles which are relatively lower in element abundance than those of the Hébécourt rhyolites, where the Hébécourt rhyolites are near or above the 100 line on the logarithmic axis, the Horne rhyolites are between 100 and 10, with Eu:Eu* of 0.53 (Kerr and Gibson, 1993) (Fig. 6.2). In addition, the shape of the Horne rhyolite REE profiles has the LREE forming an inclined line, with lighter elements higher in abundance and decreasing towards Eu, and the HREE have a flat profile (Kerr and Gibson, 1993), creating an overall REE profile transitional between true calc-alkaline and true tholeiitic REE profiles. The profiles for the Hébécourt rhyolites are flat and consistent from the LREE to the HREE with a minor negative anomaly in Eu:Eu* of 0.54, similar but less pronounced than for the Horne rhyolites. The difference in the profiles could be indicative of a different tectonic environment. The inclined LREE profile of the Horne rhyolites could be the result of an arc influence (Jenner, 1996) in an episode of early rifting of an immature back-arc system (Mercier-Langevin et al., 2010b). However it could also be the result of crustal contamination or a different source.

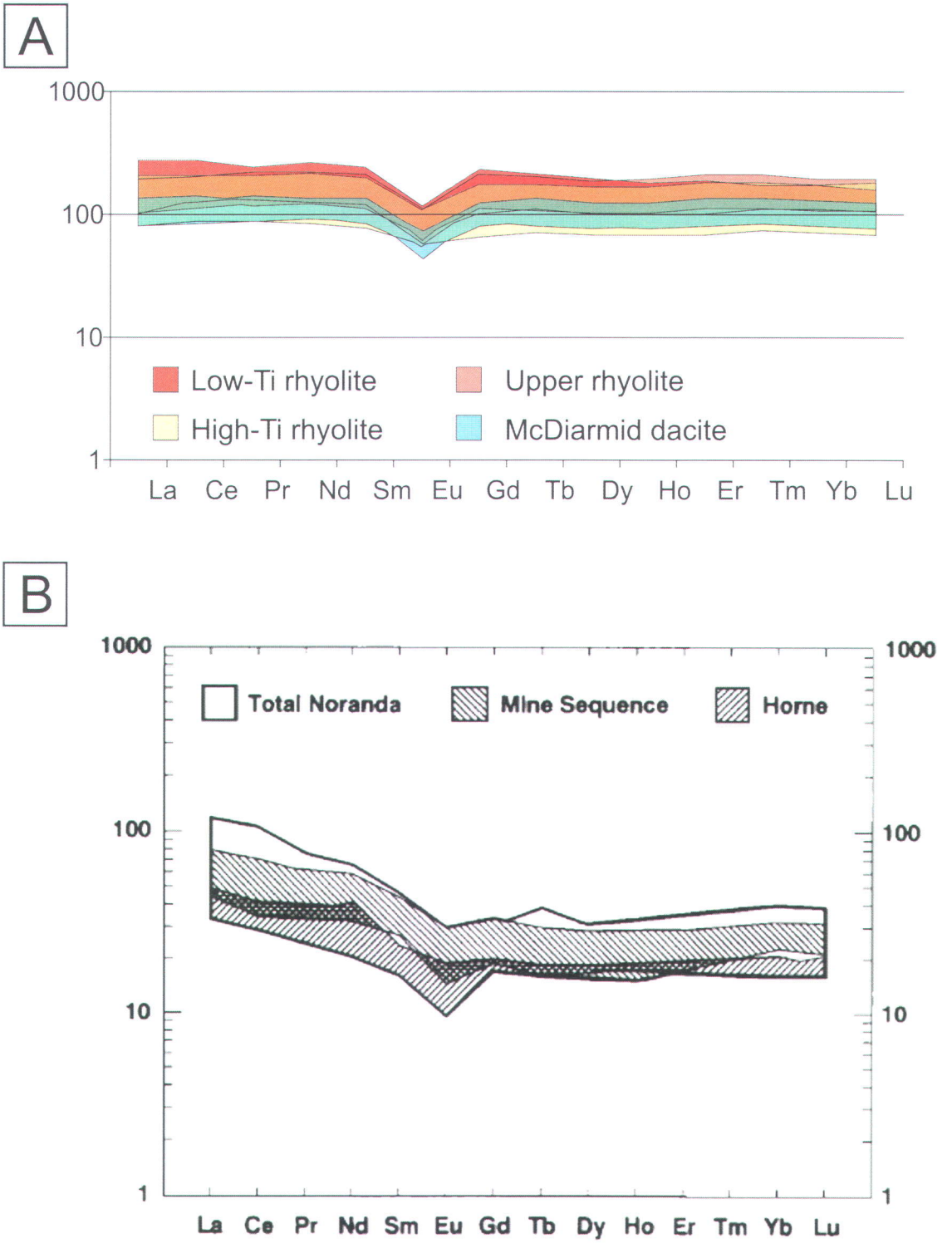

Figure 6.2. Rare earth element (REE) plots for; A) the felsic rocks of the study area and B) Mine sequence, Horne sequence and the total Noranda reference field from Kerr and Gibson (1993). Both graphs are chondrite normalised using values from Sun and McDonough (1989).

6.6 Exhalites and the sulphide-bearing stratified horizons

The term "exhalite" is sometimes overused in mineral exploration, with laminated sulphide-bearing horizons automatically assumed to represent laterally extensive marker horizons formed by sulphide precipitation and sedimentation in seawater, following venting of a hydrothermal fluid coming from a source such as a field of black smokers (Peter et al., 2003a; 2003b; Chapman et al., 2008). While true exhalites undoubtedly exist in many VMS camps, explorationists have to be careful about using the term "exhalite" too quickly.

This study has shown that careful examination of laminated sulphide-bearing horizons can lead to the conclusion that they do not always form one or several laterally extensive horizons, but can instead form several discontinuous and unconnected horizons. In such horizons, the sulphides can be truly exhalative and deposited with the enclosing sediment, but they can also be introduced later by replacement, from hydrothermal fluids moving mostly upward in the crust.

Nevertheless, even if they are not part of a classic exhalite, the sulphide minerals within these horizons still contain useful information on the location of hydrothermal up-flow zones and can aid in VMS exploration, as illustrated by this study.

7. Conclusions

VMS-type mineralization is well known in the Blake River Group. Concentrations of VMS deposits are associated with the upper Blake River Group, particularly the Noranda mining camp, which contains 22 known deposits north of Rouyn-Noranda (Gibson and Watkinson, 1990), most of which belong to the upper BRG. The Doyon-Bousquet-LaRonde mining camp also contains large VMS deposits in rocks of upper BRG age.

Rocks of the lower Blake River Group are now considered highly prospective as well, as both the Horne and Quemont gold-rich VMS deposits have recently been shown to sit in rocks of this age range, using precise U-Pb geochronology (Goutier et al., 2009; McNicoll et al., *submitted*). The world-class Horne deposit was mined from 1927 to 1976 and produced 53.7 Mt of ore at grades of 6.1 g/t Au, 2.2% Cu and 13.0 g/t Ag (Kerr and Gibson, 1993; Gibson et al., 2001). Rocks of the lower BRG in Québec and Ontario cover a vast area and spatially represent a significant part of the group. Improved understanding of the geology and hydrothermalism is therefore needed to vector exploration towards prospective sectors in the lower BRG.

However, exploration is hindered outside of mining camps (in the BRG and elsewhere) because the stratigraphy is not well known, there is a lack of marker horizons or they are undocumented, and there are fewer historical drill holes to provide information. In some districts, there is also a lack of outcrop. In many cases, no single exploration technique will be as effective due to the lack of exposure inhibiting observations and sampling, and the limited amount of previous work does not provide a large database to be compared with and expand new findings. It is often necessary to use a combination of imperfect techniques to gain a full understanding of the region.

The study area chosen was located in the lower BRG, in the northern part of the group, near the Québec-Ontario border. The knowledge of the volcanic stratigraphy in the study area was improved using whole rock geochemistry with numerous trace elements analyzed by ICP-MS. The main rhyolite in the Hébécourt Formation had previously been

undivided on maps from MRNF, and was divided informally using a variety of techniques in various company reports, but this study has divided it into two sub-units, the low-Ti and high-Ti rhyolites, using multiple methods: presence or absence of phenocrysts, abundance of Ti, and Zr/Y ratios. In addition, the boundaries of the sub-units have been better constrained with more control points in this study.

This study has also established the link between the basaltic andesite above the main rhyolite and the basaltic andesite intercalated within the Hébécourt basalt lower down in the stratigraphy. This link, in addition to the identification of Hébécourt basalt within the felsic package in Québec and above the felsic package in Ontario, has led to the conclusion that mafic volcanism was ongoing during the eruption of the felsic units.

Identification of calc-alkaline units of an extrusive nature (pillow breccias, tuffs, etc) rather then intrusive, below the Hébécourt upper rhyolite in the eastern section of the study area, and with a proximal-distal relationship from east to west, suggests that arc-type calc-alkaline volcanism began earlier than previously believed, within the time period which produced the overwhelmingly tholeiitic Hébécourt Formation. Since two different tectonic environments cannot have been present simultaneously in the same relatively small area, it appears likely that some of the trace element variations in the BRG result from effects such as crustal contamination and/or different melting depths/sources rather than a constantly changing tectonic environment.

The study area had to be divided into two areas, eastern and western, because of a difference in the stratigraphic order for the felsic units, even though the units were the same. In the east, the location of volcanic centers was established through use of physical volcanology, they were: a vent or cluster of vents for the low-Ti subunit of the main rhyolite in the vicinity of DDH HEB-02; two vents to the east and west of the Chemin de la Mine for the high-Ti subunit of the main rhyolite; a single vent for the youngest intercalation of the basaltic andesite, possibly the same as the eastern vent for the high-Ti, or at least in the same region; and a vent in the vicinity of DDH HEB-01 for the upper rhyolite.

In the west, the units are the same, with the addition of the McDiarmid dacite which was undefined before this study, but the order is different. The Hébécourt basalt is still the oldest. The contact between the basalt and the overlying high-Ti rhyolite was not observed, and the high-Ti rhyolite contains an intercalation of the upper rhyolite. Above the high-Ti is another unit of the upper rhyolite, the thickest unit, which contains an intercalation of the high-Ti rhyolite. Above this is the McDiarmid dacite which contains an intercalation of the low-Ti rhyolite. At the top of the Hébécourt Formation is a unit of the Hébécourt basalt, directly below the Reneault-Dufresnoy Formation. No vent regions were determined in the western area, however the difference in the stratigraphic order of the units and the great distance between the areas makes it highly unlikely that the felsic units in the west share any vents with the units in the east.

This project simultaneously combined physical volcanology with chemo-stratigraphy to establish the location of effusive centers in the volcanic units. The location of the volcanic vents provided context to interpret pyrite mineral chemistry in sulphide-bearing stratified horizons and hydrothermal alteration in the underlying volcanic units. This enabled the identification of hydrothermal up-flow zones and established a spatial link between hydrothermal up-flow zones and volcanic centers. The pyrite geochemistry provided useful information despite the pyrite grains not being hosted by classic exhalites.

7.1 Suggestions for future work

Future work in the study area could be profitably spent exploring lower stratigraphic levels in the region of DDH HEB-04, which is near a volcanic centre (the western vent of the high-Ti subunit) and is believed to be an area of past hydrothermal up-flow as indicated by the pyrite geochemistry in sulphide-bearing stratified horizons. This region is not associated with any known mineralization but has not had significant exploration yet.

In addition, the chemo-stratigraphy of the whole study area could be improved by an even tighter sampling program to further decrease the spacing between the samples within each

DDH, which would better constrain the boundaries of the units. In addition, new drill holes between DDHs HEB-09 and MD-01 would potentially allow the identification of vent areas for units in the western area and would also show the relationships between units in the eastern and western area (e.g. are they linked? Do they interfinger? Relative ages?).

Further work could be undertaken on the stratified sulphide-bearing horizons. The additional whole-rock geochemical analyses mentioned above, resulting in an improved chemo-stratigraphy, would help better constraining boundaries of volcanic units and then better correlations between the sulphide-bearing stratified intervals may become possible. While this study has noted which elements occur predominantly in inclusions and which in the lattice of the pyrite crystals, this could be taken further. By seeing if several elements that are within inclusions share the same spectra pattern, then it could be possible for types of inclusions to be identified. In addition, multivariate statistical analyses of the data, such as principal component analysis, could establish correlations between trace elements, or see patterns as to the behavior of elements with proximity to the hydrothermal up-flow zones.

Reference list

Abraitis, P.K., Pattrick, R.A.D., and Vaughan, D.J., 2004, Variation in the compositional, textural and electrical properties of natural pyrite: a review: International Journal of Mineral Processing, v. 74, p. 41-59.

Ayer, J., Amelin, Y., Corfu, F., Kamo, S., Ketchum, J., Kwok, K., and Trowell, N., 2002. Evaluation of the southern Abitibi greenstone belt based on U-Pb geochronology; autochtonous volcanic construction followed by plutonism, regional deformation and sedimentation: Precambrian Research 115, 63-95.

Ayer, J.A., Thurston, P.C., Bateman, R., Dubé, B., Gibson, H.L., Hamilton, M.A., Hathway, B., Hocker, S.M., Houlé, M.G., Hudak, G., Ispolatov, V.O., Lafrance, B., Lesher, C.M., Macdonald, P.J., Péloquin, A.S., Piercey, S.J., Reed, L.E., and Thompson, P.H., 2005, Overview results from the Greenstone Architecture Project; Discover Abitibi Initiative: Ontario Geological Survey; Open File Report 6154, 146 pages.

Bambic, P., 1998, Ormico Exploration limited, Hébécourt property report on the 1997 winter diamond drilling campaign: Mining exploration file, Ministère des Ressources naturelles et de la Faune (Québec), document GM 56162, 153 p.

Barrett, T.J., and MacLean, W.H., 1999, Volcanic sequences, lithogeochemistry, and hydrothermal alteration in some bimodal volcanic-associated massive sulfide systems: Reviews in Economic Geology, v. 8, p. 101-131.

Barrie, C.T., and Hannington, M.D., 1999, Classification of volcanic-associated massive sulphide deposits based on host-rock composition: Reviews in Economic Geology, v. 8, p. 1–11.

Carignan, G., and Lafrance, B., 2008, Rapport pour le programme de forage 2007, Projet Hébécourt: Mining exploration file, Ministère des Ressources naturelles et de la Faune (Québec), document GM 63800, 90 p.

Cas, R.A.F., 1992, Submarine volcanism: eruption styles, products, and relevance to understanding the host-rock successions to volcanic-hosted massive sulfide deposits: Economic Geology, v. 87, p. 511-541.

Cashin, P., and Fraser, R., 1992, Exploration report, Hébécourt J.V. property, Hébécourt township, Quebec: Mining exploration file, Ministère des Ressources naturelles et de la Faune (Québec), document GM 52416, 120 p.

Chadwick, W. W., Gregg, T. K. P., and Embley, R. W., 1999, Submarine lineated sheet flows: a unique lava morphology formed on subsiding lava ponds: Bulletin of Volcanology, v. 61, p. 194-206.

Chapman, J.B., Peter, J.M., and Layton-Matthews, D., 2008, Volcanogenic massive sulphide vectors? Decoding geochemical variability in metalliferous black shales of the Kidd-Munro assemblage; Summary of fieldwork and other activities: Ontario Geological Survey, Open File Report 6226, p. 7.1–7.7.

Chenery, S., Cook, J.M., Styles, M., and Cameron, E.M., 1995, Determination of the three-dimensional distributions of precious metals in sulphide minerals by laser ablation microprobe-inductively coupled plasma-mass spectrometry (LAMP-ICP-MS): Chemical Geology, v. 124, p. 55-65.

Chown, E. H., Daigneault, R ., Mueller, W., and Mortensen, J.K., 1992, Tectonic evolution of the Northern Volcanic Zone, Abitibi belt, Quebec: Canadian Journal of Earth Sciences. v. 29, p. 2211-2225.

Cloutier, J.F., 1975, Falconbridge Nickel Mines ltd., Sudbury Contact property, diamond drill report and review of main zone of interest: Mining exploration file, Ministère des Ressources naturelles et de la Faune (Québec), document GM 30901, 118 p.

Corfu, F., and Noble, S. R., 1992, Genesis of the southern Abitibi greenstone belt, Superior Province, Canada: Evidence from zircon Hf isotope analyses using a single filament technique: Geochimica et Cosmochimicta Acta, v. 56, p. 2081-2097.

Corfu, F., Davis, D. W., Stone, D. and Moore, M. L. 1998, Chronostratigraphic constraints on the genesis of Archean greenstone belts, northwestern Superior Province, Ontario, Canada: Precambrian Research, v. 92, p. 277-295.

Couture, J.-F., and Goutier, J., 1996. Métallogénie et évolution tectonique de la région de Rouyn-Noranda. MB 96-06, 110 pp.

Daigneault, R., Mueller, W.U., and Chown, E.H., 2002, Oblique Archean subduction: accretion and exhumation of an oceanic arc during dextral transpression, Southern Volcanic Zone, Abitibi Subprovince Canada:Precambrian Research, v. 115, p. 261–290.

Dimroth, E., Cousineau, P., Leduc, M., and Sanschagrin, Y., 1978, Structure and organization of Archean subaqueous basalt flows, Rouyn-Noranda area, Quebec, Canada: Canadian Journal of Earth Sciences, v. 15, p. 902-918.

Dimroth, E., Imreh, L., Rocheleau, M., and Goulet, N., 1982, Evolution of the south-central part of the Archean Abitibi Belt, Quebec, Part I: Stratigraphy and paleogeographical model: Canadian Journal of Earth Sciences, v. 19, p. 1729-1758.

Doyle, M.G., and Allen, R.L., 2003, Sub-seafloor replacement in volcanic-hosted massive sulfide deposits: Ore Geology Reviews, v. 23, p. 183-222.

Feely, R, A, Lewison, M, Massoth G J, Robert-Baldo G., Lavelle J. W. Byrne R H., Von Damm, K. L., and Curl, H. C. Jr, 1987, Composition and Dissolution of Black Smoker Particulates From Active Vents on the Juan de Fuca Ridge: Journal of geophysical research, v. 92, p. 11,347-11,363,

Fisher, R.V., 1961. Proposed classification of volcaniclastic sediments and rocks: Geological Society of America Bulletin 72, 1409-1414.

Franklin, J. M., 1995, Volcanic-associated massive sulfide base metal: Geological Survey of Canada, Geology of Canada, no 8, p. 158-183.

Franklin, J. M., Gibson, H.L., Jonasson, I R., and Galley, A.G., 2005, Volcanogenic massive sulfide deposits: Economic Geology, 100th anniversary volume, p. 523-560.

Fraser, R., 1991, Exploration report, Hébécourt J.V. property, Hébécourt township, Quebec: Mining exploration file, Ministère des Ressources naturelles et de la Faune (Québec), document GM 51635, 116 p.

Galley, A. G., 1993, Semi-conformable alteration zones in volcanogenic massive sulphide districts: Journal of Geochemical Exploration, v. 48, p. 175-200.

Galley, A. G., Hannington, M., and Jonasson, I., 2007, Volcanogenic massive sulphide deposits. *in* Goodfellow, W. D., *ed.*, Mineral Deposits of Canada: A Synthesis of Major Deposit-types, District Metallogeny, the Evolution of Geological Provinces, and Exploration Methods, Geological Association of Canada, Mineral Deposits Division, Special Publication No. 5, p. 141-161.

Gélinas, L., Trudel, P., and Hubert, C., 1984, Chemostratigraphic division of the Blake River Group, Rouyn-Noranda area, Abitibi, Quebec: Canadian Journal of Earth Sciences, v 21, p. 220-231.

Gibson, H., and Galley, A., 2007, Volcanogenic massive sulphide deposits of the Archean, Noranda District, Quebec, *in* Goodfellow, W. D., ed., Mineral Deposits of Canada: A Synthesis of Major Deposit-types, District Metallogeny, the Evolution of Geological Provinces, and Exploration Methods, Special Publication No. 5, Mineral Deposits Division, Geological Association of Canada, p. 533-552.

Gibson, H.L., and Watkinson, D.H., 1990, Volcanogenic massive sulphide deposits of the Noranda Cauldron and Shield Volcano, Quebec, *in* Rive, M., Verpaelst, P., Gagnon, Y., Lulin, J.-M., Riverin, G., and Simard, A., eds, The northwestern Quebec polymetallic belt: a summary of 60 years of mining exploration: Canadian Institute of Mining and Metallurgy, Special Volume 43, p. 119-132.

Gibson, H.L., Morton, R.L., and Hudak, G.J., 1999, Submarine volcanic processes, deposits, and environments favorable for the location of volcanic-associated massive sulfide deposits: Reviews in Economic Geology, v. 8, p. 13-51.

Gibson, H.L., Kerr, D.J., and Cattalani, S., 2001. The Horne mine: geology, history, influence on genetic models, and a comparison to the Kidd Creek mine: Exploration and Mining Geology 9, 91-111.

Gifkins, C., Herrmann, W., and Large, R., 2005, Altered volcanic rocks; a guide to description and interpretation: Centre for Ore Deposit Research, University of Tasmania, Australia, 275 p.

Goodwin, A.M., 1982, Archean volcanoes in the southwestern Abitibi Belt, Ontario and Quebec: form, composition and development: Canadian Journal of Earth Sciences, v. 19, p. 1140-1155.

Goutier, J., 1997, Géologie de la région de Destor (SNRC 32D/07): Ministère des ressources naturelles (Québec), report RG 96-13, 37 pages.

Goutier, J., Dion, C., Legault, M., Ross, P.-S., McNicoll, V., De Kemp, E., Percival, J., Monecke, T., Bellefleur, G., Mercier-Langevin, P., Lauzière, K., Thurston, P., Ayer, J., 2007. Les unités du Groupe de Blake River : corrélations, géométrie et potentiel minéral In, Québec Exploration 2007. Ministère des Ressources naturelles et de la Faune (Québec), DV 2007-04, pp. 13

Goutier, J., McNicoll, V.J., Dion, C., Lafrance, B., Legault, M., Ross, P.-S., Mercier-Langevin, P., Cheng, L.-Z., de Kemp, E., and Ayer, J., 2009, L'impact du Plan cuivre et de l'IGC-3 sur la géologie de l'Abitibi et du Groupe de Blake River: Ministère des Ressources naturelles et de la Faune (Québec), report GM 64195, p. 9-13.

Greeley, R., 1982, The Snake River Plain, Idaho: representative of a new category of volcanism: Journal of Geophysical Research, v. 87, p. 2705-2712.

Gregg, T. K. P., and Fink, J. H., 1995, Quantification of submarine lava-flow morphology through analogue experiments: Geology, v. 23, p. 73-76.

Hart, T.R., Gibson, H.L., and Lesher, C.M., 2004, Trace element geochemistry and petrogenesis of felsic volcanic rocks with volcanogenic massive Cu-Zn-Pb sulfide deposits: Economic Geology, v. 99, p. 1003-1013.

Heinrich, C. A., Pettke, T., Halter, W. E., Aigner-Torres, M., Audétat, A., Gunther, D., Hattendorf, B., Bleiner, D., Guillong, M., and Horn, I., 2003, Quantitative multi-element analysis of minerals, fluid and melt inclusions by laser-ablation inductively-coupled-plasma mass-spectrometry: Geochimica et Cosmochimica Acta, v. 67, p. 3473–3496.

Huston, D.L., Sie, S.H., Suter, G.F., Cooke, D.R., and Both, R.A., 1995, Trace elements in sulfide minerals from eastern Australian volcanic-hosted massive sulfide deposits; Part I, Proton microprobe analyses of pyrite, chalcopyrite, and sphalerite,

and Part II, Selenium levels in pyrite; comparison with delta ^{34} S values and implications for the source of sulfur in volcanogenic hydrothermal systems: Economic Geology, v. 90, p. 1167-1196.

Ingram, R.L., 1954, Terminology for the thickness of stratification and parting units in sedimentary rocks: Geological Society of America Bulletin, v. 65, p. 937-938.

Ishikawa, Y., Sawaguchi, T., Iwaya, S., and Horiuchi, M. 1976, Delineation of prospecting targets for Kuroko deposits based on modes of volcanism of underlying dacite and alteration halos: Mining Geology, v. 26, p. 105-117.

Jenner, G.A., 1996, Trace element geochemistry of igneous rocks: geochemical nomenclature and analytical geochemistry, in: Wyman, D. A., ed., Trace Element Geochemistry of Volcanic Rocks: Applications for massive sulphide exploration: Geological Association of Canada, Short course notes, v. 12, p. 51-77

Jensen, L. S., 1978, Geology of Stoughton and Marriott Townships, District of Cochrane: Ontario Geological Survey Report 173, 72 pages.

Jolly, W.T., 1978. Metamorphic history of the Archean Abitibi belt: Metamorphism in the Canadian Shield. Geological Survey of Canada, 63–78.

Kalogeropoulos, S.I., and Scott, S.D., 1989. Mineralogy and geochemistry of an Archean tuffaceous exhalite: the Main Contact Tuff, Millenbach mine are, Noranda, Quebec: Canadian Journal of Earth Sciences, v. 26, pp. 88-105

Kerr, D.J., and Gibson, H.L., 1993. A comparison of the Horne volcanogenic massive sulfide deposit and intracauldron deposits of the Mine Sequence, Noranda, Quebec: Economic Geology, v. 88, pp. 1419-1442.

Kerrich, R. and Wyman, D. A., 1996, The trace element systematics of igneous rocks in mineral exploration: An overview: *in* Wyman, D. A., Trace element geochemistry of volcanic rocks: applications for massive sulphide exploration, Geological Association of Canada, v. 12, pp. 1-50.

Knuckey, M.J., Comba, C.D.A., Riverin, G., 1982. Structure, metal zoning and alteration at the Millenbach deposit, Noranda, Quebec. In: Hutchinson, R.W., Spence, C.D., Franklin, J.M. (Editors), Precambrian sulphide deposits: Geological Association of Canada Special Paper, 25, pp. 255-295.

Laflèche, M.R., Dupuy, C., and Dostal, J., 1992, Tholeiitic volcanic rocks of the Archean Blake River Group, southern Abitibi greenstone belt: origin and geodynamic implications: Canadian Journal of Earth Sciences, v. 29, p. 1448-1458.

Lafrance, B., and Dion, C., 2004, Synthèse de la partie est du Groupe de Blake River, phase 1: secteur à l'est de la faille du ruisseau Davidson (32D/07 SE): Ministère

des ressources naturelles, de la faune et des parcs (Québec), report RP 2004-04, 14 p.

Lafrance, B., Moorhead, J., and Davis, D.W., 2003, Cadre géologique du camp minier de Doyon-Bousquet-LaRonde: Ministère des ressources naturelles, de la faune et des parcs (Québec), report ET 2002-07, 45 p.

Large, R., Gemmel, B., Paulick, H., and Huston, L., 2001, The alteration box plot: a simple approach to understanding the relationship between alteration mineralogy and lithogeochemistry associated with volcanic-hosted massive sulfide deposits: Economic Geology, v. 96, p. 957-971.

Legault, M., Goutier, J., Beaudoin, G., and Aucoin, M., 2005, Synthèse métallogénique de la Faille de Porcupine-Destor, Sous-province de l'Abitibi: Ministère des Ressources naturelles et de la Faune (Québec), report ET 2005-01, 35 p.

Liaghat, S., and MacLean, W.H., 1992. The Key Tuffite, Matagami mining district: origin of the tuff component and mass changes: Exploration and Mining Geology 1, 197-207.

Lydon, J. W., 1984, Ore deposit models: volcanogenic massive sulfide deposits. Part 1: A descriptive model: Geoscience Canada, v. 11, p. 195-202.

Lydon, J. W., 1988, Ore deposit models: volcanogenic massive sulfide deposits. Part 2: Genetic models: Geoscience Canada, v. 15, p. 43-65.

Martin, L., 1994, Noranda Exploration Company limited, project 338, Hébécourt township, Quebec, Report of diamond drilling: Mining exploration file, Ministère des Ressources naturelles et de la Faune (Québec), document GM 52938, 88 p.

Maurice, C. J., David, J., Bédard, J. H., Francis, D., 2009, Evidence for a widespread mafic cover sequence and its imlications for continental growth in the Northeastern Superior Province : Precambrian Research, v. 168, p. 45-65.

McNicoll, V., Dubé, B., Goutier, J., Mercier-Langevin, P., Dion, C., Monecke, T., Ross, P.-S., Thurston, P., Percival, J., Legault, M., Pilote, P., Bédard, J., Leclerc, F., Gibson, H., and Ayer, J., 2008, New U-Pb geochronology from the TGI-3 Abitibi/Plan Cuivre project: implications for geological interpretations and base metal exploration. Geological Association of Canada - Mineralogical Association of Canada (GAC-MAC-SEG-SGA) Joint Annual Meeting, Quebec City, May 2008, Abstracts Volume 33, P. 110.

McNicoll, V., Goutier, J., Dubé, B., Mercier-Langevin, P., Ross, P.-S., Dion, C., Monecke, T., Percival, J., Legault, M., and Gibson, H., *submitted*, New U-Pb geochronology from the Blake River Group, Abitibi Greenstone Belt, Québec: implications for geological interpretations and base metal exploration: Economic Geology.

McPhie, J., Doyle, M., and Allen, R., 1993, Volcanic textures: a guide to the interpretation of textures in volcanic rocks: Hobart, Tasmania, University of Tasmania, 196 p.

Mercier-Langevin, P., Dubé, B., Hannington, M.D., Davis, D.W., Lafrance, B., and Gosselin, P., 2007a, The LaRonde Penna Au-Rich Volcanogenic Massive Sulfide Deposit, Abitibi Greenstone Belt, Quebec: Part I. Geology and Geochronology: Economic Geology, v. 102, p. 585-609.

Mercier-Langevin, P., Dubé, B., Hannington, M.D, Richer-Lafléche, M., and Gosselin, G., 2007b, The LaRonde Penna Au-Rich Volcanogenic Massive Sulfide Deposit, Abitibi Greenstone Belt, Quebec: Part II. Lithgeochemistry and Paleotectonic setting: Economic Geology, v. 102, p. 611-631.

Mercier-Langevin, P., Ross, P.-S., Lafrance, B., and Dubé, B., 2008, Volcaniclastic rocks of the Bousquet scoriaceous tuff units north of the LaRonde Penna mine, Doyon-Bousquet-LaRonde mining camp, Abitibi Greenstone Belt, Quebec: Geological Survey of Canada, Current Research, v. 2008-11, p. 1-19.

Mercier-Langevin, P., Wright-Holfeld, A., Dubé, B., Bernier, C., Houle, N., Savoie, A., and Simard, P., 2009, Stratigraphic setting of the Westwood-Warrenmac ore zones, Westwood Project, Doyon-Bousquet-LaRonde mining camp, Abitibi, Quebec: Geological Survey of Canada, Current Research paper CR2009-3, 20 p.

Mercier-Langevin, P., Dubé, B., Hannington, M., Monecke, T., McNicoll, V., Gibson, H., Galley, A., Goutier, J., Davis, D., and Bécu, V. 2010a. Gold-rich VMS deposits of the Abitibi Greenstone belt: Distribution, main geological attributes and implications for exploration. Prospectors and Developers Association of Canada International Trade Show and Investors Exchange – The Abitibi Technical Session, Tuesday March 9th, 2010, Toronto, Canada. [Talk]

Mercier-Langevin, P., Hannington, M.D., Dubé, B., and Bécu, V., 2010b, The gold content of volcanogenic massive sulfide deposits. Mineralium Deposita (in press), DOI 10.1007/s00126-010-0300-0.

Moon, C. J., Whateley, M. K. G., and Evans, E. M., 2006, Introduction to mineral exploration: Blackwell Publishing, 2nd edition.

Monecke, T., Gibson, H., Dubé, B., Laurin, J., Hannington, M.D., and Martin, L., 2008, Geology and volcanic setting of the Horne deposit, Rouyn-Noranda, Quebec: initial results of a new research project: Geological Survey of Canada Current Research paper CR2008-9, 16 p.

Morton, R. L. and Franklin, J. M., 1987, Two-fold classification of Archean volcanic-associated massive sulfide deposits: Economic Geology v. 82, p. 1057-1063.

Mueller, W.U., Daigneault, R., Mortensen, J.K., and Chown, E.H., 1996. Archean terrane docking: upper crust collision tectonics, Abitibi greenstone belt, Quebec, Canada: Tectonophysics 265, 127-150

Mueller, W.U., Stix, J., Corcoran, P.L., and Daigneault, R., 2009. Subaqueous calderas in the Archean Abitibi greenstone belt: An overview and new ideas: Ore Geology Reviews 35, 4-46.

O`Neil, J., Maurice, C., Stevenson, R. K., Larocque, J., Cloquet, C., David, J., and Francis, D., 2008, The Geology of the 3.8 Ga Nuvvuagittuq (Porpoise Cove) Greenstone Belt, Northeastern Superior Province, Canada. In Van Kranendonk, M. J., Smithies, R. H., and Bennet, V. C., 2008, Earths Oldest Rocks, Amsterdam, Elsiever: p. 219-250.

Pearson, V., and Daigneault, R., 2009. An Archean megacaldera complex: the Blake River Group, Abitibi greenstone belt: Precambrian Research 168, 66-82.

Péloquin, A. S., Potvin, R., Paradis, S., Lafléche, M.R., Verpaelst, P., and Gibson, H.L., 1990, The Blake River Group, Rouyn-Noranda area, Quebec: a stratigraphic synthesis, *in* Rive, M., Verpaelst, P., Gagnon, Y., Lulin, J.-M., Riverin, G., and Simard, A., eds, The northwestern Quebec polymetallic belt: a summary of 60 years of mining exploration: Canadian Institute of Mining and Metallurgy, Special Volume 43, p. 107-118.

Percival, J.A., 2007, Geology and metallogeny of the Superior Province, Canada: *in* Goodfellow, W.D., ed., Mineral Deposits of Canada: A Synthesis of Major Deposit-Types, District Metallogeny, the Evolution of Geological Provinces, and Exploration Methods: Geological Association of Canada, Mineral Deposits Division, Special Publication No. 5, p. 903-928.

Peter, J. M., and Goodfellow, W. D., 1996, Mineralogy, bulk and rare earth element geochemistry of massive sulphide-associated hydrothermal sediments of the Brunswick Horizon, Bathurst Mining Camp, New Brunswick: Canadian Journal of Earth Sciences, v. 33 p. 252–283

Peter, J.M., Kjarsgaard, I.M., and Goodfellow, W.D., 2003a, Hydrothermal sedimentary rocks of the Heath Steele Belt, Bathurst Mining Camp, New Brunswick: Part 1. mineralogy and mineral chemistry: Economic Geology Monograph 11, p. 361-390.

Peter, J.M., Goodfellow, W.G., and Doherty, W., 2003b, Hydrothermal sedimentary rocks of the Heath Steele Belt, Bathurst Mining Camp, New Brunswick: Part 2. Bulk and rare earth element geochemistry and implications for origin: Economic Geology Monograph 11, p. 391-415.

Piercey, S.J., Chaloux, E.C., Péloquin, A.S., Hamilton, M.A., and Creaser, R.A., 2008, Synvolcanic and younger plutonic rocks from the Blake River Group: implications for regional metallogenesis: Economic Geology, v. 103, p. 1243-1268.

Powell, W. G., Carmicheal, D. M., and Hodgson., C. J., 1995, Conditions and timing of metamorphism in the southern Abitibi greenstone belt, Quebec: Canadian Journal of Earth Sciences, v. 32, p. 787-805.

Ridler, R.H., 1971. Analysis of archean volcanic basins in the Canadian Shield using the exhalite concept (abstract): Canadian Institute of Mining and Metallurgy Bulletin 64, 20.

Ross, P.-S., and Bédard, J.H., 2009, Magmatic affinity of modern and ancient subalkaline volcanic rocks determined from trace-element discriminant diagrams: Canadian Journal of Earth Sciences, v. 46, p. 823-839.

Ross, P.-S., Percival, J. A., Mercier-Langevin, P., Goutier, J., McNicoll, V. J., and Dubé, B., 2007, Intermediate to mafic volcaniclastic units in the peripheral Blake River Group, Abitibi greenstone belt, Quebec: origin and implications for massive volcanogenic massive sulphide exploration: Current Research, v. 2007-C3, p. 1-25.

Ross, P.-S., Goutier, J., McNicoll, V.J., and Dubé, B., 2008a, Volcanology and geochemistry of the Monsabrais area, Blake River Group, Abitibi Greenstone Belt, Quebec: implications for volcanogenic massive sulphide exploration: Geological Survey of Canada, Current Research, v. 2008-1, p. 1-18.

Ross, P.-S., Goutier, J., Percival, J.A., Mercier-Langevin, P., and Dubé, B., 2008b, New volcanological and geochemical observations from the Blake River Group, Abitibi Greenstone Belt, Quebec: the D'Alembert tuff, the Stadacona unit, and surrounding lavas: Geological Survey of Canada, Current Research, v. 2008-17, p. 1-27.

Ross, P.-S., Goutier, J., Mercier-Langevin, P., and Dubé, B., *submitted a*, Basaltic to andesitic volcaniclastic rocks in the Blake River Group, Abitibi Greenstone Belt: 1. Mode of emplacement in three areas: Canadian Journal of Earth Sciences

Ross, P.-S., McNicoll, V., Goutier, J., Mercier-Langevin, P., Dubé, B., *submitted b* Basaltic to andesitic volcaniclastic rocks in the Blake River Group, Abitibi Greenstone Belt: 2. Origin, geochemistry, and geochronology: Canadian Journal of Earth Sciences

Spry, P.G., Peter, J.M., Slack, J.F., 2000. Meta-exhalites as exploration guides to ore. In: Spry, P.G., Marshall, B., Vokes, F.M. (Editors), Metamorphosed and

metamorphogenic ore deposits: Society of Economic Geologists, Reviews in Economic Geology 11, pp. 163-201.

Sun, S.-S., and McDonough, W.F., 1989, Chemical and isotopic systematics of oceanic basalts: implications for mantle composition and processes, *in* Saunders, A.D., and Norry, M.J., eds., Magmatism in the ocean basins: Geological Society Special Publication, v. 42, p. 313-345.

Thurston, P.C., 2002, Autochthonous development of Superior Province greenstone belts?: Precambrian Research , v. 115, p.11–36.

Thurston, P.C., Ayer, J.A., Goutier, J., and Hamilton, M.A., 2008, Depositional gaps in Abitibi Greenstone Belt stratigraphy: a key to exploration for syngenetic mineralization: Economic Geology, v. 103, p. 1097-1134.

White, J.D.L., and Houghton, B.F., 2006, Primary volcaniclastic rocks: Geology, v. 34, p. 677-680.

Winchester, J.A., and Floyd, P.A., 1977, Geochemical discrimination of different magma series and their differentiation products using immobile elements: Chemical Geology, v. 20, p. 325-343.

Yamagishi, H., and Dimroth, E., 1985, A comparison of Miocene and Archean rhyolite hyaloclastites: evidence for a hot and fluid rhyolite lava: Journal of Volcanology and Geothermal Research, v. 23, p. 337-355.

Appendices

List of Appendices — Page

All appendices are included as PDF files on the accompanying CD.